UNIVERSITÀ DEGLI STUDI DI SALERNO
DIPARTIMENTO DI MEDICINA, CHIRURGIA E ODONTOIATRIA,
SCUOLA MEDICA SALERNITANA

Corso di Dottorato di Ricerca in:
Medicina Traslazionale dello Sviluppo e dell'Invecchiamento Attivo

XXXI Ciclo
Coordinatore: Prof. Corrado Rubino

"Functional MRI Study of Human Gustatory Cortex: Technological Advancements and Applications to Basic and Clinical Neurosciences"

Relatore:
Ch.mo Prof. Fabrizio Esposito

Candidato:
Canna Antonietta
Matr. 8800900011

Anno Accademico 2017/2018

To my mom, my dad, Alessio, Angela

Summary

Summary:

The purpose of brain plasticity is generating adaptive behaviours while predicting, interpreting, and responding to more and more complex tasks. Some of the most riveting questions in neuroscience revolve around the relationship between neural circuit structure, neural dynamics, and complex behaviour. The capability to understand the mechanisms that govern the brain under certain conditions is extremely helpful to predict human behaviour and to find possible brain alterations caused by or determining specific pathologies.

While many human brain behaviours have been largely investigated, and studied with structural and functional neuroimaging, there are still unexplored or incompletely understood domains. For example, the study of brain behaviour during taste perception and tastants evaluation is still an active field of scientific research with substantial space for neuroscientific innovation.

To date, few studies have analysed the mechanisms during the processing of gustatory stimuli and the update findings show some inconsistencies either because the use of different experimental protocols and stimulation systems, and because of the complex nature of taste sense which involves both objective and subjective factors, thus making the decoding of brain gustatory neural responses extremely complex to be definitively assessed.

The first aim of this thesis is to analyse how the human primary gustatory cortex (PGC) responds to gustatory stimulation by the use of functional Magnetic Resonance Imaging (fMRI), both specifically evaluating the responses to all the five basic tastants (sweet, bitter, sour, salty and umami) and analysing the effects determined by manipulating taste intensities.

One of the first crucial aspects of gustatory fMRI experiments is the choice of the device for taste delivery that should be able to

inject small volumes of solutions with high temporal precision and flow rates. Since no standard devices exist to perform gustatory experiments, I developed and tested a novel solution for the automatic injection of taste solutions during fMRI experiments that, thanks to the established open-architecture, open-source and low-cost nature, may contribute to an increased standardization of experimental designs in human fMRI studies of taste perception. This device is described in the second chapter of this dissertation, after a short description of the state of the art on what is known about brain mechanisms determined by gustatory stimuli.

In order to evaluate the existence within the PGC of specific subregions that differentially process taste stimuli by changing their intensity, an fMRI study performed at 3 Tesla is described in the third chapter with the injection (performed with the implemented device) of basic tastes with opposite valence, sweet and bitter, in five increasing concentrations.

This study reports the presence of a subregion in the left antero-middle insula that differentially responds to increasing concentrations according to a highly non-linear response profile, that clearly accounts for the highly complex nature of taste intensity processing within the PGC. In addition, for the first time, a spatial gradient of preferred concentrations has been highlighted in both the right and left insula, suggesting how the processing of taste intensity might require a spatially distributed neural code, as also previously observed in some animal studies.

In order to precisely localize (i) the areas within the insular cortex that primarily respond to basic taste stimulations and (ii) to verify the possible existence of a spatially organized distribution of functional responses to taste quality in the PGC, in the fourth chapter of this thesis I present the results of a parallel study performed using ultra-high magnetic field (7 Tesla) fMRI. Results from this study, the first exploring gustatory perception in humans with high spatial resolution (1mm, isotropic functional data), suggest that insula bilaterally responds to all basic tastes (sweet, bitter, salty, umami, sour) within two major clusters of activation

in the anterior and middle regions. However, the spatial distribution of individual taste preference across the insular surface was not sufficiently consistent across subjects to demonstrate the existence of a general cortical “chemotopy” whereby each basic taste simply (or simplistically) corresponds to the same predictable location within the PGC.

The second objective of this thesis, described in the fifth chapter, is to analyze the existence of possible differences in (i) the functional activations induced by the stimulation with two primary tastes (sweet and bitter) and in (ii) the inter-hemispheric functional connectivity in patients with two eating disorders (EDs), Anorexia nervosa (AN) and Bulimia Nervosa (BN), compared to healthy subjects (HC). The results obtained from the analysis of the functional response to sweet and bitter tastes have highlighted the presence of significant differences in the cingulate cortex, in the amygdala and in the insula, suggesting an altered pattern of response to pleasant and aversive tastes in several areas belonging to the reward pathway. Differences have been also found from the analysis of the inter-hemispheric functional connectivity in several brain areas involved in cognitive control and in the regulation of emotions, suggesting for the first time, this measure of connectivity as a possible new marker for the study of these two pathologies.

Riassunto:

Lo scopo della plasticità cerebrale è generare comportamenti adattivi mentre predice, interpreta e risponde a compiti sempre più complessi. Alcune delle attuali domande in ambito neuro scientifico ruotano intorno alla relazione che esiste tra la struttura, la dinamica e il comportamento del circuito neurale in presenza di stimolazioni di diversa natura. La capacità di comprendere i meccanismi che governano il cervello in determinate condizioni è fondamentale per prevedere il comportamento umano e per trovare possibili alterazioni cerebrali causate (da) o determinanti patologie specifiche.
Mentre molte funzioni del cervello umano sono state ampiamente studiate con tecniche di neuroimaging strutturale e funzionale, alcune altre rimangono ancora totalmente inesplorate o non del tutto comprese. Ne è un esempio lo studio della risposta cerebrale durante la percezione del gusto, ambito che è ancora un campo aperto per la ricerca e per l'innovazione neuroscientifica.
Ad oggi, pochi studi hanno analizzato i meccanismi durante l'elaborazione degli stimoli gustativi e i risultati attuali mostrano ancora alcune incongruenze sia per l'uso di diversi protocolli sperimentali e sistemi di stimolazione, sia per la natura complessa del senso del gusto che coinvolge sia fattori oggettivi che soggettivi, rendendo così estremamente complessa la decodifica delle risposte neuronali durante tale stimolazione.
Il primo obiettivo di questa tesi è analizzare come la corteccia gustativa primaria (CGP) risponde alla stimolazione gustativa mediante l'uso della risonanza magnetica funzionale (fMRI), valutando specificamente le risposte a tutti i cinque gusti primari (dolce, amaro, acido, salato e umami) e analizzando gli effetti causati dalla manipolazione delle intensità del singolo gusto.
Uno dei primi aspetti cruciali degli esperimenti di fMRI che prevedono stimolazione gustativa riguarda la scelta del dispositivo per l'iniezione del gusto, che si richiede essere in grado di iniettare

piccoli volumi di soluzioni con alta precisione temporale e alta risoluzione in termini di portata fluidica. Poiché non esistono dispositivi standard per eseguire tali tipi di esperimenti, nel corso di questa tesi verrà descritto un dispositivo innovativo per l'iniezione automatica dei gusti che, grazie alla sua architettura open source e a basso costo, potrebbe anche contribuire a una maggiore standardizzazione dei disegni sperimentali per gli studi di fMRI. Questo dispositivo è descritto nel secondo capitolo, dopo una panoramica sullo stato dell'arte su ciò che è noto riguardo i meccanismi cerebrali determinati dagli stimoli gustativi.
Al fine di valutare l'esistenza all'interno della CGP di regioni specifiche che elaborano in maniera differenziale diverse intensità del singolo gusto, nel terzo capitolo è descritto lo studio fMRI eseguito con uno scanner a 3 Tesla in cui viene effettuata l'iniezione di due gusti primari di opposti valenza, dolce e amaro, in cinque concentrazioni crescenti.
Questo studio mostra la presenza di una regione nell'insula di sinistra (nella porzione antero-centrale) che risponde in maniera differenziale all'aumento delle concentrazioni, secondo un profilo di risposta altamente non lineare, che evoca chiaramente la natura complessa dell'elaborazione dell'intensità del gusto all'interno della CGP. Inoltre, per la prima volta, un gradiente spaziale di concentrazioni è evidenziato sia nell'insula destra che sinistra, suggerendo come l'intensità del gusto potrebbe richiedere un'attivazione neurale distribuita spazialmente, come precedentemente osservato in alcuni studi fatti su animali.
Al fine di localizzare con precisione (i) le aree all'interno della corteccia insulare che rispondono principalmente ai gusti primari e (ii) per verificare la possibile esistenza di una distribuzione spazialmente organizzata di risposte funzionali alla qualità del gusto nella CGP, nel quarto capitolo di questa tesi vengono presentati i risultati di uno studio parallelo eseguito utilizzando acquisizioni fMRI a campi magnetici ultra-alti (7 Tesla). I risultati di questo studio, per la prima volta fatto con acquisizioni ad altissima risoluzione spaziale (1mm isotropico), suggeriscono che

l'insula risponde bilateralmente a tutti i gusti primari (dolce, amaro, salato, umami, acido) in due regioni, anteriore e centrale. Tuttavia, la distribuzione spaziale delle attivazioni, indotte dalla percezione dei vari gusti, non risulta sufficientemente coerente tra i soggetti per dimostrare l'esistenza di una "chemotopia" corticale per cui ogni gusto primario semplicemente (o semplicisticamente) corrisponde alla stessa localizzazione all'interno della CGP.
Il secondo obiettivo di questa tesi, descritto nel quinto capitolo, è quello di analizzare l'esistenza di (i) possibili differenze nelle attivazioni funzionali indotte dalla stimolazione con due gusti primari (dolce e amaro) e (ii) nella connettività funzionale inter-emisferica in pazienti affette da due disturbi alimentari, Anoressia nervosa (AN) e Bulimia Nervosa (BN), confrontate con soggetti sani (HC). I risultati ottenuti dall'analisi della risposta funzionale al dolce e all'amaro hanno evidenziato la presenza di differenze significative nella corteccia del cingolo , nell'amigdala e nell'insula, suggerendo un alterato pattern di risposta a gusti piacevoli e avversi in diverse aree del circuito legato al reward. Le differenze si riscontrano anche dall'analisi di connettività funzionale inter-emisferica in aree cerebrali coinvolte nel controllo cognitivo e nella regolazione delle emozioni, suggerendo per la prima volta questa misura di connettività come un possibile nuovo marker per lo studio di queste due patologie.

Chapter 1:

The perception of taste

1.1 Introduction

Gustation is an indispensable physiological sense and it is essential for taste evaluation, food choice and consumption. It is a complex process because it involves both chemosensory perception and cognitive evaluation, and plays a crucial role to enable recognition of chemical signals and to provide indispensable information for the evaluation of food quality and for the detection of dangerous substances. The primary role of the gustatory system is to guide individuals to select whether inject or avoid potential food sources which may carry or cause effects of contamination and poisoning. Tasting is usually driven by energy needs but also by pleasure and palatability, and these latter aspects are key factors for reward processes in determining satisfaction and physiological signals of satiety, whose derangement could become pathological.

The primary gustatory cortex (PGC) is located in the insular cortex, albeit its precise localization within the insula is still a matter of debate (Small, 2010). It has not only a primary role in recognizing incoming tastes but it is also certainly involved in the processing of the three interactive perceptual dimensions characterizing incoming taste stimuli: quality, intensity and affective valence. Furthermore, insular responses to gustatory stimuli are naturally integrated into multi-sensory systems, such as those responsible for the olfactory feelings and tactile sensations accompanying the act of tasting, as well as within the neural circuitry of memory and decision making (rejection and reward). Thereby, several factors contribute to the ultimate experience of

tasting determining an extremely complex pattern of brain activity, whose decoding and understanding represent a very difficult task.
In this first chapter, I provide the state of the art of the studies of taste perception, with a special focus dedicated to the insular cortex, the brain cortical region where the PGC is located, and to the neural phenomena occurring during the perception of basic taste stimuli.
In the second part of this chapter, a brief review of previous studies on taste perception in humans is provided, together with a discussion of the main results obtained in the fMRI studies of taste intensity, quality and affective valence.

1.2 The gustatory pathway in humans

It has been well established that humans can distinguish at least five different basic taste qualities, each of them has evolved to play a specific role in the evolution of the species.
For instance, bitter taste induces a defensive and protective mechanism to prevent from ingesting potentially toxic and dangerous foods. Contrariwise, sweet taste is naturally pleasurable and well accepted, since sugars serves as the main energy source for animals. Umami (or savory) senses amino acids in proteins and represents the taste of monosodium glutamate, present in meats, vegetables and fermented products. Salty and sour tastes evoke additional protective mechanisms aimed at assuring internal sodium or acid-base balance, respectively (Antinucci and Risso, 2017).
Taste processing is first achieved at the level of taste receptor cells (TRCs) that are clustered in taste buds on the tongue.
When a gustatory stimulus is detected by TRCs, they release neurotransmitters that activate the afferent nerve fibers for carrying taste information to the central nervous system (CNS) through a well-established pathway (Figure 1).

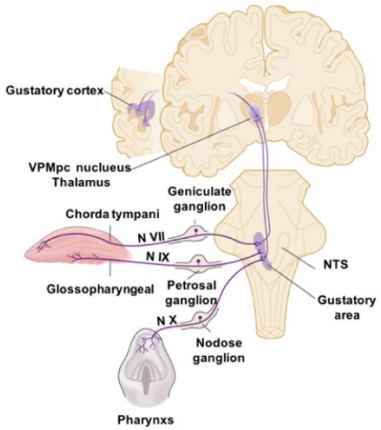

Figure 1: *Gustatory pathway in humans.*

The afferent taste fibers integrate information from multiple taste buds and relay them to the nucleus of solitary tract (NTS), located in the dorsolateral part of the bulb, that is the first synaptic station of the central gustatory system. This brain region extends rostrally from the spinal cord/medullary junction to regions in the pons located at the level of the dorsal cochlear and facial nuclei. Signal is carried from the NTS to ventro-postero-medial nucleus of the thalamus (VPMpc) and then to the primary taste cortex within the insular cortex. Projections are also present along the ventral part of the precentral gyrus.

Taste responsive neurons have been observed in the pregenual cingulate cortex, that is interconnected with the insula, thalamus and orbitofrontal cortex (OFC), the latter is the secondary gustatory area. The insular cortex has also direct and reciprocal connections with the frontal (opercular, premotor, and medial regions), temporal (auditory cortex, polar, and superior temporal sulcus), parietal (primary and secondary sensory areas), and caudolateral orbitofrontal cortices, and indirect connections with the hypothalamus, hippocampus, and striatum. Links to the amygdala, basal ganglia, and entorhinal cortex are also present. These brain

regions play a significant role not only in the interpretation of the incoming taste stimuli, which requires memory processing and cognition, but in forming complex intermodal and hedonic associations necessary for the overall gestalt of taste perception (Small, 2010).

1.3 The primary gustatory area

The PGC resides in the insular cortex.
The insula is a multi-sensory integration region which is involved in other sensory mechanisms, such as those activated by trigeminal (Hort et al., 2016) and mechanical (Baumgartner et al., 2010) stimulations, visceral pain (Zhang et al., 2018), touch (Davidovic et al., 2017), and hearing (Oh et al., 2018). For this reason, it is not immediate to separate the response induced by taste stimulation from the other sensory mechanisms occurring during the gustatory process and these factors may have influenced the full understanding of taste perception in human brain.
Furthermore, insula is a cortical region characterized by widespread anatomical connections and by heterogeneous cytoarchitecture and functional activity. It shows a smooth gradual change in its grey matter structure from the anteroventral (agranular) to postero-dorsal (granular) direction (Dalenberg et al., 2015). Together with a cytoarchitectonic parcellation of the insula, several studies have demonstrated a task-evoked subdivision; for example, studies investigating the functional connectivity of the insula (Chang et al., 2013) have indicated that the ventro-anterior agranular insula appears to be involved in the processing of chemosensory information such as olfaction and gustation, the dorso-anterior insular region has been associated with mechanisms related to higher cognitive tasks and executive control, whereas the posterior granular insula has been defined as a region of multimodal convergence of sensory, (e.g., touch, temperature, and pain), interoceptive (e.g., somatovisceral sensations) (Craig, 2003), auditory (Bamiou et al., 2003), and vestibular information (Brandt and Dieterich, 1999; Guldin and Grüsser, 1998).

The convergence of multimodal sensory signals and the ability to readout subjective states (Bamiou et al., 2003; Craig, 2009) likely explain why this brain area is intimately involved in affective processing (Damasio et al., 2000; Wager and Barrett, 2004).
In particular, it has also been associated with both the experience and observation of disgust (Phillips et al., 1997; Wicker et al., 2003), anxiety (Phillips et al., 1997), feelings of anger (Damasio et al., 2000), guilt (Chang et al., 2011), and also moral violations (Sanfey et al., 2003).
Thus, the insula is also well suited to interface between physiological sensations and higher order cognitive mechanisms (Duncan and Owen, 2000; Eckert et al., 2010; Yarkoni et al., 2009). In addition, this brain area has been demonstrated to be functionally connected with the anterior cingulate and amygdala to form the salience network (Seeley et al., 2007) and appears to be integrally involved in switching between the executive control and default networks (Menon and Uddin, 2010; Sridharan et al., 2008).
Especially in humans, the controversy about which areas in the insula are primarily involved in the decoding of taste sensations revolves around disagreements regarding the somatosensory contributions to these activations. Tasting, in fact, is always co-occurrent with oral somato-sensation, thus these two (taste and oral somatosensory) processing either overlap or lay beside each other (Hirata et al., 2005; Yamamoto et al., 1984). The subregions in the insula mostly involved in this controversy include the middle-dorsal portion and the Rolandic operculum and the posterior insula/parietal operculum/ postcentral gyrus. This latter area has been specifically proposed to be the site for oral somatosensory cortical representation in humans (Veldhuizen et al., 2011). Although most neuroimaging taste studies rely on the subtraction of a baseline (water or tasteless trial) to eliminate non-gustatory components from the taste signal, oral touch and taste are inherently related (Green and Nachtigal, 2014; Simon et al., 2008). This raises the issue of whether taste can be isolated from somatosensory representations and this combined contributions of somato-sensation and gustation to the activation of human insula

remain an important outstanding issue in the imaging of gustatory representation (Veldhuizen et al., 2011).
Another unresolved issue in the study of taste perception concerns the possible hemispheric dominance of gustatory processing: although Kurth et collegues (Kurth et al., 2010) demonstrated a right insula dominance for gustatory processing, some studies, e.g. from Velhuizen et al. (Veldhuizen et al., 2010), have failed to find any proof of laterality. To the same conclusion arrives the recent meta-analysis of Young et. al (Yeung et al., 2017), according to which basic taste processing recruits bilateral antero-ventral and middle-dorsal insula activations. However, as reported in this meta-analysis, the bilateral response to gustatory stimuli does not necessary mean a lateralization of taste perception, but may indicate that some concurrent and interacting mechanisms during the perception of taste may be lateralized.
The perception of a gustatory stimulus, in fact, primarily asks the PGC to decode three different features of taste input (referred often as perceptual dimensions in gustation), the quality of taste, its intensity or strength and its palatability (affective valence), the latter defining whether taste is considered appetitive or aversive.
A recent study of Dalenberg et. al (Dalenberg et al., 2015) has pointed out the effects of these three perceptual dimensions in the left and right insula and has demonstrated that while the left insula is primarily involved in the processing of taste quality and affective valence, the right insula gathers the processing of taste intensity.
These results, by now, are not completely exhaustive as some other works reported the bilateral insula activated by different taste intensities (Small et al., 2003; Spetter et al., 2010) and the right insula mostly involved in the discrimination among different taste qualities (Prinster et al., 2017).
As explained, the study of taste perception requires some aspects to be ultimately assessed: not only the exact location of the primary gustatory area within the insula remains to be precisely individuated but also how the PGC processes the three perceptual dimensions of taste stimuli.

1.4 The decoding of taste quality

Quality is one of taste attributes and refers to the molecular compounds of tastant solutions. The decoding of taste quality at peripheral level (in the tongue) occurs with several receptorial mechanisms that are activated during the process of tasting and that consequentially promotes the discrimination among basic tastants and the hedonic characterization (hedonic valence) determining the execution of selective behaviors (avoidance vs. acceptance) (Scott, 2004).

Generally, the mechanisms underlying sensory perception, from peripheral transduction to central neural processing of information, have been largely studied in many fields of human sensation from visual, auditory to the somato-sensory systems, where the incoming external stimuli mostly present key physical properties that are analyzed by specific receptors in the peripheral sense organs and maintained in the specific pathway until to be processed in the sensory cortices. To facilitate external stimuli discrimination, neuronal populations that respond to similar stimulus features are clustered, and response properties vary smoothly, across cortical sheets (Abdollahi et al., 2014; Ashburner, 2007; De Martino et al., 2013; Grabenhorst and Rolls, 2008; Humphries et al., 2010; Schmahmann, 2010; Seifritz et al., 2006). In these cases, while quantitative dimensions like position (characterizing tactile and visual stimulation) or frequency (characterizing visual and auditory stimulation) are naturally well suited to be represented in spatially ordered cortical locations, stimulus features of chemical substances do not include continuous physical properties, other than intensity. In fact, the quality of a chemical stimulus is categorized according to a chemical composition that does not exhibit variations along a physical dimension, common to different substances. In addition, the mechanisms of taste signal transduction and transmission (from peripheral sense organs, bud cells, to the cortical regions, e.g. to the PGC) remains still not completely determined and it remains still under debate whether taste quality signal is coded in specific labeled lines or as patterns emerging across a collection of neurons

(Roper and Chaudhari, 2017), (labeled-line vs. across-fiber theories).
The rationale of a spatially segregated and ordered cortical representation of taste qualities, especially in the PGC, may result from genetically determined stereotyped neural circuits in specific regions that could be an explanation of innate human ecological behaviors (Sosulski et al., 2011).
Particularly, cortical taste processing may tune each taste domain to identify specific nutrients, harmful substances, or chemicals associated with physiological functions (Lundström et al., 2011), thereby, an ordered cortical organization for taste would help the discrimination among tastants with mechanisms similar to those observed in other sensory cortices. Moreover, some animal imaging reports argue for chemotopy in mammalian brain cortex (Accolla et al., 2007; Chen et al., 2011; Sugita and Shiba, 2005), but a more recent imaging report argues against an ordered chemotopic cortical organization and shows no spatial distribution of taste sensitivity in mouse cortical regions (Fletcher et al., 2017). By now, only one study in humans (Prinster et al., 2017) has identified "best taste response areas" in the right PGC using fMRI but these preliminary results (performed on eight healthy subjects at 1.5 Tesla) still wait to be validated. According to these findings, taste preference is organized in compact clusters localized across the anterior and posterior parts of the right insular cortex according to a spatial distribution reminiscent of an ecological meaning of each taste or combination of tastes.
Other studies performed in humans have limited their analyses mostly to individuate areas principally responsive to tastes or their properties. The most recent study of (Dalenberg et al., 2015), for example, individuated the response of the insular cortex to taste quality in the left insula. The meta-analysis of (Yeung et al., 2018) reported effects of insular response to basic taste quality in the right antero-middle dorsal insula.
The dominance of the right hemisphere for processing the stimulus quality has been observed in several works (Kurth et al., 2010; Nakamura et al., 2011) although a large number of experiments have reported bilateral anterior and dorsal-middle insula activation

to basic tastants (Avery et al., 2016; Bender et al., 2009; Haase et al., 2007; Iannilli et al., 2012; O'Doherty et al., 2001; Veldhuizen et al., 2011). By the way, the middle dorsal insula has been argued to present neurons multimodally responsive to both gustatory and interoceptive stimuli. This could mean that this region supports a modality-general representation of food percepts from the internal and external environment, since it is shown to integrate metabolically relevant external stimuli with internal representations of the body's current state (Avery et al., 2017, 2016).

Studies analyzing taste quality have been performed also in animals. Extracellular recordings in anesthetized rodents (Maffei et al., 2013; Smith et al., 2000; Yamamoto et al., 1984; Yokota et al., 2011) have shown that the majority of taste processing neurons are located in the granular and dysgranular insula, although neurons in agranular part can also display gustatory responses (Ogawa et al., 1992).

While responses in all the three PGC's subdivisions are generally broadly tuned (Carleton et al., 2010; Simon et al., 2006), neurons in granular part have appeared more taste-selective than those in the dysgranular region. Within each subdivision, taste responsive neurons are distributed across all the cortical layers with a preference for the intermediate layers (Yokota et al., 2011). However, a more recent study (Fletcher et al., 2017), using 2-photon imaging, demonstrated in mice the presence of both tuned and broad neuronal cells in the PGC and, consequently, a common presence of quality-selective and quality-overlapped regions.

Studies have also been performed to demonstrate how different neurons in the PGC process taste in animals in terms of possible spatial organization of taste qualities on the surface of PGC (Accolla et al., 2007; Chen et al., 2011). However, the topographical organization within the PGC remains unclear also in animals.

A recent analysis performed with calcium imaging, shows that responses to different taste qualities appear to be spatially organized in the superficial layers of granular and dysgranular gustatory cortex (Chen et al., 2011). This result was recently

challenged by calcium imaging experiments in which sweet, salty, umami and bitter tastes appear to be coded by a small contingent of topographically isolated narrowly tuned neurons (Chen et al., 2011).

1.5 The decoding of taste intensity

The second attribute of taste stimulus is its intensity (or concentration) that refers to its strength or, for basic tastants, to the quantity of molecular compounds dissolved in solutions. During taste perception, the gustatory system is called to discriminate different intensities of taste stimuli for the detection of sub-micromolar quantities of noxious or toxic compounds and sub-molar concentrations of substances that promote caloric energy (Small, 2010). To this aim, gustatory cortex has the role of individuating and detecting thresholds measuring the minimum amount of a substance that is required to be present in a solution in order for a subject to detect its presence at above-chance levels. However, the neural mechanism underling this intensity-related discrimination is scarcely investigated, especially in the human insular cortex.

The study of Dalenberg et. al (Dalenberg et al., 2015) provided an analysis of insular response to five increasing concentrations of all the basic tastes finding the right insula, particularly in the dysgranular anterior part, involved in the processing of taste intensity. Other two previous studies were performed by Small et al (Small et al., 2003) and (Spetter et al., 2010). In the former study, authors used two concentrations of sucrose (sweet) and quinine sulfate (bitter) in two extreme concentrations (very low vs. very high) in order to evaluate the effects of affective values and intensity in a whole-brain analysis. They found some regions in the brain differently activated by increasing taste intensities and affective valence as the cerebellum, pons, middle insula, amygdala and caudolateral OFC.

In the latter study, four concentrations of sweet and salty tastes have been used and the middle insula found to be activated in such a way that, increasing the concentration of solution, the regional

activation increased in a monotonic linear way. Despite similar subjective intensity ratings, anterior insula activation by salt increased more with taste intensity than that by sucrose.

As for quality, no studies in humans have analyzed the possible spatial organization within the gustatory cortex in order to find a specific mechanism of responses to different stimulus intensity, essentially based on a spatial topography of neurons that may result selectively responsive with changes in tastants' concentration.

However, in addition to fMRI, electrophysiological studies have analyzed the neuronal firing rates in the PGC after the injection of tastes in different concentrations, some finding a monotonically increase of responses with intensity (Scott et al., 1991), other finding more complex trends (Stapleton et al., 2006). Furthermore, information about tastants intensity is thought to be decoded through a concentration-dependent increase in taste cell activity that in turn is transmitted through primary afferent taste fibers to gustatory neural relay areas in the hindbrain (Chen et al., 2011; Frank, 1973; Macdonald et al., 2012). In this first stage of processing, a positive correlation between intensity and taste-evoked neural activation has been evaluated both in rats and monkeys (Ganchrow and Erikson, 2018; Ogawa et al., 1972; Scott and Erickson, 1971). However, once taste signal reaches higher order taste centers, a more complex relationship between taste-evoked activity and concentration has been observed (Chen et al., 2011; Scott et al., 1991; Stapleton et al., 2006; Yamamoto et al., 1984).

For example, both (Yamamoto et al., 1984) and (Stapleton et al., 2006) found that the majority of neurons in the PGC responded to concentration changes with complex, nonlinear changes in firing rate. Changes in concentration can result in a variety of PGC responses that reflect both changes in firing rates and changes in the dynamics of the response and this could be a consequence of the fact that PGC receives and consequentially transmits information from other cortical and subcortical areas (Smith and Li, 2000) and that these areas will respond differentially to different tastants and concentrations of tastants.

1.6 The decoding of taste-related affective valence

The third attribute of taste stimulus is the affective value that means whether an ingested tastant determines reactions of pleasure or aversion.
Although the perceived pleasantness of taste differs widely between individuals (because of subjective evaluation of incoming taste), the expressing affective response to a taste stimulus is very similar across individuals (e.g. through facial expressions). fMRI studies have given useful information about areas associated with the generation of affective responses (Kringelbach, 2005). However, the pattern of these responses is more likely generated by many functionally connected brain areas, thereby advocating a network-oriented approach rather than a more locally investigation (Berridge and Kringelbach, 2008).
A study of Phillips et. al (Phillips et al., 2003) theorized a ventral emotion network encompassing the amygdala, insula, ventral striatum, and ventral regions of the pre- frontal cortex involved in the evaluation of affective valence produced by environmental stimuli that lead to the production of affective states. A growing body of neuroimaging studies have then associated this network with pleasantness coding of chemosensory stimuli: tastes, flavors, and odors e.g. (Berridge, 2009; Cerf-Ducastel et al., 2013; Crouzet et al., 2015; De Araujo et al., 2003; Nitschke et al., 2006; Small et al., 2003), indicating that the ventral emotion network might also process the pleasantness of chemosensory stimuli. However, only a limited number of these areas is found to directly correlate with affective behavioral ratings of orally presented stimuli on a single study level (e.g. (Berridge, 2009)) and few studies, by now, have determined which areas within this network are actually associated with pleasantness (e.g. (Royet et al., 2003; Rudenga et al., 2010; Small et al., 2003)).
Indeed, other previous studies have analyzed the affective valence of taste stimuli regionally, and, particularly, in the insular cortex, although it has been suggested that insular cortex codes only for

objective gustatory properties, such as tastant concentration or intensity. These studies have indicated an association between gustatory valence responses and left (Bender et al., 2009; Cerf-Ducastel et al., 2013; Hoogeveen et al., 2015) or bilateral insular activity (Small et al., 2003; Spetter et al., 2010). On the other hand, the region within the insula implicated in the processing of affective valence varies largely across studies: not only the anterior part (Dalenberg et al., 2017; Small et al., 2003; Spetter et al., 2010) but also the mid-portion of the insula and overlying operculum (Miskovic and Anderson, 2018; Nitschke et al., 2006) have been shown as crucial for affective valence response. Recently, patterns within the antero-ventral insula and posterior orbitofrontal cortex (OFC) also determined valence-related responses, independently of basic taste type (bitter, sour, etc.) (Miskovic and Anderson, 2018), possibly because the anterior insula and OFC are not only the regions where taste sense is primarily and secondarily processed, but also multimodal limbic cortices that are both implicated in reward and aversive mechanisms (Rolls, 2006).

Chapter 2:

A low-cost open-architecture taste delivery system for gustatory fMRI

2.1 Introduction

The design of gustatory fMRI experiments requires to take into account many experimental factors.
First, taste stimuli are always accompanied by tactile stimulation (Veldhuizen et al., 2011), thus the observed activation, specifically in the PGC, may be evoked by somato-sensory instead of (or in addition to) taste stimulation. In this case, to reduce these misunderstanding effects, taste stimuli are usually contrasted with water or artificial saliva, but, since these baseline solutions activate the PGC (Araujo et al., 2003; Veldhuizen et al., 2007), this contrasting procedure inevitably causes reduction in response sensitivity.
Second, several sub-regions of the insular cortex have been reported to process different features of taste, the intensity, quality and affective valence, and because the effects of these features highly correlate in many cases (Pfaffmann, 1980), it is hard to disambiguate them, especially when they are not measured and/or manipulated within the same paradigm. On the other hand, asking subject to pay attention (and to give scores) about the perceived quality, intensity and affective valence leads to increase subjects' selective attention that results in enhancement of brain activity in different parts of the insular cortex (Bender et al., 2009; Nitschke et al., 2006; Veldhuizen et al., 2007).

Third, because neuroimaging methods are rather insensitive to neuronal responses near detection threshold, researchers often use high taste concentrations that may cause disgust responses and elicit confounding mechanisms (Dalenberg et al., 2015).
For these reasons, trying to avoid all (or some of) these problems results in different stimulation paradigms that researchers have been designed across previous studies, some requiring subjects to continuously rate intensity perception (Bender et al., 2009; Cerf-ducastel et al., 2001), others requiring the rating of perceived pleasantness, quality and ⁄or intensity preceding or following the functional run (Cerf-ducastel et al., 2001; Kobayakawa et al., 1999, 1996; Ogawa et al., 2005; Zald and Pardo, 1999) or following stimulus presentation (Araujo et al., 2003; Cerf-ducastel and Murphy, 2004; Mizoguchi et al., 2002; Nitschke et al., 2006; Zald et al., 2002; Zald and Pardo, 1997), and others requiring subjects to report if a given stimulus of declared properties was detected (or not) (Small et al., 1997; Veldhuizen et al., 2007; Zald and Pardo, 2000).
Some experiments have measured the brain responses during passive tasting (Barry et al., 2001; Frank et al., 2003; Frey and Petrides, 1999; Kinomura et al., 1994; O'Doherty et al., 2001, 2002; Schoenfeld et al., 2004; Small et al., 2003; Yamamoto et al., 2003), other in presence of cognitive tasks to further explain the variability of the activations beyond perception (Wang and Spence, 2017), with recent works showing how even the responses in the primary gustatory cortex may change in relation to the level of attention paid by subjects to the taste intensity or pleasantness (Grabenhorst and Rolls, 2008; Veldhuizen et al., 2007).

However, differences across studies exist not only in terms of experimental design but also for what concerns the timing of stimulus injection. For example, some previous studies have delivered small volumes of tastants to a specific part of the tongue either quickly (De Araujo et al., 2003; De Araujo and Rolls, 2004; Kringelbach et al., 2004; O'Doherty et al., 2001) or over a period of a few seconds (Dalenberg et al., 2015; Hoogeveen et al., 2015; Small et al., 2004, 2003). Although, in most cases, subjects were refrained from swallowing immediately after stimulus delivery (to

avoid contamination of the fMRI response to taste with movement resulting from swallowing), in general, holding a taste in the mouth for longer periods has some drawbacks: (i) an extended period of tasting will affect taste perception, particularly in lying supine positions (Marciani et al., 2006), (ii) uncontrolled movements of the tongue during tasting contaminate to a greater extent the fMRI response and (iii), more critically for studies of flavor perception, postponed swallowing delays the main retro-nasal delivery of aroma volatiles that occurs with physiological swallowing (Buettner et al., 2001). For these reasons, the first crucial step in a gustatory experiment is the setting of the experimental design and, in particular, the control mechanism of taste delivery and injection timing, as these may easily become critical factors.

In an attempt to advance the researcher's control of the experimental design for gustatory fMRI experiments, the focus of the present chapter is on the presentation of a novel stimulation device for the delivery of taste solutions.

This device, rather than being used for a preliminary and single-subject based application, has allowed an examination of intensity-related changes in the insular cortex in a group of twenty healthy subjects (that will be described in details in the following chapter). Early gustatory fMRI studies were performed with manual injection of tastes (Cerf-ducastel et al., 2001; Dalenberg et al., 2015; De Araujo et al., 2003; Hoogeveen et al., 2015; O'Doherty et al., 2001). More recently, different research groups have started to build custom (hand-made) devices (Goto et al., 2015; Haase et al., 2007) mostly based on the use of electronic syringes (as in (O'Doherty et al., 2001) and in (Haase et al., 2007)) or infusion pumps (as in (Sarinopoulos et al., 2006)). Nowadays, commercial devices for taste injection (*gustometers*) are also available. For example, considering the device proposed by (Haase et al., 2007) and by (Veldhuizen et al., 2007), the gustometer is a portable device that consists of a laptop computer that controls independently programmable syringe pumps to deliver precise amounts of liquid to the subject at precisely timed intervals and durations. Each pump holds a 50 or 60 mL syringe connected to a beverage tubing terminating into a specially designed manifold

anchored to the MRI head coil and interfaced with the subject. Another solution has been proposed by (Goto et al., 2015), where the gustometer is made by solenoid valves connected to a microcontroller that regulates the injection, a time–intensity sensory evaluation meter that allowed the participants to select the level of their subjective taste intensity over time and an intra-oral device to deliver taste solution to anterior, lateral and posterior part of the tongue.

Although the described devices have been previously used for gustatory fMRI experiments, the lack of a miniaturized design may represent an important limitation when the experiments are to be performed in different locations, as could be the case of multi-center studies or when offline experiments in a laboratory are to be interleaved with the fMRI experiments in a clinical site. In addition, the effective modularity of these devices depends largely on the costs of each component, particularly on the sensors used to control the delivery from syringe pumps, thereby the actual expandability of the device could be unpractical or in some cases impossible.

Differently from previous architectures, a novel modular and fully portable device based on the use of peristaltic micropumps, has been designed for gustatory fMRI experiments. The use of micropumps has gathered two main advantages: (i) these are connected to tanks and therefore do not require re-charging the volumes of solution during the experiment; (ii) they can be controlled to deliver small volumes of taste solutions (< 1ml) at a high rate (from 1 ml/min to 200 ml/min) enabling time-resolved event-related fMRI experiments. In addition, this device is easy-to-use and fully scalable, i.e. it gathers the possibility to increase the number of channels by adding micro-pump modules directly by the end user virtually without limitations, thus enabling arbitrary complex and multi-dimensional taste experiments. Ultimately, this gustometer is an open- architecture and low-cost device, with an easy and open-source software interface to customize the taste delivery volume and timing to the specific needs of any fMRI study involving taste stimulation. Another feature is that it can be miniaturized to have extremely small

dimensions and thus made fully portable (e.g. using rechargeable lithium battery power) for conducting off-line and multi-center gustatory experiments using the same stimulation device.

This chapter starts with the full description of the working prototype of this gustometer assembled with six independent channels, five of which are reserved for taste solutions and one for pure water or artificial saliva as neutral solution. A description of the hardware and software architecture in full details is provided together with the protocol to connect the gustometer to other stimulation software. To illustrate the performances of the gustometer, in this chapter are reported the results of its application to a single-subject fMRI experiment conducted on a 3 Tesla MRI scanner and designed according to an event-related stimulation paradigm. In a first session, the experiment consisted on the injection of the five basic tastes (sweet, bitter, sour, salty and umami) plus neutral in a random order. In a second and third session, it consisted on the use of five different (parametrically increasing) concentrations of two different tastes with opposite pleasantness (sweet, bitter).

2.2 Architecture of the device

A picture of the prototype gustometer is shown in Figure 2 (Figure 2a shows the pictures of the actual prototype, Figure 2b shows the actual design with sizes).

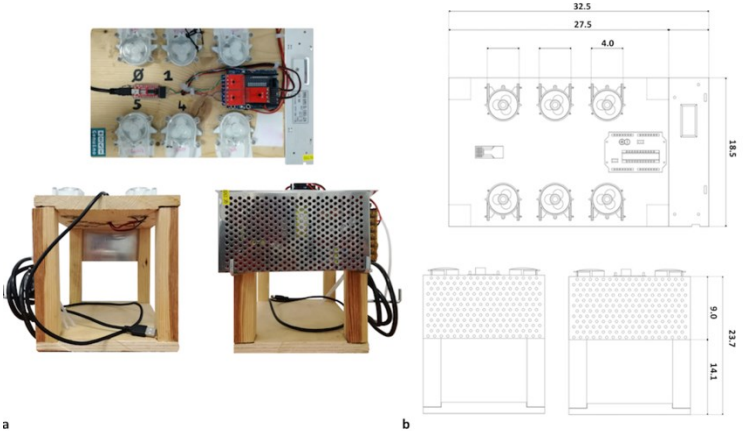

Figure 2: *a) Pictures of our exemplar gustometer; b) actual design with sizes expressed in centimeters.*

The device is designed to be positioned in the console room while tubes and the mouthpiece are the only parts of the device entering in the scanner area. Particularly, the only component that is actually in contact with the subject is the mouthpiece (and the extreme parts of the collected tubes) that should be sterilized after each experiment to ensure safe condition for each subject. The mouthpiece is thought to be hold by subject mouth and is designed to fix separately each of taste-channel lines. The design of the mouthpiece has been developed to ensure the convergence of channels and to avoid a common tube termination. This design decision has been made in order to prevent from fluid contamination, a critical problem that occurs during fMRI experiments that both require single or multiple tastes injection. In fact, in many circumstances, especially for gustatory experiment

requiring several repetitions of taste injection, the volumes feasibly adoptable for rewashing do not guarantee the mouthpiece to be perfectly cleaned. Thus, holding separate channels for tastes until subject mouth ensures that each taste would be clearly and differentially perceived.
The execution of an fMRI experiment with this gustometer supposes the pre-filling of the tubes before the beginning of the acquisition. In this way, during inactivity the surface tensions applied to the two extreme sections of the tubes are equal and this allows to avoid any drip of the fluid (Bernoulli theorem). During stimulation, we consider a fixed delivery time of 600ms, which is the amount of time necessary for the micropump to inject the quantity of taste that, in our experiment, we fixed to 1mL (flow rate = 100mL/min). Considering that the tubes are pre-filled before the fMRI experiment, this time necessary for fluid to arrive to subject's mouth can be considered negligible and does not depend on the length of the tubes and on the distance between the scanner and the gustometer placement.
The device architecture is divided into two main sections: the first one consists of the control and interfacing system with the stimulation computer, the second one is represented by the system of peristaltic pumps for the administration of taste solutions.
The support of this first prototype is realized in wood but it can be realized in PLA using a 3D printer.
In the following figure (Figure 3) is shown the schematic adopted in our device:

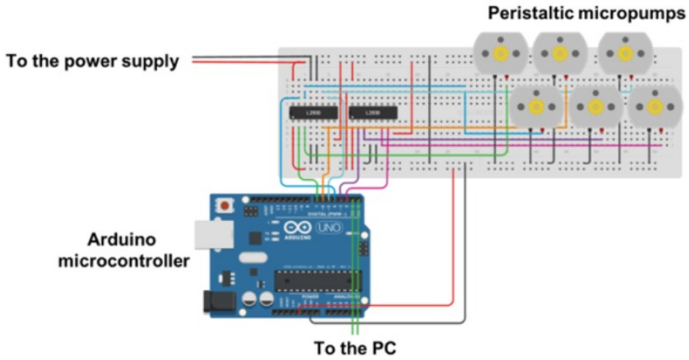

Figure 3: *Schematic adopted in our device: the Arduino microcontroller controls the pumps injection via the controller module and the communication between the stimulation computer and the microcontroller is hosted by a serial interface.*

2.3 The controller module

The control module has been realized with an Arduino-based microcontroller.

Arduino is an open-source computer hardware project for building digital devices and interactive objects that can sense and control objects in the physical and digital world. It allows to develop complex projects in an easy, flexible and cheap manner. The module is connected to the stimulation computer using a serial RS232 port, which allows to receive the commands synchronized with the fMRI acquisition, to start and stop delivery of the solutions.

The software is divided into two sections: the first one concerns the control of the pumps, the second one handles the management of the communication protocol with the stimulus system. The pumps are controlled with an optional standard Arduino interface, an L1191, which allows the Arduino to directly control the DC motor of the pump, thus enable solution delivery.

The motor activation time of peristaltic pumps is linearly proportional to the quantity of administered solutions. To drive the pumps, a software has been created that accepts an integer triad

allowing to parameterize the management of the single pump. The communication protocol is very simple and allows the stimulation computer to communicate easily with the Arduino processor through the R232 serial port. The code consists of three integers representing the pump number, the motor rotation time, the waiting time for operation.
The state machine diagram of the controller module is reported in the following scheme:

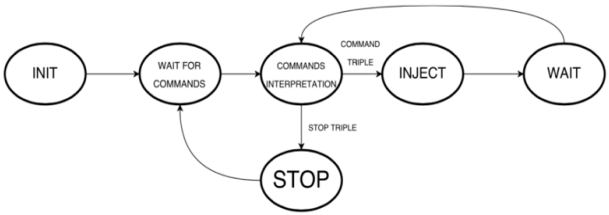

Figure 4 : *State machine diagram of the controller module. The module is programmed to receive (n+1)*3 command triples, where n is the number of injections to perform during the experiment. Each triple encodes the id field that takes information about the pump to be activated, the quantity field which represents the quantity of liquid to inject and the time field that is the time to wait before the next injection.*

Furthermore, it is possible to activate different pumps simultaneously by replacing the first integer (the pump id) with a one-hot encoding scheme that sends one (or more) byte to pilot the corresponding pumps. For example, the string 00000011 will activate the pumps with ids 1 and 2. When the device is switched on, the software waits for the administration protocol of the solutions. The software can handle various modalities to activate the pumps allowing the execution of different experiments. It accepts predefined or random sequences of pump activation, and each pump can be turned on after a fixed time interval, or can be driven directly by the impulse sequence. Moreover, it is possible to set up the amount of delivered solution for each pump independently.

2.4 Peristaltic pumps

One of the core components of the gustometer is the peristaltic micropump. This device is composed by a DC motor, three independently actuated rolls and by a compressible tube ½ meter long. The rolls are located around the center of the external (and closed) chamber of the pump where is also placed the compressible tube laying between the rolls' external and chamber's internal walls. When the DC motor turns the rolls press on the tube thus determining the fluid flow. This tube terminates at one side into fluid tank, that could be both sterilized plastic or glass containers, and is connected to a long (silicone or PVC) tube (terminating to mouthpiece) at the other side. During rotation, the rolls compress the fixed compressible tube thus allowing the fluid to be taken from tank and pumped to subject. The motor angular velocity determines the flow rate of the pumps. The peristaltic pumps can be software-driven to control the solution flow rate, that varies from 1 mL/min to 200 mL/min. The main advantage of the peristaltic micropumps is the possibility to change the hose to adapt the system to different solutions and flow rates. Each pump is connected with sterilized lines that allow the solution flow to reach the subject inside the MRI exam scanner, ending with a disposable mouthpiece.
The number of tubes are equal to the number of peristaltic pumps, thus avoiding fluid contamination during the experiment. The device is connected to the stimulation computer via a USB port. The same computer is also connected to the MR triggering system via another USB port.

2.5 Application of the prototype in a task-based fMRI experiment

2.5.1 Subject and scanner sequence

One healthy, right-handed and not-smoker subject (male, 26 y) was enrolled for this study and the acquisitions were performed at 3T scanner (Magnetom Skyra, Siemens, Erlangen, Germany)

equipped with a 20-channel head coil at the Department of Diagnostic Imaging of the University Hospital "San Giovanni di Dio e Ruggi di Aragona" of Salerno (Italy).
Subject arrived in two separate days in the MR room without eating and drinking (just plain water allowed) for two hours before the scanning with a signed written informed consent.
The acquisition protocol for these experiments included a three-dimensional T1-weighted Magnetization Prepared Rapid Gradient-Echo (MPRAGE) sequence with the following parameters: TR=2400ms, TE=2.26ms, TI=950ms, flip angle= 8°, slice thickness= 1.0 mm, matrix size= 256x256, number of slices =192 and voxel size=1.0 x 1.0 x 1.0 mm^3, a BOLD-fMRI sequence, gradient-echo echo-planar (EPI) imaging acquired with a Multiband ((Feinberg et al., 2010; Moeller et al., 2011; Xu et al., 2013)) factor of 4, TE =30ms, TR = 1000ms, matrix size = 96 x 96, voxel size = 2.5 x 2.5 x 2.5 mm^3, 60 slices, 910 dynamic scans, direction of phase encoding acquisition Anterior-Posterior, and two identical fMRI sequences with opposite phase encoding and 5 dynamic scans for distortion correction (see below).
In the first day, subject performed an experiment based on the perception of the five basic tastes (sweet, bitter, sour, salty, umami), while in the second day an experiment based on the perception of parametrically increasing concentrations of sweet and bitter tastes. The latter experiment consisted on two identical acquisitions, one performed at 9:00 AM and the other at 15:00 PM, and the taste presented were respectively sweet and bitter.

2.5.2 Taste and concentrations

For the first experiment the following concentration setting has been used:

- sweet (sucrose) 220 mM;
- bitter (quinine hydrochloride) 0.05 mM;
- salt (sodium chloride) 96 mM;
- sour (citric acid) 5mM;
- umami (monosodic glutamate) 21 mM.

For the experiment based on five different concentrations, 50mM, 117mM, 245mM, 447mM, 658mM of sucrose for sweet, and 0.06mM, 0.25mM, 0.5mM, 0.75mM, 1.25mM of quinine hydrochloride for bitter were used.
All taste solutions in both the experiments were prepared the day before the MRI acquisition and stored at controlled low temperature (4°C) for the night. Two hours before the scanning they were stored at room temperature (~20°) to keep the same starting condition for all experiments. Solutions were brought to the site of experiment in a polystyrene box and the filling of the tubes were carried out 10 minutes before the starting of the experiments.

2.5.3 Experimental protocol

Synchronization with fMRI acquisitions and stimulus delivery were controlled using Presentation® software. The experimental protocol is described in Figure 5.

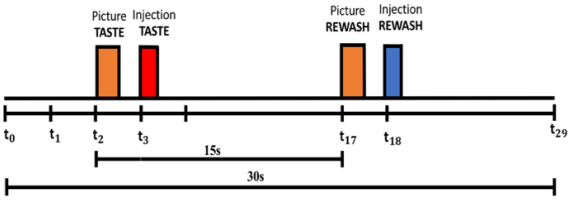

Figure 5: *Experimental protocol based on repetition of injection phases.*

It consisted on an event-related design composed by different injection phases, the blocks containing four different stimuli: two visual cues and two solution deliveries (taste and water for rewash). For each injection phase, the starting time is "t_0" that occurs every 30 TRs. The other events are: taste visual cue (t_2): the word “taste” (white upper case letters, Arial font size 60) was presented on a

video display unit (connected to a back-projection screen in the MRI room) for 800ms; taste-injection (t_3): the pump of the gustometer containing taste was activated for 600ms and one milliliter of solution with a specific taste was delivered in the mouth of the subject; rewash visual cue (t_{17}): the word "rewash" (white upper case letters, Arial font size 60) was presented on a video display unit (connected to a back-projection screen in the MRI room) for 800ms; water-injection (t_{18}): the pump of the gustometer containing water was activated for 600ms .
A single injection phase is repeated five times to deliver all of the tastes/concentrations. This latter block of injection of all the tastes/concentration is repeated six times and during each repetition the order of tastes/concentrations was shuffled. During the experiments, subjects were instructed to swallow immediately after the rapid taste and water injections.

2.5.4 Preprocessing and data analysis

Image data preprocessing and statistical analyses were performed in BrainVoyager, (Brain Innovation, Maastricht, The Netherlands), albeit EPI distortion correction was performed using tool TOPUP (Andersson et al., 2003), which is a part of FMRI Software Library (FSL; http://fsl.fmrib. ox.ac.uk/fsl).
The anatomical T1w images were skull extracted, corrected for spatial intensity inhomogeneity and normalized to the Talairach space. In particular, for the concentration-based experiment, the T1w images of the second scan were aligned to the T1w images of the first scan, and the images of the two runs were then skull extracted, corrected for spatial intensity inhomogeneity and normalized to the Talairach space.
Multi band EPI time-series were corrected for movement artefacts by the re-alignment of all the volumes to the first using Levenberg–Marquardt algorithm, optimizing three translation and three rotation parameters on a resampled version of each image.
Besides being used to correct movement artefacts in the data, the motion parameters were carefully inspected to control that no excessive residual motion was present. The resulting head motion-

corrected time series were also corrected for the different slice scan times using a cubic spline interpolation procedure and then exported from BrainVoyager to NIFTI format for the distortion correction which was performed with the TOPUP tool of FSL. The obtained functional data were imported back to BrainVoyager and filtered in the temporal domain using a high-pass filter with cut-off set to 0.008Hz to reduce linear and non-linear trends in the time courses.

Finally, using the results of the image registration with three-dimensional anatomical scans, the functional image-time series were warped into Talairach space and resampled into 2-mm isotropic voxel time series and then spatial smoothed with a 4 mm gaussian kernel.

Single subject general linear model (GLM) has been performed separately for each study, by including the predictors for tastes/concentrations as predictors of interest while predictor for rewash and the six parameters of motion as confound. Predictors consisted of double-gramma impulse functions at the onset of each stimulus.

In both the taste- and intensity-based experiments, statistical t-maps were computed for each taste and concentrations from the estimated GLM beta weights and residuals.

The statistical threshold was set to p=0.005 false discovery rate (FDR) corrected over the whole slab of imaging.

To assess the sensitivity to the elicited gustatory effects, we performed region of interest (ROI) analyses in the clusters showing activation to tastes and concentration using a one-way ANOVA model for taste-based experiment (five levels) and a two-way ANOVA model for concentration-based experiment (two levels for tastes and five levels for concentration). In the same clusters, to inspect the temporal profiles, we computed the event-related averaged fMRI time-courses.

2.6 Results

Taste-based experiment: The stimulation with all basic taste qualities activated several areas within the gustatory pathway. Regions of activations were localized in the insular cortices but also in other brain regions, as in the pre- and post-central gyrus, in the cingulate cortex, in the caudate nuclei, putamen and in the parietal and temporal cortices.
The peaks of all significant activations with the corresponding Talairach coordinates and the cluster sizes are reported in Table 1.

	Regions	x	y	z	p	Cluster size
Sweet	RH Insula	31	19	14	<0.001	136
	RH postcentral gyrus	59	-19	18	<0.001	733
	RH putamen	25	1	-6	<0.001	334
	RH cuneus	13	-69	10	<0.001	2747
	RH medial frontal gyrus	12	64	0	<0.001	374
	LH cuneus	-13	-65	8	<0.001	348
	LH postcentral gyrus	-56	-23	23	<0.001	407
Bitter	**Regions**	**x**	**y**	**z**	**p**	**Cluster size**
	RH insula	35	17	6	<0.001	520
	RH parahippocampal gyrus	41	-37	-12	<0.001	1064
	RH middle temporal gyrus	41	-51	8	<0.001	736
	RH superior frontal gyrus	33	47	30	<0.001	1168
	RH inferior parietal lobule	43	-43	40	<0.001	1546
	RH Putamen	25	-1	-6	<0.001	1868
	RH medial frontal gyrus	11	-13	64	<0.001	741
	RH precuneus	17	-75	55	<0.001	769
	RH superior frontal gyrus	13	-69	10	<0.001	10813
	RH cuneus	9	-89	25	<0.001	317
	RH posterior cingulate cortex	13	-35	38	<0.001	788
	LH cingulate gyrus	-1	-3	38	<0.001	4902
	RH caudate	7	9	6	<0.001	447

	RH postcentral gyrus	3	-41	61	<0.001	381
	LH superior frontal gyrus	-5	65	28	<0.001	476
	LH caudate	-7	7	10	<0.001	4200
	LH cingulate gyrus	-11	-25	36	<0.001	301
	LH middle frontal gyrus	-25	-7	62	<0.001	705
	LH inferior frontal gyrus	-47	13	27	<0.001	3292
	LH superior frontal gyrus	-23	-39	42	<0.001	325
	LH insula	-33	17	16	<0.001	579
	LH precentral gyrus	-33	31	39	<0.001	598
	LH middle temporal lobe	-45	-61	-10	<0.001	2303
	RH parahippocampal gyrus	41	-37	-12	<0.001	1064
Sour	**Regions**	**x**	**y**	**z**	**p**	**Cluster size**
	RH postcentral gyrus	59	-19	18	<0.001	801
	RH postcentral gyrus	47	-31	34	<0.001	799
	RH insula	37	19	6	<0.001	227
	RH middle temporal gyrus	41	-73	18	<0.001	377
	RH inferior parietal lobule	33	-53	40	<0.001	807
	RH postcentral gyrus	13	-49	70	<0.001	553
	LH cingulate gyrus	-1	-3	38	<0.001	1682
	LH medial frontal gyrus	-11	-21	56	<0.001	602
	LH postcentral gyrus	-23	-47	66	<0.001	551
	LH precuneus	-29	-55	38	<0.001	490
	LH insula	-29	25	2	<0.001	321
	LH fusiform gyrus	-45	-61	-10	<0.001	1847
	LH precentral gyrus	-41	3	26	<0.001	910
Umami	**Regions**	**x**	**y**	**z**	**p**	**Cluster size**
	RH postcentral gyrus	57	-11	16	<0.001	1912
	RH insula	36	19	6	<0.001	233
	RH precentral gyrus	49	-9	-18	<0.001	448
	RH inferior parietal lobule	43	-51	52	<0.001	319
	RH inferior parietal lobule	37	-31	30	<0.001	466
	LH cuneus	-1	-79	6	<0.001	6873
	LH fusiform gyrus	21	1	-6	<0.001	304
	RH posterior cingulate	19	-57	4	<0.001	941
	RH superior parietal lobule	17	-73	58	<0.001	363

	RH medial frontal gyrus	5	-9	56	<0.001	328
	LH postcentral gyrus	-59	-19	22	<0.001	2442
Salty	**Regions**	**x**	**y**	**z**	**p**	**Cluster size**
	RH inferior parietal lobule	61	-35	26	<0.001	2419
	RH postcentral gyrus	59	-19	18	<0.001	1108
	RH postcentral gyrus	47	-31	34	<0.001	687
	RH insula	35	17	6	<0.001	756
	LH cingulate gyrus	-1	-3	38	<0.001	791
	LH caudate	-7	7	10	<0.001	316
	LH fusiform gyrus	-27	-69	-14	<0.001	310
	LH inferior temporal girus	-55	-23	26	<0.001	1383
	RH inferior parietal lobule	61	-35	26	<0.001	2419

Table 1: *Peaks of the main effects of basic tastes, with the statistical threshold set to 0.005 FDR corrected. The reported tastes are respectively sweet, bitter, sour, umami, salty.*

Focusing the attention on the right insular cortex, all tastes activated (partly overlapping) clusters in the anterior insula.
To estimate the sensitivity and size of these effects and to display the temporal profile of the event-related fMRI activation, a region of interest (ROI) was defined as union of these clusters and a ROI-based GLM was estimated. A one-way analysis of variance (1-ANOVA) on the ROI-GLM beta values (considering taste as single factor with five levels) revealed that the effect of taste was statistically significant (p_{taste} <0.001). Maps of activation, the temporal analysis and the mean beta values are reported in the following Figure 6.

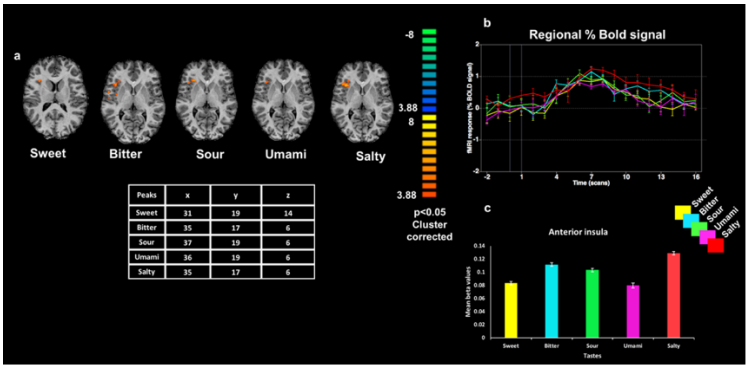

Figure 6: *a) Maps of main effects for individual tastes along the anterior insula cluster, b) event-related averaged time-courses (scaled as % BOLD signal changes from pre-stimulus baseline) to all tastes along the anterior insula cluster, c) a bar graph of the extracted mean ROI beta values (scaled as % BOLD signal changes from).*

More in details, Figure 6a reports the maps of main effects (and the peaks coordinates) for individual tastes along this cluster as well a bar graph (Figure 6c) of the extracted mean ROI beta values (scaled as % BOLD signal changes from baseline as a measure of the effect size). This latter graph shows that, although significant activation was found in all the considered tastes, the highest effect occurs for salty taste. In the same figure, we also report the event-related averaged time-courses (scaled as % BOLD signal changes from pre-stimulus baseline) for the responses to all tastes in the anterior insula cluster (Figure 6b). From this plot, it is possible to observe how, compared to the other tastes, the responses to salty taste are significantly higher specifically after 6-7 seconds from the onset of the 600ms injection.

Intensity-based experiment: The main effects of the different concentrations of sweet and bitter tastes produced a common significant activation in the right middle insula, except for the first concentration of bitter. This latter condition produced a cluster of significant activation in the same middle insula region at a slightly lower statistical threshold ($p = 0.05$ FDR corrected). The peaks of main effects of sweet and bitter tastes across the five concentrations have been presented in Figure 7.

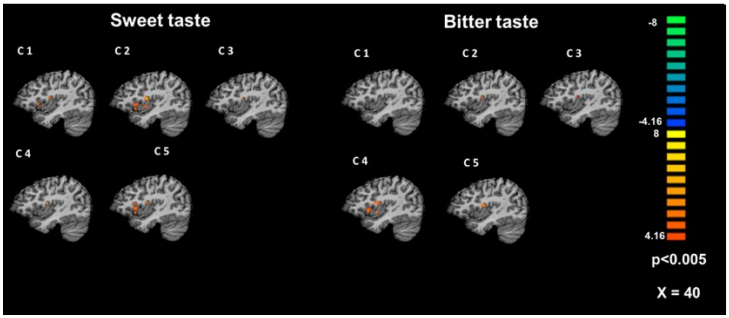

Figure 7: *Maps of main effects in the right insula of sweet (left panel) and bitter (right panel) to the five concentrations with a statistical threshold of p =0.005, FDR corrected.*

In addition, respectively the first, second, fourth and fifth concentrations of sweet and the fourth concentration of bitter activated a cluster in the right anterior insula. In this latter case, the peaks of significant activations are reported in Table 2.

Taste - Concentration	x	y	z	p	Cluster size
Sweet c1	31	15	14	p<0.001	156
Sweet c2	31	15	14	p<0.001	412
Sweet c4	33	15	13	p<0.001	61
Sweet c5	39	17	2	p<0.001	475
Bitter c4	31	15	14	p<0.001	795

Table 2: *Peaks of the main effects in the right anterior insula cluster, obtained in the different concentrations of sweet and bitter tastes, with the statistical threshold set to 0.005, FDR corrected.*

In the common cluster of activation in the middle insula (Figure 8), the ROI-based GLM was estimated and the event-related averaged time-courses is reported in Figure 8b (scaled as % BOLD signal changes from pre-stimulus baseline) and in Figure 8c the trend of the mean beta values as a measure of the effect size.

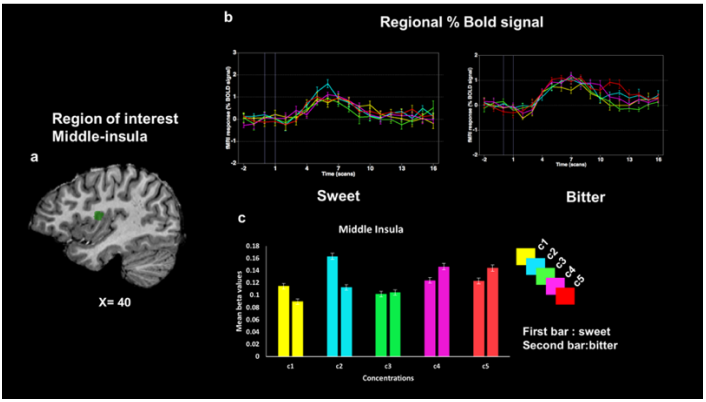

Figure 8 : *a) Cluster of common activation in the right middle insula, b) event-related averaged time-courses (scaled as % BOLD signal changes from pre-stimulus baseline) to all concentrations for sweet and bitter along the common middle insula cluster, c) a bar graph of the extracted mean ROI beta values (scaled as % BOLD signal changes from baseline).*

These latter graphs show that the highest effect occurs for the second concentration for sweet between 4-8seconds, while for bitter the fourth concentration showed the highest activation especially after 8-9s. A two-way ANOVA on the ROI-GLM beta values from this cluster revealed that taste, concentration and interaction effects were statistically significant (p_{taste} =0.04, p_{conc} , $pi_{nteraction}$ <0.001). Activations were also found in the left middle insula and the maps of main effects are reported in the following Figure 9.

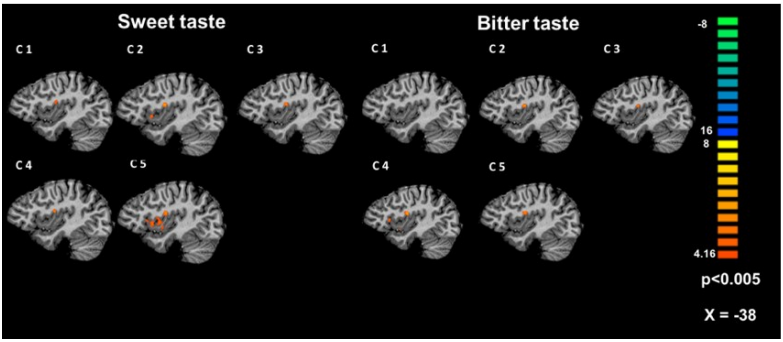

Figure 9 : *Maps of main effects in the left insula of sweet (left panel) and bitter (right panel) to the five concentrations with a statistical threshold of p =0.005, FDR corrected.*

In Figure 10b,c respectively the averaged time courses (scaled as % BOLD signal changes from pre-stimulus baseline) and the mean bar graph over voxels are provided.

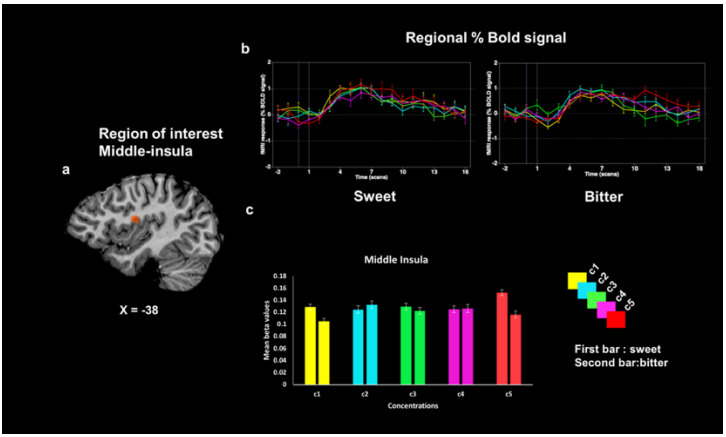

Figure 10: *a) Cluster of common activation in the left middle insula, b) event-related averaged time-courses (scaled as % BOLD signal changes from pre-stimulus baseline) to all concentrations for sweet and bitter along the common middle insula cluster, c) a bar graph of the extracted mean ROI beta values (scaled as % BOLD signal changes from baseline).*

The event-related time-course analysis further confirmed that the highest sweet response was obtained for the fifth concentration of sweet, the difference being significant for the entire post-stimulus interval (as also shown in the bar graph). In contrast, the highest bitter response was obtained for the fifth concentration of bitter only after a delay of 9s from the injection and the start of the perception, whereas the regional analysis of the mean responses did not show a significant difference between concentrations (as shown in the bar graph). In the left middle insula, the 2 way ANOVA on the ROI beta values revealed significant effects of taste, concentration and interaction (respectively p_{taste} =0.001, p_{conc} = 0.04 and $p_{interaction}$ <0.001).
The anterior insula resulted activated from the second and fifth concentrations of sweet and from the fourth concentration of bitter, as shown in Table 3.

Taste - Concentration	x	y	z	p	Cluster size
Sweet c2	-35	11	6	p<0.001	180
Sweet c5	-43	15	0	p<0.001	153
Bitter c4	-35	20	14	p<0.001	168

Table 3 : *Peaks of the main effects in the left anterior insula cluster, obtained in the different concentrations of sweet and bitter tastes, with the statistical threshold set to 0.005, FDR corrected.*

2.7 Discussion

In this chapter, I presented the performances of a novel device for the study of human taste perception.
Besides the full description of the device, which was implemented according to a scalable and open architecture, the results of a pilot single-subject 3 Tesla fMRI study have been provided, in which a working prototype of the device was used to control the injection of either all basic tastes (sweet, bitter, sour, salty and umami) or multiple concentrations of a given taste (sweet or bitter), according to an event-related stimulation paradigm.

Differently from custom hand-made devices (Goto et al., 2015; Haase et al., 2007) mostly based on the use of electronic syringes (as in (O'Doherty et al., 2001) and in (Haase et al., 2007)) or infusion pumps (as in (Sarinopoulos et al., 2006)), the proposed device uses peristaltic micropumps for the injection of small volumes of taste solutions (< 1ml) at a high flow rate (> 1ml/s). As shown by the results, this device is particularly suitable for time-resolved event-related fMRI experiments. In fact, because pumps are connected directly to tanks, a sufficient number of trials could be programmed without the need to break the experiment.

To assess the correct functioning of the device, both the whole brain and regional responses in the insular cortex have been evaluated, to both basic taste qualities and intensities and for both a pleasant taste like sweet and an aversive taste like bitter. The obtained results demonstrate the effectiveness of the device in eliciting significant clusters of fMRI activity in the insular cortex as well as in other regions, among those frequently detected in response to taste stimuli according to recently published neuroimaging meta-analyses (Yeung et al., 2018, 2017). For example, extra-insular activations were found in the pre and post central gyrus, caudate nuclei, putamen, in the cingulate cortex as well as in the temporal and parietal regions.

By focusing the investigation on the insular cortices, which is where the taste perception originates in the cerebral cortex, the temporal profile of the event-related responses to different taste qualities has been further highlighted in a time-resolved manner as well as the sensitivity and effect size of these responses to different concentrations of solutions with opposite affective value.

For example, analyzing the trend of beta values in relation to the different tastes, it could be observed how the perception of the salty taste produced a peak of maximum activation significantly greater than the other tastes after 7-8s delay from the impulsive stimulus, highlighting the importance of monitoring the precise temporal profile of taste-related activation, which is only possible when controlling the delivery of the solutions over small intervals of time

in an even-related design. In the same way, analyzing the trend of beta values in response to different tastes intensities, in the right insula, for example, a significantly different activation for the fifth concentration of bitter after 9-10s from the stimulus injection and for the second concentration of sweet between 4-8 seconds has been obtained.

The temporal profile of insular response after each fast taste injection obtained by the event related averaging analysis shows some time-related differences in taste perception and this latter aspect has been previously and more accurately demonstrated with high temporal resolution electrophysiological studies in both animals and humans where it was established that taste quality- and intensity- related responses occurred with different duration and onset latencies (Crouzet et al., 2015; Kobayakawa et al., 2008; Samuelsen et al., 2012). Thus, the rapid injection ensured by this gustometer in combination with a higher temporal resolution, especially varying the timing of the gustatory stimuli, may allow to evaluate, without affecting taste perception, the dynamic aspects of gustatory activations. However, the event-related analysis proposed here was just focused at analyzing the mean % BOLD signal change of all the activated voxels within the insulae and over a period between the time of the fast taste injection and the time of the rewash event.

When analyzing the activations due to different concentrations of sweet and bitter tastes, it was possible to observe that the scaling of the activations with the intensity may follow different profiles for different taste, e.g. a pleasant and an unpleasant taste, highlighting the potential importance of multi-dimensional paradigms for addressing the cortical processes elicited by taste perception. Particularly, the concentration (intensity) effect found in the middle insula of both the hemispheres nicely resembles the effects reported in previous works of (Small et al., 2003; Yeung et al., 2017). Thus, these illustrative results on a single subject have clearly encouraged the use of the presented device in a complete multi-subject study for the evaluation of both the effects of quality

and intensity of tastants across time and space along the gustatory pathway (in the next chapter, in fact, a study of insula processing during the perception of increasing intensities of sweet and bitter is provided on a group of twenty healthy subjects).
In this regard, it is important to emphasize that all components used for the device are low-cost components. Particularly, these are easily replaceable and especially the lack of valves, seals and glands makes the maintenance of the device comparatively inexpensive. Importantly, the micro-pump based design prevents backflow effects, an important aspect to consider when performing gustatory fMRI experiment to avoid missing injections (missing trials). Another important aspect to consider is that this design ensures no fluid contamination as the only part of the pump in contact with the fluid is the inner part of the tube, which is easy to sterilize, clean or replace.
This is the first implementation with a practical demonstration of a low-cost device that is usable for all kinds of fMRI taste experiments. Particularly, more emphasis is given to the fact that the gustometer is easily portable (e.g. from an fMRI site to a lab for off-line tests or to another fMRI site) and easily replicable by other researchers, and therefore especially suitable for multi-center fMRI studies. Furthermore, the scalability of the design and the low-cost nature of the materials will possibly boost the experimental design of more complex multi-dimensional studies of the taste pathway.
The architecture of the working device presented here was made up of six channels only, which was enough for guaranteeing the parallel and independent injections of all known basic tastes. However, the expandability of the number of channels is made possible in the presented architecture by adding and easily interfacing more microcontroller modules.
In summary, the main advantages of this realized device architecture are: (i) versatility: this gustometer supports different stimulation protocols that can vary in flow rates and injection times; (ii) open architecture/open source: the gustometer has been designed and developed with open architecture hardware

components and open source software tools; (iii) expandability: this system is based on a flexible architecture and therefore additional modules can be easily developed (e.g. a Bluetooth wireless communication module); (iv) cost-effectiveness: the device is realized with cost-effective components (peristaltic pumps, Arduino Uno microcontroller, driver and materials for the support).

For what concerns the settings, the volume of each injection and the injection rate are easily programmable by the user. Thus, this gustometer would allow implementing both block design and event-related protocols in time-resolved fMRI experiments, in the latter case allowing to inject small volumes (down to 1 milliliter of solution) in small intervals of time (600 milliseconds), thus producing an almost ideal series of impulsive taste stimuli at conventional repetition times (1-2 seconds) used in fMRI experiments. The flexibility of the system also allows interfacing the device with any stimulation paradigm and with other devices such as response recording systems or other stimulation systems. In addition, as this gustometer is completely adaptable and open-source, it is possible to use it for real-time fMRI to implement a continuous neurofeedback stimulation or within a BCI designed to translate taste perception into specific (re)actions. For example, in the development of novel treatment strategies, using the neural activity from extra-insular regions to directly control the gustatory stimulation may gather an obvious neurofeedback paradigm to up- or down-regulate the taste perception in subjects with eating disorders who have been recently shown to display abnormal levels of insular activations in response to bitter and sweet stimuli (Monteleone et al., 2017).

Last, the peristaltic micropumps used for this gustometer work in a low-pressure regime. However, because of the miniaturized nature of our device, it can be easily moved at any heights the user needed and this peculiarity makes our gustometer particularly feasible for any subject position, for example in upright position for MEG, fNIRs, EEG or response time studies.

Chapter 3:

Intensity related distribution of sweet and bitter taste fMRI responses in the insular cortex

3.1 Introduction

The human gustatory system is evolutionary organized to analyze and code the tastants, based on their chemo- and somato-sensory features, as well as their hedonic properties, to promptly determine whether the carrier substances should be ingested, because of their energetic or nutritive content, or, rather, avoided and rejected, due to possible contamination and potential poisoning effects (Gutierrez and Simon, 2011; Jezzini et al., 2013; Yeomans, 1998). It is well established that humans can discriminate at least five basic tastes (sweet, bitter, sour, salty and umami), and that the quality of a taste is assigned with an hedonic value determining selective behaviors (Wang et al., 2018). However, during the processing of taste features, the gustatory system also needs to distinguish the intensity (or concentration) of a given tastant. In fact, when increasing or decreasing the intensity of a tastant, the expected ingested quantity of the substance may possibly change the predictable consequences of the ingestion itself. Thereby, the intensity information should be also analyzed by the gustatory system and eventually coded during taste perception (Scott, 2004). The cortical processes underling the intensity-related perception of taste have been scarcely investigated in humans. Particularly, a

detailed spatial pattern of intensity-related activations within the human insular cortex in response to parametrically varied intensities of a taste stimulus, is currently lacking in the literature and some relevant inconsistencies were noted among previous reports. For example, among previous human studies using fMRI with taste stimulation, the most recent work by Dalenberg et al. (Dalenberg et al., 2015) has provided a detailed factorial analysis of the insular responses to taste quality, concentration and affective valence, demonstrating that the left insula is more specialized for detecting the quality of a tastant and its affective valence, independently of the concentration, whereas the right insula, and particularly in the dysgranular anterior part of it, is more sensitive to intensity variations albeit according to a non-linear response. However, for the latter observation, no further details and no definitive interpretation were provided.

Moreover, a recent pilot study (Prinster et al., 2017) has suggested the possibility that the right insular cortex, while not being necessarily specialized for detecting the quality of each basic tastant, may still exhibit a different spatial distribution of neural activation in relation to the perceived quality of a tastant, albeit the possible modulating effect of concentration was not investigated. In addition, the lateralized specialization of the right hemisphere for the concentration-related processing was also partly inconsistent with two previous studies, respectively from Small et al (Small et al., 2003) and Spetter et al (Spetter et al., 2010), reporting evidence that (i) both the left and right middle insula regions can be sensitive to taste intensity (irrespective of valence) (Small et al., 2003), and (ii) the bilateral middle insula activation linearly increases across four different concentrations (Spetter et al., 2010), whereas the findings in (Dalenberg et al., 2015) highlighted a non-linear (quadratic) trend of the functional activity in the right insula in response to the varying concentrations. On the other hand, some electrophysiological studies have been performed in animals, analyzing the neuronal firing rates in the insula after the injection of tastes at different concentrations, which reported both

monotonically increasing (Scott et al., 1991) and far more complex (non-linear) changes (Stapleton et al., 2006) of firing rates with the intensity of taste.
To possibly shed more light about the effects of taste intensity on the neural activity within the human insular cortex, the aim of the present study was to analyze and report the detailed spatial distribution of neural activity elicited by the perception of five different concentrations by using fMRI in twenty normal subjects. Similar to (Small et al., 2003), we administered two tastes with opposite valence (sweet and bitter). Similar to (Dalenberg et al., 2015), we used five different concentrations of each tastant, which were carefully chosen after preliminary off-line tests on a separate cohort of subjects in such a way that, besides the correct detection of the expected quality and valence, all parametrically increased concentrations were reported as linearly increasing intensity of taste perception during random injections. To maximally reduce the duration of the tasting phase and to minimize the impact of tongue movements during taste perception (Marciani et al., 2006), an event-related stimulation paradigm was designed by relying on the rapid injection (600ms) of small volumes (1mL) of tastants. Moreover, to maximally preserve the intrinsic spatial resolution of the original fMRI data in determining the cortical distribution of intensity-related taste activations, no spatial smoothing was applied to the fMRI images and a high resolution cortical registration method was applied to maximize the spatial correspondence of the insular cortex across all individual brains.

3.2 Materials and Methods

3.2.1 Participants

Twenty-four healthy adult volunteers (mean age ± standard deviation = 24 ± 3 y) were enrolled in this study on the basis of a written informed consent. Participation was in accordance with the requirements of the local ethical committee at the University

Hospital “San Giovanni Di Dio e Ruggi di Aragona” of Salerno. Included participants were right handed, non-smoker and without any history of taste, smell, neurological and psychiatric disorders. Participants using any form of medication that possibly affected taste perception (i.e. gastrointestinal complaints, dry mouth, nausea, and taste disturbance) were not enrolled in the study. Participants were instructed not to eat or drink during 2 hours prior to the scanning session (only plain water allowed). The eating behavior of each participant was assessed with the “Predimed test” (Martınez-Gonzalez et al., 2012).

3.2.2 Experimental Procedure

In a preliminary offline study, we enrolled a sample of thirteen young healthy subjects (mean age ± standard deviation = 25 ± 6 y) to perform a visual assessment score (VAS) test in order to choose an optimal set of increasing concentrations. This test was organized as two separate sessions for sweet and bitter tastes. In each session, each subject received 1 mL of tastant with a concentration randomly chosen among eight prepared concentrations followed by 1mL of water for rewash. After injection, the subject was asked to give a score between 0 mm (very low perceived intensity) to 10 mm (very high perceived intensity) on the basis of the following question “How strong do you feel the taste?”. The injection of all the concentrations was performed with the home-made gustometer described in Chapter 2 (Canna et al., 2018), and each concentration was presented twice. For each repetition, the order of the concentrations was randomly shuffled.
The starting sets of solutions (prepared in water) included 50mM, 60mM, 117mM, 245mM, 447mM, 658mM, 800mM, 976mM of sucrose for the sweet taste and 0.05mM, 0.06mM, 0.12mM, 0.25mM, 0.50mM, 0.75mM, 1.00mM, 1.25mM of quinine hydrochloride for the bitter taste. To establish the final set of five concentrations for the fMRI experiment, for each taste separately, a 2w-ANOVA model was defined using concentration and repetition as within-subject factors and post-hoc pair-wise

comparisons were performed to discard those consecutive concentrations that did not yield a significant difference in the intensity perception ($p>0.05$).
The taste solutions for both the offline and MRI acquisition were prepared the day before the examinations and stored at controlled low temperature (4°C) for the night. Two hours before the scanning, they were stored in normal temperature (~20°) to keep the same starting condition for all the subjects. Solutions were brought to the site of experiment in a polystyrene box and the filling of the tubes for all the experiments were carried out 10 minutes before starting the acquisitions.
All subjects enrolled for the fMRI experiment were also asked to rate the selected intensities in an off-line test using the same VAS. The off-line test was performed the day before the fMRI scan but with the same gustometer (Canna et al., 2018) used in the fMRI acquisition, albeit only one repetition of the stimuli was presented.

3.2.3 MRI data acquisition

MRI image data sets were acquired on a 3T MRI scanner (MAGNETOM Skyra, Siemens, Erlangen Germany) equipped with a 20-channel RF receive head coil. The imaging protocol consists of two identical fMRI sessions, the first of which was performed during the morning (between 9:00 and 12:00 AM) and the other during the afternoon (between 15:00 and 18:00 PM). During the first session, we used sweet taste solutions while in the second session we used bitter taste (more detailed are provided below). Each session included a 3D anatomical T1weighted Magnetization Prepared RApid Gradient Echo (MPRAGE) sequence with TR/TE = 2400/2.25ms, resolution = 1mm isotropic, matrix size = 256 × 256, 192 slices, a gradient-echo echo-planar imaging (GRE-EPI) with a multi-band (MB) factor of 4 (MB-EPI (Feinberg et al., 2010; Moeller et al., 2011; Xu et al., 2013)), TE = 30ms, TR = 1000ms, matrix size = 96 x 96, voxel size = 2.5 x 2.5 x 2.5 mm^3, 60 slices, 910 dynamic scans, direction of phase encoding acquisition Anterior-Posterior. The same GRE-EPI series

was repeated two more times with only 5 dynamic scans and opposite (Anterior- Posterior, Posterior-Anterior) phase encoding directions for the purpose to correct GRE-EPI image distortions (Andersson et al., 2003; Smith et al., 2004). Each scanning session was 20 minutes long: 15 minutes for functional acquisition, 5 minutes for anatomical acquisition.
Synchronization between fMRI acquisition and stimulus delivery was controlled using Presentation® software (Neurobehavioral Systems, Inc., Berkeley, CA, www.neurobs.com).
Our stimulation protocol has been designed as a time-resolved event related protocol, during which we injected 1mL of taste in 600ms, as previously described in Chapter 2 (Figure 5).

3.2.4 MRI data processing

Image data preparation, (part of) preprocessing and statistical analysis were performed in BrainVoyager, (Brain Innovation, Maastricht, The Netherlands, www.brainvoyager.com). GRE-EPI image distortion correction was performed using the tool TOPUP (Andersson et al., 2003) from the FMRI Software Library (FSL; http://fsl.fmrib. ox.ac.uk/fsl). Additional analyses were performed using custom scripts written in MATLAB R2016a (The MathWorks Inc., Natick, MA, USA, www.themathworks.com).
For each individual subject, the anatomical T1w images of the first and second sessions were skull stripped and corrected for intensity inhomogeneities. The T1w images from the first scan were transformed to Talairach space. The T1w images from the second scan were aligned to the AC-PC transformed T1w images of the first scan via a 6-parameter affine transformation and then the same Talairach transformation was applied. In Talairach space, the images of the two scans were averaged, yielding an anatomical image with higher signal to noise. The average T1w image was then used for segmentation and cortical surface reconstruction, yielding the initial surface meshes for the cortex-based alignment (CBA) procedure (Frost and Goebel, 2012).

In order to perform a cortex-based data analysis, the gray/white matter boundary was segmented using the automatic region-growing methods based on the analysis of intensity histogram, as implemented in BrainVoyager. Morphological operations were used to smooth the borders of the segmented data and to separate the left from the right hemisphere. The obtained segmented hemispheres were then submitted to a “bridge removal” procedure, which ensures the reconstruction of maximally topologically correct mesh representations (Kriegeskorte and Goebel, 2001). Segmented images were also carefully inspected, and, when needed, manually corrected to avoid residual topological errors and further improve mesh reconstructions. The borders of the segmented hemispheres were tessellated along the border to produce a (folded) surface mesh of each hemisphere which was morphed to an inflated mesh while keeping the link to the original reference (folded) mesh and to guarantee the correct localization of functional data. We used all default parameter settings of the CBA procedure and, particularly, chose the "moving target" approach, according to which, all individual brains are iteratively aligned to a dynamically updated average brain only based on the cortical folding patterns. A folding pattern represents the alternation of gyri and sulci of the brains and can be quantitatively assessed by calculating the curvature values from the shape analysis of the surface mesh. During the CBA procedure, the algorithm essentially aligns as much as possible corresponding gyri and sulci among individual brains with the result of reducing the anatomical inter-subject variability (Frost et al., 2014; Frost and Goebel, 2012; Goebel et al., 2006). The CBA procedure is identically repeated for each separate hemisphere, allowing the mapping of the individual cortical surface mesh vertices to an average cortical surface mesh.

3.2.5 FMRI data processing

MB-EPI time series from both sessions were corrected for the different slice scan acquisition times using a cubic spline interpolation procedure and for movement artefacts by a rigid re-alignment of all the volumes to the first volume based on a Levenberg–Marquardt algorithm, optimizing three translation and three rotation parameters on a resampled version of each image. The estimated motion parameters were carefully inspected to control that no excessive residual motion was present (more than 2 pixel size in head translation or more than 2 degree in head rotation). The head motion-corrected time series were then exported to NIFTI image format for the GRE-EPI distortion correction which was performed with the TOPUP tool of FSL (Andersson et al., 2003; Smith et al., 2004). Last, the fMRI time-series were filtered in the temporal domain using a high-pass filter with cut-off set to 0.008Hz to reduce linear and non-linear trends in the time-courses and then all images were transformed to Talairach space (with resampling to 2 mm isotropic voxels). The folded cortex meshes were used to sample the functional data at each vertex resulting in one mesh time course data set for each scan and each subject.

In order to focus the fMRI data analysis on the insular cortex, two 1 mm resolution volume masks covering the left and right insulae were imported in Talairach space from the Harvard Oxford atlas (originally available in the Montreal Neurological Institute (MNI) space from the FSL). The volume masks were projected from the volume space to the target brain mesh resulting in two cortical patches of interest (POI) on this mesh. To ensure that no insular regions were missing in the projection, a slight dilation of 3 vertices was applied to each POI.

The first and second level analyses were performed separately for the left and right insular POIs. For the first level analysis, a single study deconvolution-based GLM was applied to the mesh time-courses with “stick” predictors defined over each interval of 13 s

(corresponding to 13 time points) from the time of injection. In this way, we defined 13 predictors of interest for each concentration of each tastant covering the taste perception response phase (before the injection of plain water for rewashing). Additional predictors (of no interest) were added to the GLM to model the responses during the rewash phase. The six motion parameters were also added in the GLM model as confound predictors. A correction for serial correlation was applied using fit-refit procedure with a second-order auto-regressive model applied to the GLM residuals. Z-transformation was applied to the time courses before the GLM fitting. For the second-level analysis, a random-effects (RFX) GLM was applied and the main effects of all five predictors corresponding to the five delays between 4s and 8s (i.e. around the expected peak of the BOLD response) were combined into one single contrast per concentration and per taste, and mapped onto the target mesh. A 2w-ANOVA was also performed, considering taste and concentration as within-subject factors with respectively two (sweet, bitter) and five (all concentrations) levels. A statistical threshold was applied to the F- and t- maps, which protected against false-positive clusters at 5% (cluster- level corrected for multiple comparisons over the mesh after 1000 Montecarlo simulations (Forman et al., 1995).

The image contrasts extracted from the RFX-GLM analyses of all concentrations and tastes were also used to determine group-level preference maps (Prinster et al., 2017). Group-level preference maps were obtained separately for the two tastes (and hemispheres) by assigning a different color code to each activated vertex according to the condition (concentration) yielding the highest contrast: blue (first concentration), light blue (second concentration), green (third concentration), yellow (fourth concentration) and red (fifth concentration). Taste preference maps were also obtained for each individual subject (and hemisphere) using a custom made MATLAB script. Namely, the 10 contrast maps (five concentrations of two tastes) were extracted from first level GLM analysis, masked with the cortical POI and spatially

normalized over the POI using z-transformation. For a vertex by vertex preference analysis, the five z-scores (per taste condition) were first ranked and the concentration corresponded to the first rank was assigned to the corresponding vertex. Preference maps of each subject were also spatially correlated with the group-level preference map using Spearman correlations (Prinster et al., 2017).

3.3 Results

Figure 11 shows the trends of VAS scores across eight preliminary chosen concentrations for sweet (a) and bitter (b) tastes. For both sweet and bitter tastes, the intensity perceived by the group of subjects clearly exhibit an increasing trend that appears saturated at the highest concentrations.

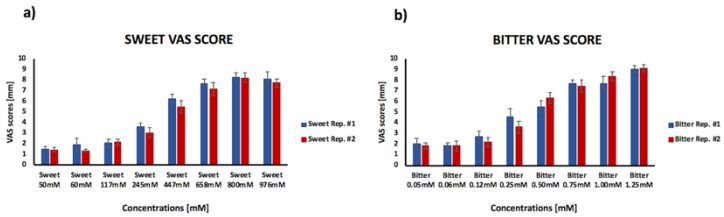

Figure 11: Trend of VAS scores for sweet (a) and bitter (b) for each of the two repetitions of taste injection during the offline test.

Thereby, from the initial set of these eight concentrations, the following five concentrations were chosen for the fMRI experiments: sweet 50mM, 117mM, 245mM, 447mM, 658mM and for bitter 0.06mM, 0.25mM, 0.50mM, 0.75mM, 1.25mM. The t and p-values of the significant statistical tests for the pair-wise comparisons of consecutive concentrations are reported in Table 4 a and b.

	Concentrations	t(25)	p
Sweet concentrations	1-3	2.45	0.02
	3-4	3.41	0.001
	4-5	5.4	<0.001
	5-6	3.16	0.003

Table 4a: *Results from the offline VAS test with sweet taste reporting the significant effects of concentrations.*

	Concentrations	t(25)	p
Bitter concentrations	2-4	4.36	<0.001
	4-5	3.19	0.002
	5-6	3.28	0.002
	6-8	3.86	<0.001

Table 4b: *Results from the offline VAS test with bitter taste reporting the significant effects of concentrations.*

Four of the twenty-four subjects were excluded from the image analysis because of excessive movements during fMRI scanning. Table 5 summarizes the demographic characteristics of our subjects.

Age (mean ± standard deviation)	BMI (mean ± standard deviation)	Sex	Predimed Results (mean ± standard deviation)
24 ± 3	24 ± 2.6	11 M, 9 F	7.5 ± 1.5

Table 5: Demographic characteristics of the subjects considered in the fMRI data analysis.

Figure 12 shows the correlations between the group-averaged intensity ratings and the concentrations used in the fMRI experiment. For both tastes, this correlation was statistically significant (sweet: p=0.004, bitter: p=0.002).

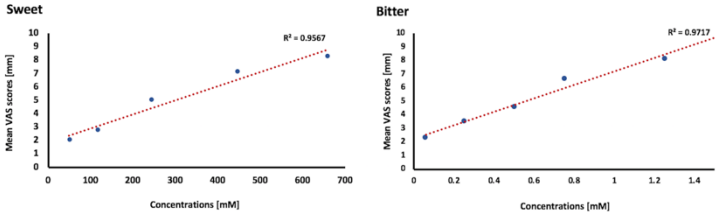

Figure 12 : *Correlation between mean subjective intensity ratings (VAS) and concentration values for sweet and bitter tastes, performed on the group of enrolled subjects for the fMRI experiment.*

When jointly modeling taste quality and concentration (2w-ANOVA) in the right hemisphere, we did not obtain statistically significant effects of either taste or concentration factors. The analysis of the main effects of taste at each separate concentration (1w- ANOVA) within the right insular cortex revealed the presence of three compact clusters located in the anterior, middle- posterior and inferior insula (Figure 13, first row).
However, when displaying the contrasts across different concentrations, the extensions of these clusters were dramatically reduced for the intermediate concentration for both tastes (Figure 13, second and third rows).

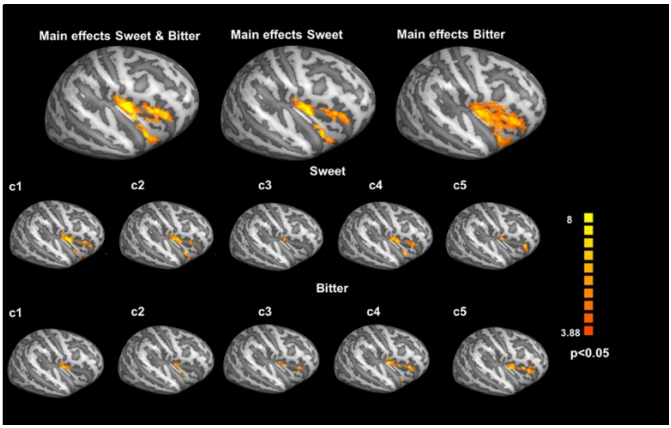

Figure 13: *Main effects of sweet and bitter tastes at all delays between 4 and 8 s from injection. The maps represent the main effect to tastes taken together and separately (first row) and to the concentrations taken separately (second and third rows).*

From the 2w- ANOVA analysis in the left hemisphere we did not obtain statistically significant effects of taste but the concentration factor produced a cluster of statistically significant effect within the anterior-middle insula, as shown in (Figure 14).

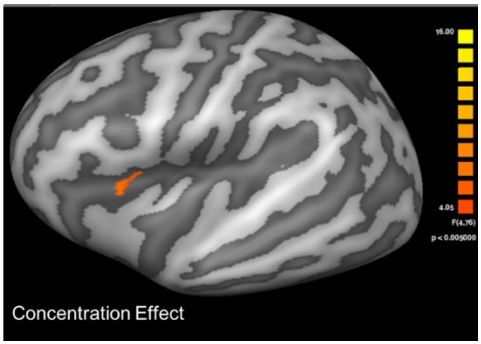

Figure 14: *Effect of concentration obtained by the 2w-ANCOVA analysis in the left insula, p<0.05 cluster corrected using Monte Carlo simulations (cluster threshold forming p=0.005).*

After extracting the mean regional beta values, a post-hoc analysis using two-sample Student t-test revealed that for sweet taste, a significant difference occurs between the second and third concentrations (p=0.002) and between the third and fourth concentrations (p=0.01) while for bitter taste a significantly difference between the third and fourth concentration (p=0.003).

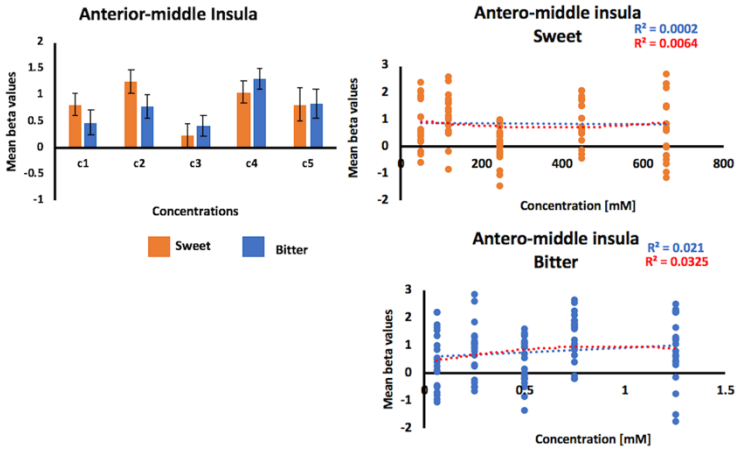

Figure 15: *Left side: bar-graph with standard errors of the mean beta values in the left antero-middle insula. Right side: mean beta values for each subjects for sweet and for bitter tastes with corresponding polynomial fitting curves and R-square (blue : first order, red : second order).*

In Figure 15, it is reported the bar graph (with standard errors) of the mean beta of both sweet and bitter values in the cluster resulted significant from the ANOVA test. In the same figure, the mean beta values for each subject and the linear and quadratic fits (with R^2) are provided. For both sweet and bitter tastes, no significant linear and quadratic trends were found ($p > 0.05$).

The separate analysis of the main effects of taste in the left insula produced two compact clusters of activation in the anterior and middle insula. When analyzing the main effects for separate

concentrations, while for sweet taste two clusters resulted significant for all concentrations except for the third, for bitter taste two clusters resulted significantly activated for the second, third and fourth concentrations, while the first concentration activated only one cluster in the middle insula and the fifth concentration only one cluster in the anterior insula. These maps are reported in Figure 16.

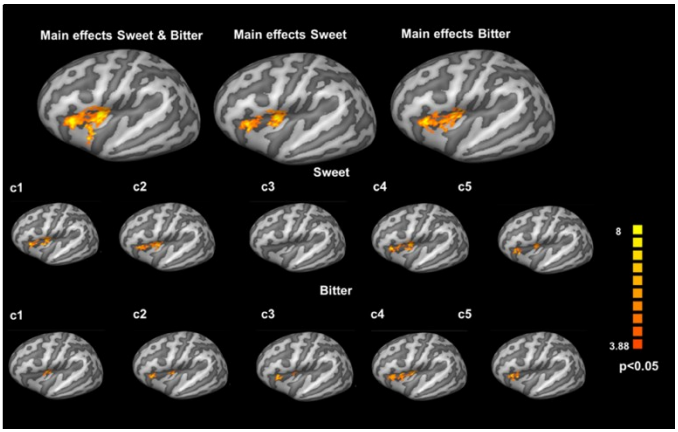

Figure 16: *Main effects in the left insula of sweet and bitter tastes at all delays between 4 and 8 s from injection. The maps represent the main effect to tastes taken together and separately (first row) and to the concentrations taken separately (second and third rows).*

To descriptively assess the continuous spatial distribution of the insular activation across all concentrations, group-level preference maps were calculated to represent the "preferred" taste intensity within and across all the above reported clusters, as shown in Figure 17.

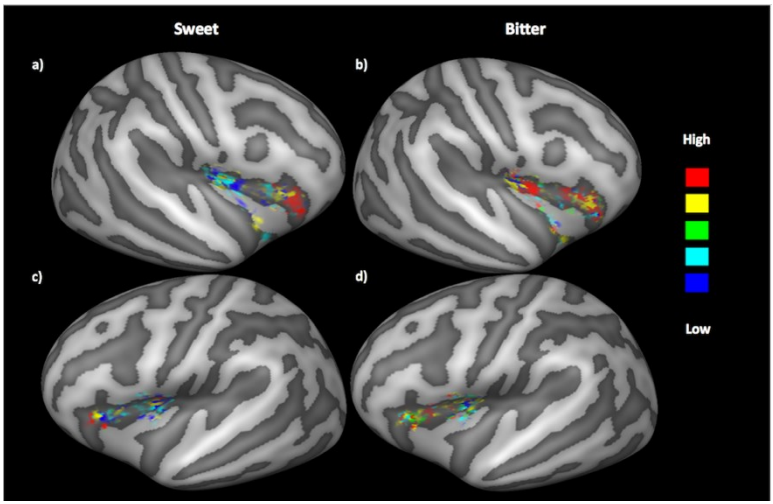

Figure 17: *Group-based preference maps in the right (a, b) and left (c, d) insulae of sweet (left column) and bitter (right column) tastes, represented in the regions of main effects.*

In the right insula, for the sweet taste (Figure 17a), the spatial change in the preferred concentration suggests the presence of an anterior-posterior spatial gradient for the high-to-low concentrations extending from the anterior cluster (higher concentrations preferred) towards the middle-posterior cluster (lower concentrations preferred), whereas the cluster in the inferior part of the right insula exhibits two sub-clusters with co-existing equal preference for a high (fourth) and a low (second) intermediate concentration. For the bitter taste (Figure 17b), the higher concentrations appear more represented across all three clusters of the right insula, although some preference for the second concentration is visible in the middle-posterior cluster and between the middle-posterior and inferior part of the insular cortex. In the left insula, for sweet taste (Figure 17c), the lower concentrations appear more represented across all two clusters with significant main effects, although an anterior-posterior spatial gradient for high-to-low concentrations is visible within the anterior cluster. For the bitter taste (Figure 17d), an anterior-poster spatial gradient for

high-to-low concentrations is observed from the anterior to the middle cluster of the left insula.

In order to assess how much information from the above spatial patterns was actually present in the single subjects, single-subject preference maps were also generated (from the first-level GLM fits). The individual preference maps of four representative subjects are shown in Figure 18 and Figure 19 for the right insula and in Figure 20 and Figure 21 for the left insula. Respectively, the tastes represented in these figures are sweet and bitter over the entire insular POIs (with the black border of the above group-level clusters drawn on the mesh).

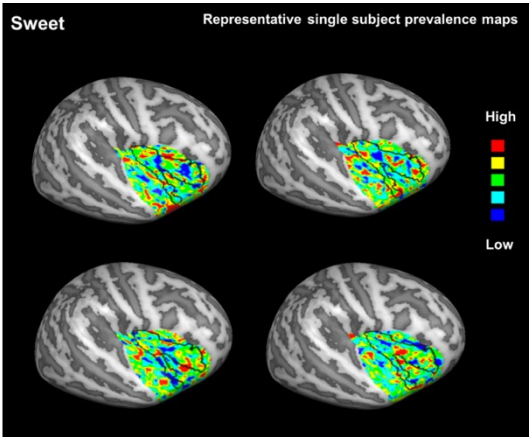

Figure 18: *Representative individual preference maps of the spatial distribution of best representative concentrations for sweet taste in the right insula.*

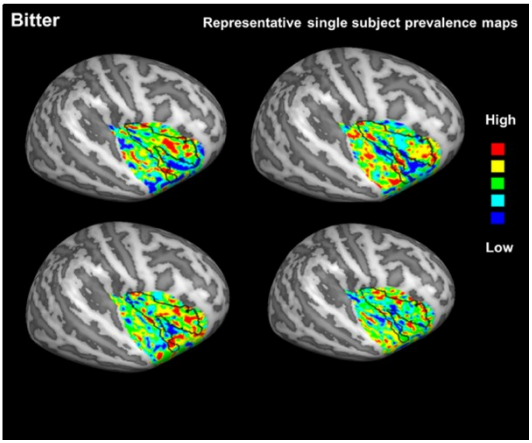

Figure 19: *Representative individual preference maps of the spatial distribution of best representative concentrations for bitter taste in the right insula.*

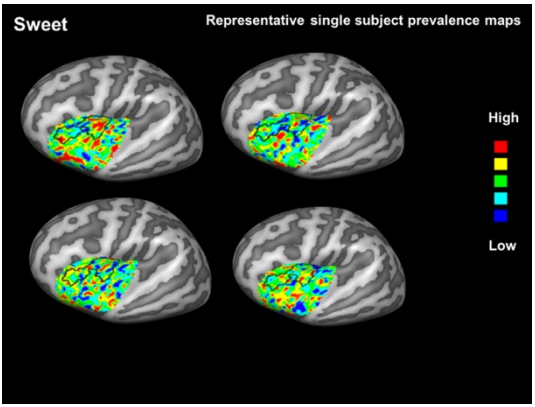

Figure 20: *Representative individual preference maps of the spatial distribution of best representative concentrations for sweet taste in the left insula.*

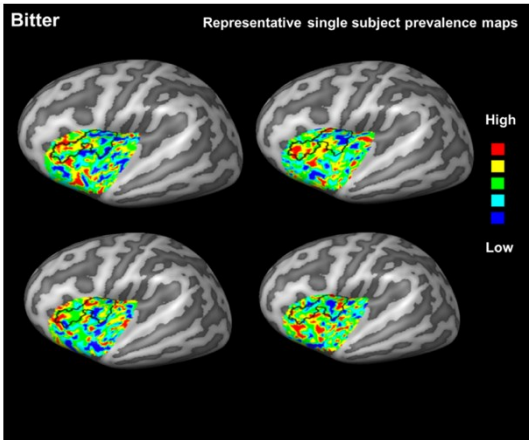

Figure 21: *Representative individual preference maps of the spatial distribution of best representative concentrations for bitter taste in the left insula.*

To quantify the adherence of all single subject to the group preference pattern, the spatial correlation coefficient (Spearman correlation) between each individual preference map and the group-level preference map is reported for all subjects in Table 6 and in Table 7 (respectively for right and left insula) and this data shows that at least 80% of subjects exhibited a significantly positive spatial correlation ($p<0.05$) in both hemispheres.

Subjects	Sweet		Bitter	
	rho	p	R	rho
1	0.10	<0.001	1	0.10
2	0.01	0.52	2	0.01
3	0.11	<0.001	3	0.11
4	0.12	<0.001	4	0.12
5	0.05	<0.001	5	0.05
6	0.08	<0.001	6	0.08
7	0.11	<0.001	7	0.11
8	0.10	<0.001	8	0.10
9	0.18	<0.001	9	0.18
10	0.13	<0.001	10	0.13
11	0.16	<0.001	11	0.16
12	0.18	<0.001	12	0.18
13	0.12	<0.001	13	0.12
14	0.07	<0.001	14	0.07
15	0.16	<0.001	15	0.16
16	0.11	<0.001	16	0.11
17	0.13	<0.001	17	0.13
18	0.06	<0.001	18	0.06
19	0.17	<0.001	19	0.17
20	-0.02	0.17	20	-0.02

Table 6 : *Spearman spatial correlation between each individual preference map and the group-level preference map in the right insula.*

Subjects	Sweet		Bitter	
	rho	p	R	rho
1	0.02	0.31	1	0.02
2	-0.03	0.09	2	-0.03
3	0.04	0.01	3	0.04
4	0.04	0.02	4	0.04
5	-0.01	0.41	5	-0.01
6	0.13	<0.001	6	0.13
7	0.10	<0.001	7	0.10
8	0.08	<0.001	8	0.08
9	0.12	<0.001	9	0.12
10	0.07	<0.001	10	0.07
11	0.09	<0.001	11	0.09
12	0.13	<0.001	12	0.13
13	0.18	<0.001	13	0.18
14	0.11	<0.001	14	0.11
15	0.12	<0.001	15	0.12
16	0.11	<0.001	16	0.11
17	0.14	<0.001	17	0.14
18	0.03	0.07	18	0.03
19	0.06	<0.001	19	0.06
20	0.07	<0.001	20	0.07

Table 7: *Spearman spatial correlation between each individual preference map and the group-level preference map in the left insula.*

3.4 Discussion

In this chapter, by using fMRI, we have analyzed the cortical processes elicited by the perception of five parametrically increasing intensities of a pleasant (sweet) and an unpleasant (bitter) taste stimulus in the human insular cortex. This experiment principally aimed at disclosing whether the insular cortex includes clusters with a robust specialization for the intensity processing of these tastants, and whether a spatial gradient of preference exists among the insular responses to the varying intensity of the taste perception. To maximize the spatial information in the cortical responses, we acquired 3 Tesla fMRI data at relatively high spatial resolution (2.5mm isotropic) and avoided any spatial smoothing. Moreover, we used a high resolution cortical registration method to improve the anatomical correspondence across individual cortices (Prinster et al., 2017). To the best of our knowledge, no previous studies reported the detailed spatial distribution of taste intensity responses in the insular cortex. Here we found that (i) the left, but not the right, insular cortex includes a compact specialized cluster for processing taste intensities independently of the quality and valence of the tastant; (ii) the spatial distribution of the highest responses across the main effects of the insular activation delineate an anterior-posterior spatial gradient for high-to-low concentrations according to the "preferred" concentration.

All the insular regions activated during taste perception were perfectly overlapping with those reported in two recent meta-analyses of taste perception in humans (Yeung et al., 2017) and (Yeung et al., 2018) covering several gustatory fMRI studies based on the injection of basic taste solutions to healthy subjects. However, when assessing the main effects at some specific concentrations, some of the clusters were reduced or disappeared depending on the intensity of the tastant, suggesting the presence of intensity-related effects in the activation patterns. For example, the anterior and middle-posterior clusters of the right insula were found activated by all single concentrations except for the third (intermediate) concentration of the sweet tastant, suggesting that (i) a non-linear relationship is likely to exist between concentration

and neural activation in some clusters and (ii) a spatial gradient of "preference" might exist in the spatial distribution of the insular responses to the taste concentration.
To possibly isolate the presence of compact clusters with taste or intensity specialization, a full factorial (2 taste x 5 concentrations) analysis was performed. From this analysis, one specialized cluster for the processing of taste intensity was obtained in the antero-middle part of the left insula, whereas no quality or intensity-by-quality interaction effects were detected in both the right and left insula.
The lack of specialized effects for taste quality, in both the left and right hemispheres, could be possibly ascribed to the use of small acquisition voxels and unsmoothed data which might have reduced the sensitivity of our analysis, in favor of a possibly higher specificity of the preference analysis. Future works using ultra-high field fMRI are needed to increase the contrast-to-noise of the analysis without sacrificing the specificity of the spatial analysis.
The finding of a significant effect of taste intensity in the left insular cortex is only apparently contrasting with the finding of (Dalenberg et al., 2015) of a right insula more specialized for taste intensity processing (and a left insula more specialized for taste quality processing). On the other hand, the factorial modeling in (Dalenberg et al., 2015) was performed on the first two principle components of the group-level data over the entire insula and not at each individual brain location (e.g. voxel, or vertex in our case). As a consequence, no clusters with specialized intensity-related function or intensity preference maps could be reported to respectively address the location and distribution of taste intensity rankings over the insula. Thus, the existence of a spatially distributed processing for the taste intensity responses in the right insula was not excluded by previous studies and, actually, the presence of such a spatial code might be postulated on the basis of the taste intensity preference maps that we show in both the right and left insula. Indeed, from this preference analysis, we observed a changing local preference from high to low concentrations in both the right and left insula with an intriguing complementary pattern between sweet and bitter tastes in the two hemispheres: for sweet

taste, an anterior-posterior spatial gradient for high-to-low concentrations was more evident in the right insula; for bitter taste, an anterior-posterior spatial gradient for high-to-low concentrations was more evident in the left insula. In both cases, these spatial distributions would be compatible with the idea that the processing of taste intensity could be configured for a spatially distributed processing code, as previously discussed in some other works (see (Jones et al., 2006; Simon et al., 2006)). In addition, in vivo imaging studies of neuronal activity in rats, have also reported different spatial patterns of activation in response to appetitive (saccharin) and aversive (quinine) tastes (Accolla and Carleton, 2008; Yiannakas and Rosenblum, 2017). In particular, the evidence for distributed gustatory processing in the primary gustatory cortex was gathered by the fact that taste identity, palatability and, in particular, intensity were more efficiently decoded when the activity of different spatially localized neuronal populations were taken into account (Jones et al., 2006; Katz et al., 2002).

Previous studies had also highlighted that specific regions of the insula are responsible for processing at the same time several and, sometimes opposite, aspects of taste perception. This could be particularly the case of the anterior insula that is engaged in the processing of food rewards (Monteleone et al., 2017; Sescousse et al., 2013; Van der Laan et al., 2011), pleasantness (Dalenberg et al., 2017; Small, 2010) as well as in the experiencing of aversive smells (Wicker et al., 2003), anticipation of aversive stimuli (Nitschke et al., 2006) and aversive taste learning (Bermudez-Rattoni, 2014; Wegman et al., 2018). Similarly, the middle insula is known to be involved in several mechanisms, including the simple response to oral somatosensory stimuli (De Araujo and Rolls, 2004; Rolls, 2016). However, the bilateral middle insula is also reported to be the area processing taste intensity (Small et al., 2003; Spetter et al., 2010) with the middle-posterior part being specifically more activated by unpleasant tastes causing aversive reactions (Nitschke et al., 2006; O'Doherty et al., 2001). This could partially explain why the preference for low concentration in the middle posterior clusters is less consistent between sweet and bitter tastes compared to the preference for high concentration in the

anterior clusters.
We observed both similarities and differences between right and left insula in relation to the intensity preference maps. Importantly, the left insula seems to cover a slightly broader spectrum of preferred intensities across the anterior and middle clusters and the left insula patterns also appear more similar between sweet and bitter tastes. This pattern even encompasses a small specialized cluster in the antero-middle insula where the intensity factor becomes statistically significant in the 2w- ANOVA, whereas no such localized specialization emerged for the right insula.
The two hemispheric patterns appear more similar for the anterior clusters (where the high concentrations are best represented) and more different for the middle posterior clusters. In fact, for the middle posterior clusters, we found that the preference for lower concentrations was present for both tastes only in the left hemisphere whereas this preference was visible only for sweet taste in the right hemisphere. This aspect is consistent with the recent pilot study (Prinster et al., 2017), where the differential preference for sweet and bitter tastes was also highlighted in comparison to all five basic tastes across the right insular cortex. In this previous study, it was indeed found that the preference for sweet and bitter tastes was visible in the middle posterior and inferior insula whereas the other basic tastes (sour, umami and salty) expressed their spatial preference in the anterior part of the right insula.
Given the merely descriptive nature of the preference mapping, a spatial consistency analysis of these patterns across all individual subjects was also performed. Despite the high variability in the obtained spatial distributions, the similarity of the individual insular patterns of spatial variation in the "preferred" intensity with the group preference map was significantly high for most subjects (>=80%) and for both tastants.
When focusing on the insular region that showed a significant effect to taste intensity, a single cluster emerged in the anterior-middle part of the left insula. In this region, we observed a highly non-linear trend of the responses to the concentration of both sweet and bitter tastants. This trend was not linear and therefore provides a new account for the complex nature of taste intensity perception

processes in the human insular cortex. More specifically, the activation responses were lower (and minimal) at intermediate concentrations in comparison to immediately lower and higher concentrations, for both sweet and bitter tastes. Not even a quadratic trend was significantly explaining the measured responses as reported in (Dalenberg et al., 2015) for the principle component scores of the entire right insular cortex, whereas two other human studies (Kobayakawa et al., 2008; Spetter et al., 2010) reported a linearly increasing response across four different intensities of sweet in the left middle insula.

Several studies performed in animals have accounted for the complex non-monotonic nature of insular responses to taste intensity. For example, while some electrophysiological studies reported a monotonic increase of firing rates in the insula neurons with increasing tastant concentration (Scott et al., 1991), far more complex (non-linear) trend emerged when other aspects, such as the tasting phase (e.g. the number of licking cycles before ingestion), were taken into account (Stapleton et al., 2006), thereby gustatory neurons were found to respond more to sucrose (sweet) tastants of higher or lower concentrations depending on the latency of observation. Thus, changes of functional activation in response to taste intensity is likely also influenced by the exact number and latencies of the different tasting phases occurring when the subject holds the taste in mouth for a given period. In our experiment, although we tried to minimize the duration of the tasting period by implementing a rapid taste injection (600ms) of very small amounts of solution (1mL), we substantially failed to obtained a linear relationship between cortical activation and taste intensity, probably due to the impossibility to control the exact number of tasting cycles occurring at each concentration. On the hand, it has been also reported that the primary gustatory cortex response may change in relation to the level of attention paid by subjects to the taste intensity or pleasantness (Bender et al., 2009; Nitschke et al., 2006; Veldhuizen et al., 2007; Wang and Spence, 2017). Thus, although our paradigm did not require subjects to focus on stimuli and give any scores about both the intensity and pleasantness of the stimuli during the fMRI experiment, we cannot exclude that top-

down effects have come into play and contributed to modulating the responses across different concentrations.

In conclusion, this chapter reports that the processing of taste intensity activates multiple regions within the bilateral insular cortex including at least two clusters in the middle and anterior portions of the human insula. The difficulty in localizing specialized clusters for parametric taste intensity processing at the used spatio-temporal scales was possibly addressed and explained by the existence of spatially continuous cortical processes, whereby the response of a "preferred" intensity appears distributed over smaller clusters according to anterior-posterior spatial gradients for high-to-low concentration changes. Future investigations at ultra-high magnetic fields are needed to ultimately disclose whether compact insular clusters exist and can be targeted to parametrically control the intensity of the perceived taste or whether the suppression of specific confounders would help reducing the inter-subject variability in the spatial distribution of the taste intensity-related responses.

Chapter 4:

Study of gustatory cortex using Ultra High field fMRI: Initial Results

4.1 Introduction

Taste quality reflects the nature of a tastant and the brain insula is the region where gustatory process starts in the cortex. By now, the exact location within the insula where resides the PGC is still under debate, as discussed in details in the Chapter 1. In addition, one of the most intriguing questions regarding taste processing is whether it could be hypothesized a spatially ordered representation of tastes in the insular cortex, similar to that demonstrated for auditory and visual cortices.

The possible existence of the chemotopic organization within the insular cortex remains, in fact, one of the unsolved questions about taste perception mechanisms in the human brain and, by now, no functional MRI studies have completely clarified whether tasting determines a spatially-segregated response in the insula or not. This failure could be linked to both experimental difficulties or physiological considerations.

First, it is possible that tastants' specific signals are differentially processed (in terms of quality) in lower brain stations (e.g. in the NTS or the thalamus) before arriving to the insular cortex. Second,

it is possible to hypothesize that gustatory processing comes as a network-based processing thus requiring, in addition to the insular cortex, the integration of several other brain regions contributing to taste identification and functional representation (Jones et al., 2006; Simon et al., 2006). Third, from a more technical point of view, the failure in individuating some differentially activated sub-regions in the insula (each processing a specific tastant quality) could have been due to the intrinsically limited spatial resolution of 3 Tesla (or lower) MRI data for single-subject mapping, as well as by the high inter-individual anatomical variability in group-based mapping.

Contrariwise, some (Chen et al., 2011; Yokota et al., 2011) (but not all, (Fletcher et al., 2017)) works in animals were able to demonstrate a chemotopic segregation of primary taste processing by the use of high temporal and spatial imaging methodologies.

One way to give a first preliminary answer to these questions in the human brain is by the use of ultra-high spatial resolution fMRI and, in this chapter, it is illustrated the study performed with the use of ultra-high-field (UHF) 7T functional MRI on nine healthy subjects. The scientific questions of this study concern to (i) the identification of the insular areas primarily responsive to taste both in the group-level and in a single-subject based analyses and (ii) the possible hypothesis of a common spatial organization of taste-related insular response to all basic tastes across subjects.

Because brain mechanisms activating by tasting also involve subjective factors (e.g. context, pleasantness, etc..), the analysis of brain gustatory responses, even with high resolution fMRI data, will remain an extremely complex and open task in neuroscience. Nonetheless, what makes this study important is that even the exact location of the PGC could be revisited, and the fundamental information gained from this experiment could pave the way to novel and more anatomically and functionally informed procedure for the analysis of complex tastants in other fields of neuroscience.

4.2 Materials and Methods

4.2.1 Participants

Nine healthy adult volunteers (right handed, 5 males and 4 females, mean age ± standard deviation 27 ± 2 years, BMI age ± standard deviation 22 ± 2) not reporting any olfactory, gustatory, neurological or psychiatric disorder, and free from the use of any medication or smoking, took part in this study. The Ethical Committee of the Faculty of Psychology and Neuroscience at Maastricht University granted approval for this study (protocol number ERCPN 159_15_12_2015_S6) and each enrolled subject signed a written informed consent. One subject was discarded by the analysis because of technical problems during the fMRI acquisition. The demographic characterization of the final group of enrolled subjects is reported in Table 8.

Subject #:	Age	Sex	BMI
1	26	M	24
2	23	F	19
3	29	M	22
4	29	M	22
5	29	M	22
6	27	F	24
7	26	F	21
8	29	F	20

Table 8 : *Demographic characterization of the enrolled subject.*

4.2.2 Behavioral and laboratory screening

One week before the fMRI scanning, each enrolled subject performed some preliminary laboratory tests aimed at: (i) selecting individually calibrated tastant concentrations, (ii) choosing the neutral taste (artificial saliva) and (iii) being trained for the execution of the fMRI experiment (see below for all details).

This preliminary laboratory screening was organized in four different consecutive phases.

During the first phase, each subject was asked to choose among four progressively diluted samples of artificial saliva. The four concentrations were obtained by diluting a stock solution in distilled water with dilution factors respectively equal to 12.5%, 25%, 50%, and 75%. The starting stock solution of artificial saliva was prepared with 2.5mM of sodium bicarbonate (Sigma Aldrich Inc., MO) and 25mM of potassium chloride (Sigma Aldrich Inc., MO) (O'Doherty et al., 2001) in distilled water.
The dilution that tastes most like nothing to the subject was selected in 2 alternative-forced-choice procedures in which the 4 solutions were presented in two pairs (randomly chosen) and the subject was asked *"Which of these two solutions tastes most like nothing?"*. Table 9 reports the selected dilution (from the stock) of artificial saliva for each subject.

Subject Nr:	12.5%	Dilution 25%	Dilution 50%	Dilution 75%
1				x
2			x	
3			x	
4			x	
5				x
6			x	
7				x
8				x

Table 9: *Artificial saliva dilution individually calibrated for each enrolled subject.*

In the second phase of the laboratory session, each subject was asked to select an optimal concentration of bitter, sour, salty and umami tastes, to ensure that each of them will result as perfectly recognizable without causing any disgust or aversive feelings. This procedure aimed, first, at guaranteeing that each subject would be perfectly able to recognize each taste during all the functional runs (where tastes were injected in a shuffled order across repetitions and runs) and second, at individuating the optimal (individually-calibrated) set of taste intensities that allows

subjects to avoid any sense of disgust during the experiment (especially in the final runs).
Thus, several concentrations of quinine hydrochloride (bitter), NaCl (salt), citric acid (sour) and monosodium glutamate (umami) were prepared in distilled water with the following concentrations:

- Bitter : 0.06mM, 0.125mM, 0.250mM and 0.5mM;
- Salt : 100mM and 200mM;
- Sour : 15mM and 20mM;
- Umami 100mM, 150mM and 200mM.

Sweet concentration was set to 117mM (on the basis of some preliminary experimental tests, data not shown) but, in this laboratory screening, we asked each participant whether the selected concentration was perfectly recognized and did not determine any disgust feelings.

During the third phase of the laboratory session, once set the saliva and tastes' concentrations, we injected (in a random order) each taste in a double-repetition test. We used the selected artificial saliva both as neutral taste and for the rewash (after each taste delivery). In addition, during each injection we asked subject first to recognize the perceived taste and, second, to report a score between 0mm (very low perceived) and 10mm (very strong perceived) on a visual assessment score (VAS) test.
In Table 10 and in Table 11 are reported the selected concentrations for each subject and the collected intensity scores.

Subject Nr:	Sweet (mM)	Bitter (mM)	Salty (mM)	Sour (mM)	Umami (mM)
1	117	0.125	100	15	100
2	117	0.125	100	20	100
3	117	0.25	100	20	150
4	117	0.125	100	20	100
5	117	0.125	100	20	100
6	117	0.125	100	15	100
7	117	0.125	100	20	100
8	117	0.06	100	15	100

Table 10 : *Concentration selected for each enrolled participants for the fMRI experiment.*

Subject Nr:	Sweet	Bitter	Salty	Sour	Umami
1	6	5	5	7	7
2	7	5	5.5	7	5.5
3	3	4	2.5	5	5
4	5	6.5	4	7.5	5
5	7	7.5	8.5	7.5	7
6	9.5	7.5	8.5	7.5	6.5
7	4	6	7	6.5	8.5
8	7	6.5	7	8	7.5

Table 11 : *Visual assessment score (VAS) collected for each participant. The results were obtained after meaning the VAS scores of the two repetitions.*

In the fourth and last part of the session, we trained the subject simulating one run of the fMRI experiment by the use of a mock scanner.

For this laboratory screening, stock solution and diluted tastant solutions were prepared the day before and all solutions were stored over-night at 4°C. One hour prior the screening, solutions were kept at normal temperature (~20°C) to ensure the same starting condition for all participant.

4.2.3 fMRI data acquisition and experimental protocol

Subjects underwent the fMRI experiment on a 7 Tesla MAGNETOM MRI scanner equipped with a 32-channel Nova medical RF coil at the Scannexus facility in Maastricht, The Netherlands (www.scannexus.nl). The acquisition protocol included a three-dimensional T1-weighted Magnetization Prepared Rapid Gradient-Echo (MPRAGE) sequence with the following parameters TR= 3100ms, TE= 2.52ms, TI= 1500ms, flip angle= 5°, slice thickness= 0.6 mm, matrix size= 384 x 384 number of slices = 192 and voxel size=0.6 x 0.6 x 0.6 mm^3, a three-dimensional proton density (PD) sequence with the following parameters TR=1440ms, TE=2.52ms, flip angle= 5°, slice thickness= 0.6 mm, matrix size= 384 x 384, number of slices = 192 and voxel size=0.6 x 0.6 x 0.6 mm^3 and an fMRI Blood Oxygenation Level Dependent (BOLD) sequence, a gradient-echo echo-planar (GRE-EPI)

imaging acquired with a Multiband factor of 2 (Feinberg et al., 2010; Moeller et al., 2011; Xu et al., 2013), TE = 19 ms, TR = 1500 ms, voxel size = 1.2 x 1.2 x 1.2 mm3, 50 slices, 460 dynamic scans, direction of phase encoding acquisition Anterior-Posterior. The same GRE-EPI series was repeated 6 times (runs) for six subjects and 5 times (runs) for two subjects. Two other identical fMRI sequences with opposite phase encoding and 5 dynamic scans were also acquired for distortion correction performed during the preprocessing of functional data (Andersson et al., 2003; Smith et al., 2004).

During each functional run, consisting on three repetitions of each taste, stimulus injection was performed automatically using a gustometer composed on seven independently programmable BS-8000 syringe pumps (Braintree Scientific, Braintree, MA) controlled by a stimulation computer via a 9-pin serial adaptor and telephone wiring. Each pump holds a 50mL syringe, each containing a specific tastant solution. Two of the pumps were dedicated to the injection of the artificial saliva. Last, each syringe was connected to a 25-foot length of FDA rated Tygon beverage tubing (Saint-Gobain Performance Plastics, Akron, OH) with an inside diameter of 3/32".

The synchronization between fMRI acquisitions and stimulus delivery was controlled using a MATLAB custom script (The MATHWORKS Inc., Natick, MA, USA) and some functions of Psychotoolbox.

The experimental design was built as an event-related design that consisted of six identical blocks of five basic events or injection phases, during which subject received a specific tastant and artificial saliva for rewashing, both anticipated by visual cues. Between the taste injection and rewash, a phase for taste recognition was introduced. During this phase, a picture representing the correspondence between tastes and buttons were shown to subject who, using two button presses (one per hand) were asked to recognize taste and to press the correspondent button. The block of injection phase was repeated six times to ensure the

injection of all the tastants and tasteless solution (also used as "pure taste" condition). The taste order was shuffle during each of the three repetitions composing a single run.
The representation of the single injection phase is provided in Figure 22.

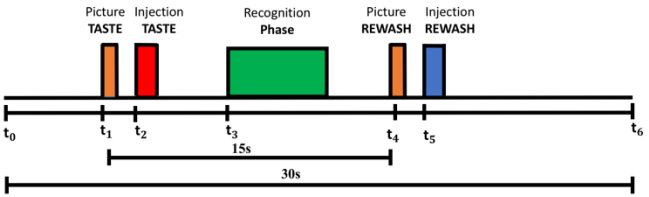

Figure 22 : *Single injection phase consisting on two visual cues occurring at the triggers (t_1, t_4) and two injection phases occurring at triggers (t_2, t_5) for taste and saliva for rewash. Between the two injection phases a picture representing the correspondence between buttons and taste was presented (trigger t_3) and each subject was asked to recognize the perceived taste.*

Referring to this figure, the following events (repeated every 25 TRs) occurred at:
1. Taste visual cue, trigger t_1: the word "TASTE" was presented on a video display unit (connected to a back-projection screen in the MRI room) for 1000ms.
2. Taste-injection, trigger t_2: the pump of the gustometer was activated for 1400ms and 0.7mL of solution with a specific taste was delivered.
3. Recognition phase, trigger t_3 with a jittered delay (in a range of 1-3 triggers after the onset of t_3): a legend showing the correspondence between buttons (coding between 1-6) and corresponding taste plus saliva was presented on a video display unit (connected to a back-projection screen in the MRI room) for 6500ms.

4. Rewash visual cue, trigger t_4: the word "REWASH" was presented on the video display unit for 1000ms.
5. Water-injection, trigger t_5: two pumps of the gustometer were activated for 1400ms and a total volume of 1.4 mL of saliva was delivered.
For the fMRI experiments, the taste solutions were prepared the day before and stored at controlled low temperature (~4°C) over-night. One hour before the scanning, they were stored in normal temperature (~20°) to keep the same starting condition for all the subjects. Solutions were brought to the site of experiment in a polystyrene box and the tube filling were carried out 10 minutes before the starting of the acquisition.

4.2.4 MRI Data Processing

Image data preparation, some preprocessing steps and statistical analysis were performed in BrainVoyager, (Brain Innovation, Maastricht, The Netherlands, www.brainvoyager.com). Image inhomogeneity correction of the anatomical data was performed with SPM12 (Wellcome Trust Centre for Neuroimaging, London, UK; http:// www.fil.ion.ucl.ac.uk/spm) while distortion correction of functional data was performed using the tool TOPUP (Andersson et al., 2003) from the FMRI Software Library.
Additional analyses were performed using custom scripts written in MATLAB.

For each individual subject, the anatomical T1w and PDw images were first sampled to $1mm^3$ isotropic and then the resulted T1w images were divided for the resulted PDw images (T1w/PDw) producing an anatomical set of images with higher contrast between gray and white matter.
The obtained T1w/PDw volume was skull-stripped using the anatomical mask produced with the skull-stripping tool of BrainVoyager (applied on the T1w images) and then, after exported in NIFTI format, was corrected for field inhomogeneity

using SPM12. The resulted volume was imported back in BrainVoyager and then normalized to the Talairach space.

Multi band GRE-EPI time series from all the runs were corrected for the different slice scan acquisition times using a cubic spline interpolation procedure and for movement artefacts by a rigid re-alignment of all the volumes to the first volume based on a Levenberg–Marquardt algorithm, optimizing three translation and three rotation parameters on a resampled version of each image. The estimated motion parameters were carefully inspected to control that no excessive residual motion was present (more than 1 pixel size in head translation or more than 1 degree in head rotation). The head motion-corrected time series were then exported to NIFTI image format for the GRE-EPI distortion correction and, after that, re-imported in BrainVoyager and filtered in the temporal domain, using a high-pass filter with cut-off set to 0.008Hz to reduce linear and non-linear trends in the time-courses. Last, all these images were transformed to Talairach space with a final spatial resolution of 1 mm isotropic.

For each subject and each run, a single study GLM was performed considering the five basic tastes (sweet, bitter, salty, sour and umami) plus neutral solution as "predictors of interest" while the visual cues, the pictures during taste recognition as well as the neutral solution used during the rewashing phase as predictors of confound. Prior to the GLM fitting, the time courses as well as the predictors were z-transformed. Last, a correction for serial temporal autocorrelations in the time-courses was applied using a second-order autocorrelation model (AR2).

In order to perform second-level analyses, two masks of the left and right insula (voxel's resolution 1mm isotropic) were considered from the Harvard Oxford atlas, provided by the FSL software. These masks were first imported in BrainVoyager, normalized to Talairach space and then merged to create a single mask.

For the second-level analysis, a group-based RFX-GLM analysis was firstly performed across all voxels within the bilateral

insula and the main effects of the five basic tastes plus neutral were extracted. A statistical threshold was applied to the t- maps, which protected against false-positive clusters at 5% (cluster- level corrected for multiple comparisons after 1000 Montecarlo simulations (Forman et al., 1995)).
1w-ANOVA was also performed, considering as (taste-related) factors all the basic tastes plus neutral solution across all voxels belong to the left and right insula.

For the single subject analysis, we performed a fixed effects GLM (FFX-GLM) across all voxels within the bilateral insula and the main effects of the five basic tastes plus neutral were extracted and reported with a statistical threshold of p=0.05, Bonferroni corrected.
From both the group-based and single subject-based analyses, we extracted the peaks of activation for all tastes and some representative maps are provided. All the analyses were performed considering the neutral solution (during the taste trials) as condition of interest, since the regression with neutral solution was also performed during the first-level GLM fitting where the rewashing phase was added in the model as confound.

4.3 Results

All subjects were able to recognize more than the 85% of the injected tastes during the entire fMRI experiment.
The ANOVA test performed in the group-based analysis did not reveal any taste effects when considering the basic tastants plus neutral as factors. In this analysis, in fact, the maps of main effects show some common regions of activation both within the right and left insulae.
For example, in the right insula two common areas of activations were found in the middle insula (as shown in Figure 23) and in the anterior insula (as shown in Figure 24), to all basic tastes and to the neutral solution.

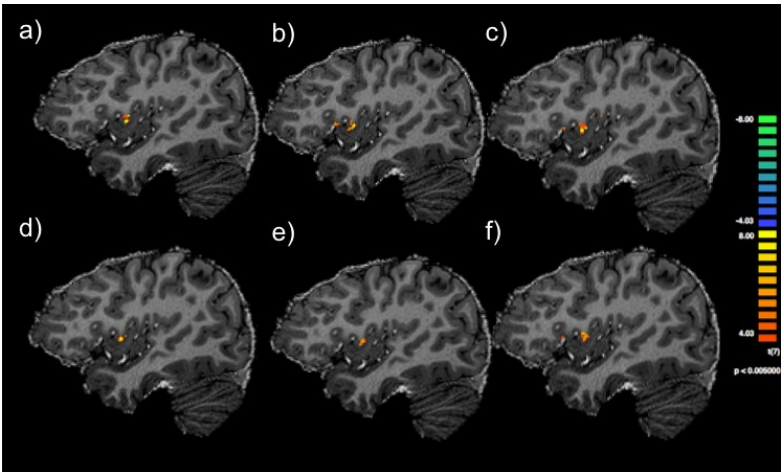

Figure 23: *Main effects in the right middle insula to all tastes, a) sweet b) bitter, c) salt, d) sour, e) umami, f)neutral.*

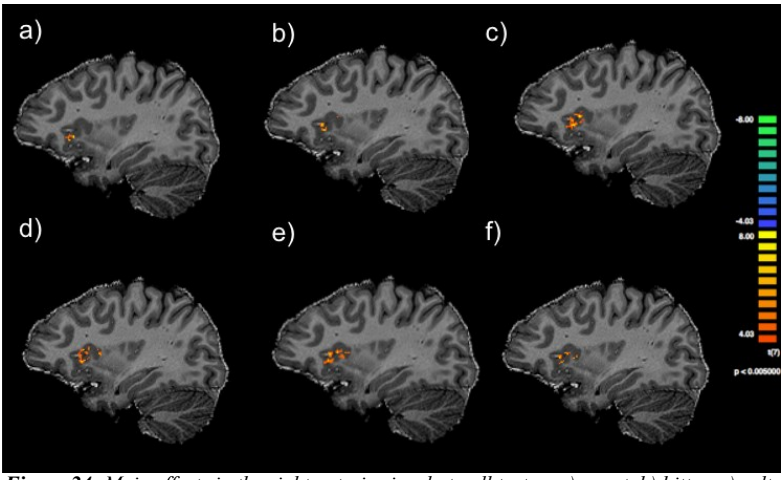

Figure 24: *Main effects in the right anterior insula to all tastes: a) sweet, b) bitter, c) salt, d)sour, e) umami, f) neutral.*

In the left insula, two areas of common activation were found, one in the anterior insula (as shown in Figure 25) and one in the inferior insula (as shown in Figure 26).

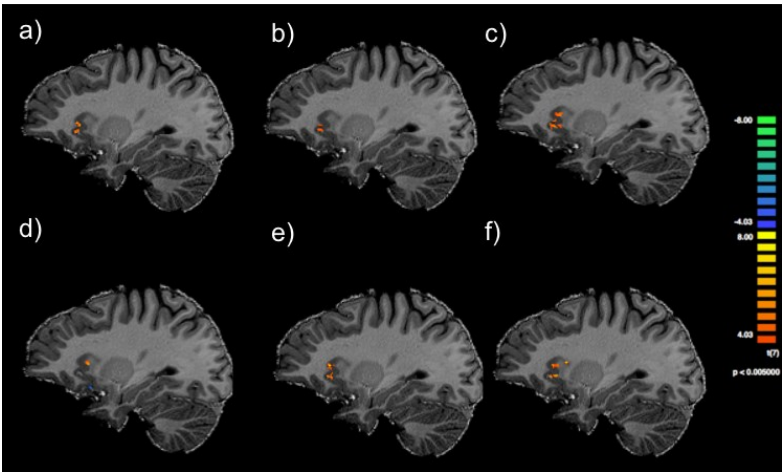

Figure 25: *Main effects in the left anterior insula to all tastes: a) sweet, b) bitter, c) salt, d)sour, e) umami, f) neutral.*

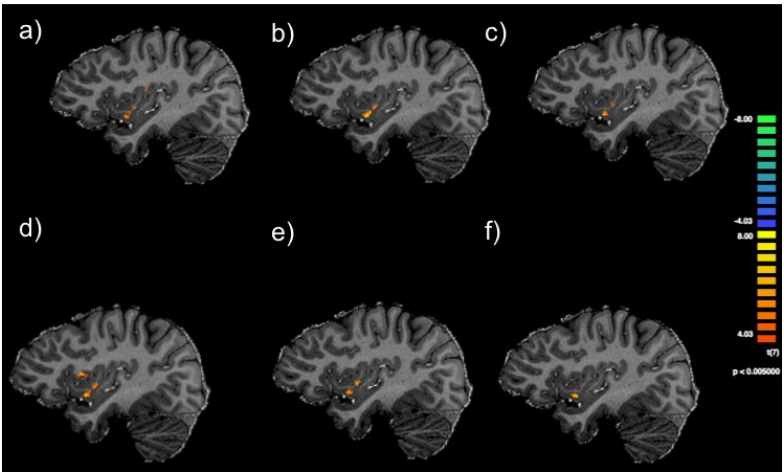

Figure 26: *Main effects in the left inferior insula to all tastes: a) sweet, b) bitter, c) salt, d)sour, e) umami, f) neutral.*

For both the left and right insulae, the peaks of activations are reported respectively in the Table 12 and in the Table 13.

Left Insula	x	y	z	t	p
Sweet	-39	8	11	9.07	<0.001
Bitter	-37	5	-5	12.36	<0.001
Salty	-30	16	6	9.55	<0.001
Sour	-33	11	6	14.58	<0.001
Umami	-41	9	-2	11.65	<0.001
Neutral	-28	3	15	14.13	<0.001

Table 12 : *Peaks of significant activations of each tastants in the left insula from the group-based RFX-GLM analysis.*

Right Insula	x	y	z	t	p
Sweet	39	7	3	11.62	<0.001
Bitter	32	20	5	9.20	<0.001
Salty	32	16	12	13.17	<0.001
Sour	40	1	8	16.85	<0.001
Umami	39	6	2	15.75	<0.001
Neutral	36	6	15	15.71	<0.001

Table 13 : *Peaks of significant activation of each tastants in the right insula from the group-based RFX-GLM analysis.*

In order to illustratively show the spatial localization of the peaks of activation, they are reported as nodes within the insulae in the following Figure 27 and Figure 28 obtained using the BrainNet viewer (Xia, Wang, He, BrainNet Viewer) of MATLAB.

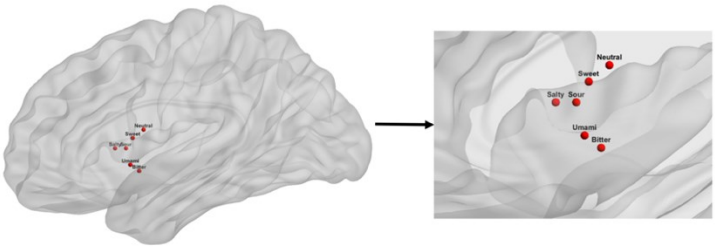

Figure 27 : *Representative localization of peaks of activations to all the basic tastes plus neutral within the left insula.*

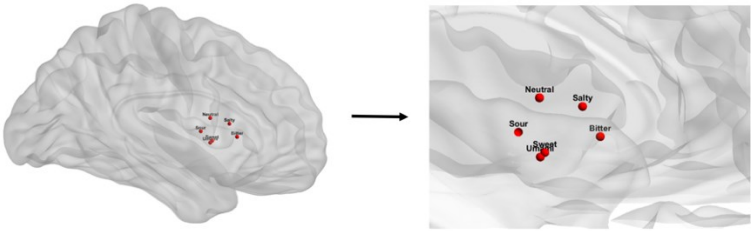

Figure 28: *Representative localization of peaks of activations to all the basic tastes plus neutral within the right insula.*

For the single subject analysis, we provide the following table reporting, for each subject and each taste. the peaks of significant activations:

Subject #1:				
Left Insula	**x**	**y**	**z**	**t**
Sweet	-37	-9	8	13.83
Bitter	-37	-9	8	12.55
Salty	-38	-6	5	12.89
Sour	-37	-9	8	12.74
Umami	-37	-9	8	14.46
Neutral	-38	-5	4	12.59
Right Insula	**x**	**y**	**z**	**t**
Sweet	39	-4	16	13.53
Bitter	39	-4	16	14.13
Salty	39	-4	16	14.32
Sour	39	-4	16	13.05
Umami	39	-4	16	14.32
Neutral	39	-4	16	14.22
Subject #2:				
Left Insula	**x**	**y**	**z**	**t**
Sweet	-36	-8	15	12.66
Bitter	-36	-8	15	13.56
Salty	-36	-8	15	14.21
Sour	-36	-8	15	14.78
Umami	-42	-4	0	12.74
Neutral	-36	-8	15	11.48
Right Insula	**x**	**y**	**z**	**t**
Sweet	37	-6	18	14.66
Bitter	37	-6	18	13.71
Salty	37	-6	18	15.33
Sour	37	-6	18	15.70
Umami	37	-6	18	14.79

Neutral	37	-6	18	14.07
Subject #3:				
Left Insula	**x**	**y**	**z**	**t**
Sweet	-35	-11	17	11.77
Bitter	-35	-11	17	10.97
Salty	-35	-11	17	13.33
Sour	-35	-11	17	11.38
Umami	-35	-11	17	13.90
Neutral	-35	-11	17	11.75
Right Insula	**x**	**y**	**z**	**t**
Sweet	44	6	-5	9.80
Bitter	39	-1	0	9.46
Salty	43	6	-4	9.44
Sour	34	-8	19	10.79
Umami	36	-7	11	10.59
Neutral	42	7	-4	8.73
Subject #4:				
Left Insula	**x**	**y**	**z**	**t**
Sweet	-41	-10	11	10.23
Bitter	-41	-10	11	8.53
Salty	-35	-5	6	10.49
Sour	-36	3	-8	10.59
Umami	-36	-5	5	9.86
Neutral	-36	-5	6	8.62
Right Insula	**x**	**y**	**z**	**t**
Sweet	39	-4	6	10.86
Bitter	39	-9	12	8.73
Salty	39	-9	12	10.64
Sour	39	-8	12	11.11
Umami	39	-8	12	10.61
Neutral	39	-9	12	9.20
Subject #5:				
Left Insula	**x**	**y**	**z**	**t**
Sweet	-33	-6	20	10.83
Bitter	-33	-7	20	9.51
Salty	-33	-7	20	10.59
Sour	-37	4	-10	10.88
Umami	-33	-7	20	9.50
Neutral	-33	-6	20	10.35
Right Insula	**x**	**y**	**z**	**t**
Sweet	37	5	-1	9.83
Bitter	44	-5	8	9.79
Salty	46	10	3	9.99
Sour	46	9	3	10.36
Umami	45	-4	8	8.99
Neutral	44	-5	8	9.34
Subject #6:				
Left Insula	**x**	**y**	**z**	**t**
Sweet	-33	-10	12	11.99

Bitter	-39	-7	9	12.81
Salty	-35	-10	11	12.74
Sour	-35	-10	11	14.32
Umami	-35	-10	11	13.42
Neutral	-35	-10	11	12.17
Right Insula	**x**	**y**	**z**	**t**
Sweet	43	-4	6	11.15
Bitter	35	-9	18	11.91
Salty	34	-9	18	12.65
Sour	35	-9	18	12.69
Umami	35	-9	18	12.63
Neutral	35	-9	18	12.00
Subject #7:				
Left Insula	**x**	**y**	**z**	**t**
Sweet	-37	0	-3	14.10
Bitter	-37	-3	0	13.60
Salty	-37	-13	6	12.41
Sour	-37	-13	6	11.67
Umami	-37	-3	0	13.45
Neutral	-37	-3	0	13.96
Right Insula	**x**	**y**	**z**	**t**
Sweet	39	-9	12	13.11
Bitter	39	3	-7	13.55
Salty	38	-10	12	13.30
Sour	39	3	-7	11.44
Umami	38	-10	12	13.07
Neutral	38	-9	12	13.07
Subject #8:				
Left Insula	**x**	**y**	**z**	**t**
Sweet	-32	-9	17	11.83
Bitter	-32	-9	17	11.52
Salty	-32	-9	17	10.83
Sour	-32	-9	17	12.18
Umami	-33	-9	17	11.01
Neutral	-32	-9	17	11.14
Right Insula	**x**	**y**	**z**	**t**
Sweet	32	-11	19	10.90
Bitter	34	-5	19	9.25
Salty	32	-11	19	9.57
Sour	32	-11	19	10.70
Umami	34	-5	19	9.06
Neutral	32	-11	19	10.24

Table 14: *Single subject analysis, peaks of activations for each subject and for each taste (plus neutral).*

In addition to the proposed table, the maps of the main effects (t-maps with a statistical threshold p=0.05, Bonferroni corrected) of three subjects (randomly chosen) are shown. From these maps,

since common areas of activations can be observed in the anterior, middle and inferior insula bilaterally, it is also possible to verify not only that no spatially segregated areas within the insula differentially process the five basic tastes, but also to evaluate an high variability across subjects in terms of the statistical strength of the reported activations. In fact, while for example the subject #1 shows distributed functional responses to all taste within the insular cortices, subjects #2 and #7 reported more compact and precisely isolated clusters in the anterior, middle and inferior insulae.

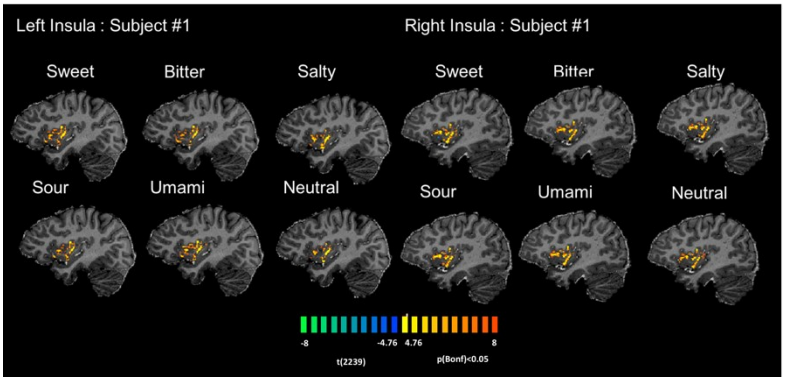

Figure 29 : *Subject #1, t-maps of left (left-side) and right (right side) insulae to all tastes (plus neutral) with a statistical threshold p=0.05, Bonferroni corrected.*

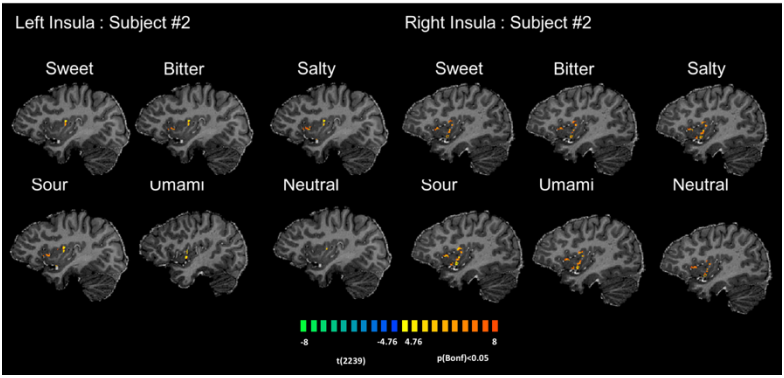

Figure 30: *Subject #2, t-maps of left (left-side) and right (right side) insulae to all tastes (plus neutral) with a statistical threshold p=0.05, Bonferroni corrected.*

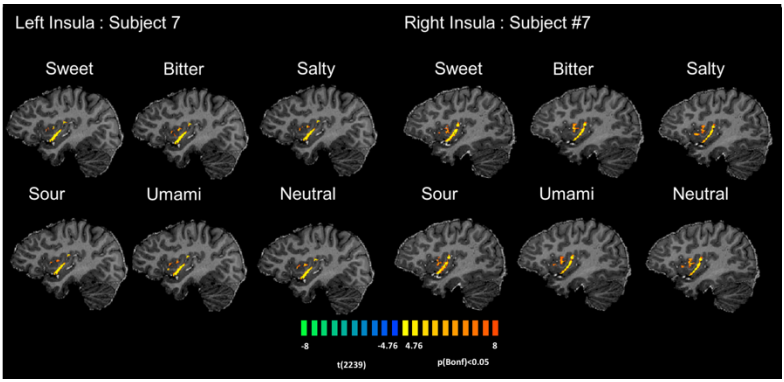

Figure 31: *Subject #7, t-maps of left (left-side) and right (right side) insulae to all tastes (plus neutral) with a statistical threshold p=0.05, Bonferroni corrected.*

4.4 Discussions

In this chapter, it has been described the study performed with ultra-high field fMRI for the evaluation of the insula response to basic tastes. It is the first study investigating gustatory cortex with the use of high spatial resolution functional data (1mm^3 isotropic) and it was aimed at defining (i) the clusters within the insula

responding to all the known basic tastes, sweet, bitter, salty, sour and umami both in a group-based and in a single-subject based analyses and (ii) at determining whether the activations obtained in response to the different basic taste qualities may allow the hypothesis of a spatially ordered distribution (chemotopy) of quality-related response within the insular cortex.

In this study, the concentrations of taste solutions were determined on the basis of individual perception in order to determine which taste intensity would be perfectly recognized during the experiment and to avoid any possible disgust feeling, especially across functional runs. In fact, the fMRI experiment was based on 6 consecutive runs for six subjects and 5 consecutive runs for 2 subjects, during which a total number of eighteen/fifteen repetitions of each taste stimulus was delivered. In order to performed our analysis with the same number of taste trials, for each individual, the first five runs were considered.

The first result of this study has been the localization of the insular regions, responsive to basic tastes both in a group-based and in a single subject based manner.

When looking at the maps of the main effects, the activations obtained from the group-based analysis determined two areas of activation respectively in the right and left insular cortex. Particularly, in the right insula, activations were found in the anterior and middle areas whereas in the left insula activations were found in the anterior and inferior areas.

These regions of activations were previously observed in several works (Dalenberg et al., 2015; Small et al., 2003; Spetter et al., 2010) as well as perfectly overlap with recent metanalyses, reporting results obtained after collecting several studies performed in healthy subjects with the use of basic tastants' solutions (Yeung et al., 2018, 2017). It is important to consider that the finding presented here comes from ultra-high fMRI data, without any spatial smoothing in order to better localize the peaks of activations to all the basic tastes.

The ANOVA analysis performed on the contrasting maps of the RFX-GLM procedure did not show any clusters of significant effects produced by the different taste qualities. However, when focusing on the peaks of significant activations, it is possible to observe how the strongest responses were localized in different cortical points across the anterior-middle insula, as illustratively represented by the Figure 27 and Figure 28. In fact, the represented peaks of activations could be easily distinguished in both the left and right insula, although specifically the sweet and umami appear as the most closed activations within the right insula. In the single subject maps of the main effects, despite an high variability in the statistical power of the activations, the areas with significantly taste activations are localized in the anterior, in the middle and in the inferior insula bilaterally.

However, when looking at the peaks of significant activations reported in the proposed Table 14 for all the enrolled subjects, unlike the analysis performed at a group level, it is possible to notice a high spatial consistence of activations to all basic tastes and to neutral solution.

These results poorly support the hypothesis of a spatially segregated distribution of basic tastes representation within the insular cortex, and because this is the first fMRI study evaluating where basic tastes activate the insula in a single subject/single taste manner, a direct comparison with literature is not straightforward. In addition, no previous studies have reported results of a taste effect in the insular cortex to different taste qualities with ultra-high fMRI and, consequently, future other investigation in this direction will be necessary to confirm the present findings.

However, this study encourage to perform gustatory analyses not only in a voxel by voxel basis but also in a layer dependent fashion, as previously suggested in the animal study of Yokota et al. (Yokota et al., 2011) where the authors observed a preferred distribution of taste responsive (and selective) neurons in the intermediate layers. However, the cytoarchitecture of the human insula is particularly complex for the spatially smoothed

distribution of a granular versus dysgranular architecture but also for the presence of continuous opercula, and this could pose layer reconstruction issues.
In addition, the analysis I performed was essentially based on a univariate approach, that could hide important effects associated with multivariate patterns essential for decoding taste qualities, as successfully shown in a recent study performed with high temporal resolution EEG procedure (Crouzet et al., 2015).
The application of standard multi voxel pattern analyses (MVPA), although potentially useful for the understanding of the gustatory processes, in this study, would be penalized by the low number of taste trials, an aspect that could easily lead to overfitting or poorly replicable results. Future applications of more sensitive MVPA strategies (also in cases of low number of trials) in determining the possible voxel selectivity to taste should be performed, for example with longitudinal acquisition on the same subject, thus allowing to increase the number of taste injection repetitions.
Another crucial aspect that certainly limits the study of taste perception with fMRI is that gustatory processing is also a time dependent processing and the temporal resolutions of fMRI acquisition and, particularly, of the sequences used here, do not allow the evaluation of the dynamic evolution of taste responses that could be really important in determining the effective response at voxel level (Crouzet et al., 2015; Kobayakawa et al., 2008; Samuelsen et al., 2012).
For this latter consideration, future studies that involve the contemporary presence of high-spatial and high-temporal imaging (e.g. EEG-fMRI) could be essential to comprehensively asses the presence or absence of the chemotopic organization of the insular cortex to taste quality.

Chapter 5:

Study of taste perception in eating disorders

5.1 Overview

fMRI studies on the gustatory processes in humans have been proven to be fundamental for the evaluation of aberrant abnormalities in psychiatric (Monteleone et al., 2017; Oberndorfer et al., 2013) and neurological pathologies (Doty et al., 2016).
In this chapter I describe the fMRI study of brain mechanisms occurring during taste processing in two types of EDs, AN and BN in comparison with HC.
In particular, two different analyses were performed on the same group of patients and controls in order to reveal (1) the possible presence of some differences occurring during the perception of pleasurable sweet and aversive bitter tastes in the gustatory pathway; (2) the possible abnormalities in the inter-hemispheric (intrinsic) functional connectivity, as possible co-occurrent marker for these two pathologies.

5.2 Introduction

AN and BN are complex psychiatric disorders of great importance for public health policies, as they are associated with a high burden of morbidity and mortality due to their severe medical and psychological consequences (Mehler et al., 2015; Treasure et al.,

2010). Several studies have aimed to elucidate their pathophysiological mechanisms, but unfortunately, the etiopathogenesis of these EDs continues to remain elusive, with the result that their treatment is often unsuccessful (Bulik et al., 2008; Walsh, 2013). A recently proposed hypothesis suggests that an altered evaluation of reward stimuli might be involved in the pathophysiology of EDs (Kaye et al., 2009; Keating et al., 2012; Monteleone and Maj, 2013), and fMRI techniques have been employed to investigate the brain's processing of reward induced by both food-related and non-food-related stimuli in AN and BN, (Keating et al., 2012).

In particular, it has been shown that, compared to healthy controls, AN patients exhibit abnormal activation of different brain areas, including the parietal, the orbito-frontal, the dorso-lateral prefrontal, the anterior cingulate and the medial prefrontal cortex (Frank, 2015, 2014) after exposure to visual food cues, especially for highly palatable foods. Similarly, altered insula, striatum or orbitofrontal responses to sweet stimuli have been found in recovered or symptomatic AN and BN patients (Frank, 2015, 2014). These findings suggest a dysregulation of brain mechanisms involved in the processing of food-related rewarding stimuli in the pathophysiology of EDs. It is reasonable to assume that the way in which the brain processes pleasant stimuli has a pathophysiological significance in EDs, but the neurophysiology of disgusting stimuli may also be significant in the aberrant eating behaviors of AN and BN, since disgust plays a role in the modulation of food intake (Martins and Pliner, 2005) and patients with EDs are characterized by altered disgust sensitivity (Aharoni and Hertz, 2012; Harvey et al., 2002). Specifically, patients with AN or BN have been found to experience specific types of food, especially high-calorie food, as disgusting (Davey et al., 1998) and bulimic patients have been shown to report feelings of disgust at the end of binge-eating episodes (Cooper et al., 1988). It has been proposed that assigning disgusting properties to food may enable AN and BN patients to transform food into a forbidden element that cannot be ingested.

Furthermore, it is plausible that an altered disgust sensitivity to aversive foods may allow BN patients to ingest even non-pleasurable food during their binge episodes. Therefore, although other research studies have suggested that the involvement of disgust emotion in EDs is modest (Davey, 2011), some authors have proposed that investigating the way in which the brain processes disgust elicited by aversive taste stimuli may help to further understand the pathophysiology of EDs (Vicario, 2013). One published study has explored the activation of brain areas elicited by both rewarding and aversive taste stimuli in individuals recovering from AN (Cowdrey et al., 2011). However, those authors employed complex taste stimuli, such as chocolate and strawberry drinks, which do not enable an investigation of basic taste processing, since complex stimuli may also elicit emotional and cognitive responses.

Thus, the first aim of this study was to illustrate the responses to a pleasant (sucrose solution) and an aversive (quinine hydrochloride solution) basic tastes in the gustatory pathway of symptomatic patients with AN and BN compared to healthy subjects. The experimental hypothesis for this study has been that, compared to matched healthy subjects, symptomatic AN and/or BN patients would display different patterns of brain activation not only to the pleasant pure sweet stimulus but also to the aversive pure bitter stimulus. However, because of controversial literature results, reporting both hypo- and hyper-activation of brain areas to taste stimuli (Frank, 2015, 2014), no specific hypothesis regarding the direction of the expected pattern of brain responses to the two tastants has been established.

The second aim of this study was to reveal possible functional brain asymmetry of resting-state fMRI. More specifically it has been observed whether brain regions implicated in reward, cognitive control, starvation and emotion regulation would also show altered inter-hemispheric functional connectivity, and whether such possible alterations would be linked to structural brain properties, such as gray matter atrophy and altered diffusivity

properties in the corpus callosum, a major white matter structure containing anatomical pathways connecting several functionally linked resting-state networks (Van Den Heuvel et al., 2009). Because the parameters of an individual's hemodynamic response function (HRF) (onset-delay, time-to-peak, and width) can vary across regions independently of the underlying functional connectivity (e. g., due to vascular differences), for the first time, it has been further characterized the possible alterations in inter-hemispheric connectivity in terms of the regional inter-hemispheric spectral coherence (IHSC), a frequency-domain correlation analysis that is less sensitive to HRF variability (Sun et al., 2004) than time-domain correlation analysis, that allows evaluating the resting-state fMRI signals also in specific frequency sub-bands (Esposito et al., 2013; Zuo et al., 2010). In particular, the IHSC provides a frequency-by-frequency evaluation of the resting-state functional connectivity between homotopic regions. This measure has been used as an additional tool to characterize the synchronicity of resting-state fMRI signal fluctuations between homotopic regions in the presence of possible VMHC abnormalities between ED patients and controls.

5.3 Materials and Methods

5.3.1 Participants

Subjects consecutively admitted to the outpatient unit of the Eating Disorders Center in the Department of Psychiatry at the University of Naples "Luigi Vanvitelli" were recruited if they met the following inclusion criteria: a) current diagnosis of AN or BN, according to DSM-5, confirmed by the Structured Clinical Interview for DSM-5 Disorders Research Version (First et al., 2015); b) female gender; c) age > 18; d) willingness to cooperate in the experimental procedures and to sign a written informed

consent; e) no psycho- pharmacological treatment during the preceding 6 weeks; f) no history of neurological or medical diseases and drug abuse/dependence; g) no history of head trauma with loss of consciousness; h) no concomitant comorbid Axis I psychiatric disorder. Twenty women with AN (4 of the binge-purging subtype and 16 of the restrictive subtype) and 20 women with BN were enrolled for this study. Twenty healthy women, with no history of psychiatric disorders, as ascertained by the Mini International Neuropsychiatric Interview (Sheehan et al., 1998), were also recruited. Inclusion criteria for healthy controls were as reported for patients in b), c), d), f) and g).
The study was approved by the Ethics Committee of the University of Naples "Luigi Vanvitelli" and performed in accordance with the ethical standards laid down in the 1964 Declaration of Helsinki and its later amendments. Each participant provided her informed consent prior to inclusion in the study.

5.3.2 MRI data acquisition

All subjects underwent an fMRI experiment consisting in the administration and tasting of sweet and bitter solutions while lying in the magnet at 3:00 PM, after 6 h fasting.
Solutions of sucrose (sweet) 0.292 M and quinine hydrochloride (bitter) 0.5mM were used for sweet and bitter tastes: the concentrations used were firstly tested on a group of fifteen volunteers (who do not participate to the fMRI experiment) in order to define the minimum concentrations that were clearly perceived as sweet and bitter tastes and whose perception disappeared within 30 seconds, which was the time interval elapsing between two subsequent taste stimuli (taste solution 20 sec + rinsing water 10 sec) in the fMRI task paradigm (see below).
The two gustatory stimuli plus water, used as reference taste, were administered via two medical injectors (Spectris Solaris, Medrad$_{TM}$) equipped with two syringes each, electronically controlled through a home-made digital I/O device connected to a

laptop. Solutions and water were alternated and rinsing water was delivered after each stimulus; a dedicated line was used for each stimulus in order to avoid cross-contamination. The three lines were pulled together and fixed to the center of the lips thus avoiding shifting of the tubes. Synchronization between fMRI acquisitions and stimuli delivery was controlled with Presentation software.
Subjects were instructed to swish and swallow after each solution injection. Each taste event consisted of the delivery of 1mL of solution over 1 s (1 mL/s injection speed), and then after 20 s rinse water was administered in a 2 mL bolus to avoid taste persistence. The time between two consecutive injections was set to 10 s. The alternation of stimuli and rinsing water prevented physical and perceptual overlapping between the different tastes. Each stimulus was delivered six times. Total fMRI scan duration was 10 min and 23 s with the acquisition of 308 dynamic scans and total beverage volume of 54 mL. Images were acquired on a 3T scanner (Achieva, Philips Medical System, Eindhoven, Holland) and the experimental protocol included an EPI single-shot acquisition (TE=35ms, TR=2000ms, 80x80 matrix, in-plane voxel size 2,87 x 2,87 mm, 30 slices 4 mm thick with no gap), a T1-weighted 3D TFE SENSE volume (sagittal; matrix 256 x 256; FOV 256 x 256 mm; 136 slices; slice thickness 1.2 mm; no gap; in-plane voxel size 1mm x 1mm; flip angle 8°; TR 6,8 ms; TE 3.2 ms, 1 average), a resting-state fMRI sequence (TE=32ms, TR=1700ms, 80x80 matrix, in-plane voxel 3,2 x 3,2 mm, 34 slices 4 mm thick with no gap, 240 dynamic scans) and a diffusion-weighted sequence (TE=102ms, TR=9300ms, 2 averages, matrix 128x128 in-plane voxel size 2x2 mm, 50 slices, slice thickness 2mm, 0.4mm slice gap, B-value 0-1000 mm/sec^2, 16 directions).

5.3.3 Psychopathological and behavioral measures

Prior to brain imaging, all the participants completed self-assessments for: 1) eating-related psychopathology by means of the Eating Disorder Inventory-2 (Garner, 1991); 2) personality

temperament and character dimensions by means of Cloninger's Temperament and Character Inventory-Revised (TCI-R) (Fossati et al., 2007). After scanning, the healthy controls and AN and BN women underwent a taste perception test in order to assess differences in the perception of the two test solutions between the groups. To this end, they underwent the same experimental procedure of administration and tasting of sweet and bitter solutions adopted in the fMRI experiment and had to rate the intensity of their taste perceptions on general Labeled Magnitude Scale (gLMS) (Green et al., 1996). Participants also rated their pleasantness responses to each tastant on a visual analogue scale (VAS), which used a 10cm line with labels at the extremities indicating the most negative (-5) and the most positive ratings (+5); zero in the middle indicated a neutral response.

5.3.4 Data analysis

Task-based FMRI data were processed with the software BrainVoyager QX (Brain Innovation, Maastricht, The Netherlands).
All the scans of functional data were re-aligned to the first included volume scan using a Levenberg–Marquardt algorithm. Motion parameters were carefully inspected to control that no excessive residual motion (>1 functional voxel) was present and then included in the statistical analysis as confounds. The resulting head motion-corrected time series were corrected for the different slice scan times using a cubic spline interpolation procedure and then filtered in the temporal domain. For temporal filtering, a high-pass filter was used to reduce linear and non-linear trends in the time courses; the cut-off was set to seven cycles per time course. The time series of the task-based fMRI data were then spatially filtered (smoothing) using a 6-mm full-width-at-half-maximum Gaussian kernel.

For the analysis of fMRI activations during taste perception, to draw population-level inferences from statistical

maps, six taste-specific linear contrasts were calculated as the difference between the two tastes (sweet and bitter) and the neutral taste (water) for three pairs of consecutive repetitions of the stimuli, and then entered a second-level analysis of variance with subjects treated as random observations. At each voxel, a 2w- ANOVA table was calculated, with one within-subject factor for the taste effect (including six levels coding sweet and bitter tastes vs. water across the three blocks of repetitions) and one between-subject factor for the group effect (including three levels for the three groups of AN patients, BN patients and healthy controls). From this table, t-maps of one- and two-group main and differential effects (respectively from one- and two-sample t tests) were computed for each separate stimulus type and their interactions and these were then overlaid on the average Talairach-normalized anatomical scan. For all comparisons, a single brain mask of 15782 mm^3 was used containing all regions known to belong to the cortico-striatal taste pathway (see, e. g (Oberndorfer et al., 2013)). This mask included bilaterally the insula, the dorso-lateral prefrontal cortex (DLPFC), the caudate, the putamen and the pallidum, the thalamus, the amygdala, the parietal cortex, the orbito-frontal cortex, the brainstem and the anterior cingulate cortex (ACC). In order to build this mask, these regions were initially extracted from the Harvard Oxford atlases as separate masks and then merged together to form a single mask that was registered to Talairach space. To localize all brain regions with statistically significant main and differential effects within this mask, a statistical threshold was applied to the t-maps, which protected against false-positive clusters at 5% (cluster- level corrected for multiple comparisons over the entire mask after 1000 Montecarlo simulations) (Forman et al., 1995). Differences in behavioral and clinical variables were statistically assessed by means of ANOVA with or without repeated measures, where appropriate.

For inter-hemispheric functional connectivity, I followed standard methods for the preprocessing and analysis of resting-state functional data, as implemented in the Data Processing

Assistant for Resting-State fMRI (DPARSF 4.0) (Yan Chao-Feng and Zang Yu-Feng, 2010), REST 1.8 (Song et al., 2011), and SPM8 (http://www.fil.ion.ucl.ac. uk/spm) running on MATLAB R2012a (The MathWorks Inc., Natick, MA, USA).

Resting-state Echo-planar imaging volumes were corrected for slice timing differences and head-motion, band-pass filtered (0.01–0.08 Hz), spatially normalized to the MNI echo-planar imaging template, resampled to a voxel size of 3 x 3 x 3 mm^3, and smoothed with a Gaussian kernel of 6 mm full width at half maximum (FWHM). In order to minimize physiological artifacts, the six motion parameters resulting from the head motion correction, as well as nuisance signals from white matter and cerebrospinal fluid, were regressed out from the filtered time-series.

After regression, the residual time-series were used to calculate the voxel mirror homotopic connectivity (VMHC) maps. To obtain a VMHC map for each participant, the individual 4D residual time-series data set were further registered to the MNI-152 symmetric template. In the MNI-152 symmetric template voxel space, the Pearson correlation coefficient (r) was computed at each voxel in one hemisphere between the residual time series of that voxel and the time series of the symmetrical voxel in the other hemisphere. To improve the normality of the expected statistical distribution, the correlation r values were Fisher transformed to z values.

T1-weighted native space images were segmented into gray and white matter and normalized to MNI standard space using DARTEL (Ashburner, 2007). The resulting gray matter probabilistic maps were modulated by the Jacobian determinants of the deformations to account for local compression and expansion due to linear and non-linear transformation (Good et al., 2001) and then smoothed with a Gaussian kernel of 6 mm FWHM. These maps were used to assess any differences in terms of atrophy between patients and HC (voxel-based morphometry, VBM) and to create a symmetric gray matter mask for VMHC analysis. For the latter purpose, all smoothed gray matter maps were averaged and resampled to a voxel-size of 3 x 3 x 3 mm^3, then again averaged

with a left–right flipped version of the same maps, and, last, these were finally thresholded at an intensity of 0.2.
Diffusion-weighted images were preprocessed and analyzed with FSL. Eddy current distortions and head motions were corrected with FMRIB's Diffusion Toolbox. Non-brain tissue was removed with the Brain Extraction Tool. Subsequently, DTIFIT was used to fit the diffusion tensors and generate fractional anisotropy (FA) maps. These FA maps were nonlinearly registered to MNI space (template MNI152_T1_2mm_brain) and subsequently smoothed with a Gaussian kernel of 4 mm FWHM. An anatomical mask of the corpus callosum was produced with Wake Forest University (WFU) pickatlas (http://fmri. wfubmc.edu/software/pickatlas) and FA values within the corpus callosum were extracted in all participants.

Signals from resting state fMRI volumes normalized to the symmetric group template were also used to perform an IHSC analysis between the homotopic regions in which a significant difference had emerged in the previous VMHC analysis comparing both HC and AN patients and HC and BN patients.
To this aim, spherical VOIs (radius 6.00mm) centered in the peaks of significantly inter-hemispheric differences were created and then extracted the mean regional time courses of each subject for all the considered VOIs.
For each selected pair of homotopic time series, x(t) and y(t), the power spectral density (Pxx(f) and Pyy(f)) and the cross power spectral density (Pxy(f)) were computed in MATLAB using the Welch's periodogram approach (256-point discrete Fourier transform (DFT), Hanning window, overlap: 50%). Then, for each frequency f, IHSC measures were computed using the following formula:

$$IHSC(f) = Coh_{xy(f)} = \frac{|P_{xy}(f)|^2}{P_{xx}(f)P_{yy}(f)}$$

IHSC values were obtained for all subjects and VOIs in the range of frequencies between 0.01Hz and 0.08Hz and were also averaged in two sub-ranges, 'Slow-4' (0.027–0.073Hz) and 'Slow-5' (0.01–0.027Hz) according to previous works (Zuo et al., 2010), (Esposito et al., 2013).

Two-tailed voxel-wise t-tests were conducted using REST software on z-transformed VMHC maps to compare patients (respectively AN and BN) and HC within the symmetrical gray matter mask, with age as covariate. The threshold for significance was corrected for multiple comparisons at a global $p < 0.05$ (single voxel: $p < 0.01$; $|T| > 2.58$), requiring a cluster size of at least 110 and 94 voxels for the comparison between AN and HC as well as between BN patients and HC, as obtained from 1000 Monte Carlo simulations conducted with AlphaSim as implemented in REST. The Monte Carlo simulation was performed within the symmetrical, unilateral gray matter mask. Regions of interest (ROIs) were created for clusters exhibiting significantly different VMHC in patients compared to controls and mean regional VMHC values within these regions were extracted.

To exclude a possible effect of atrophy, a two-sample t-test between patients and HC, both in the whole brain VBM and in each ROIs (after normalization to the total intracranial volume) were performed, which exhibited differences in the homotopic connectivity. In addition, absolute left–right differences in gray matter volumes were computed for each subject in each homotopic cluster and these indices of asymmetry were compared across cohorts using a one-way ANOVA test, with group as factor.

In order to investigate the relationship between the structural connectivity of the corpus callosum and homotopic connectivity, an analysis of covariance (ANCOVA) was computed to produce statistical maps of correlation between regional values of VMHC and regional FA values of the corpus callosum in the considered groups, corrected for multiple comparison using Monte Carlo simulations within the corpus callosum.

One within (frequency range) and one between (group) factor ANOVA test (1W1B-ANOVA) was performed on mean IHSC values of the three groups in all the considered VOIs. A post-hoc two-sample t-test was finally performed to assess the difference between groups in each frequency range. Spearman correlation coefficients were calculated between regional values of VMHC and age, body mass index (BMI) and disease duration (measured in years).

5.4 Results

5.4.1 Clinical and behavioral measures

From the initial sample of subjects (used for the task-based), fifteen AN females (mean age 26 ± 3.4 years), thirteen BN female (mean age 25.5 ± 6.3 years) and sixteen age-matched female HC (mean age 26.6 ± 7.1 years) were considered for the inter-hemispheric functional connectivity, after a screening of time series that exceeding 3 functional voxels in the motion correction of the resting state data.
A 3-way ANOVA with repeated measures performed on the offline taste perception intensity scores showed no significant effects for group ($F_{2,57} = 0.04$, $p = 0.9$), for time ($F_{5,285} = 1.16$, $p = 0.3$) and for their interactions: group x time ($F_{10,285} = 0.51$, $p = 0.8$), group x tastant ($F_{2,57} = 0.05$, $p = 0.9$), tastant x time ($F_{5,285} = 0.17$, $p = 0.9$) and group x tastant x time ($F_{10,285} = 0.84$, $p = 0.8$). These results demonstrate that the two tastants were clearly perceived by all 3 groups without any significant difference in both the intensities and the perception time patterns among the groups. Similarly, a 2-way ANOVA on the pleasantness ratings of the two tastants showed no significant effect for group ($F_{2,114} = 0{,}80$ $p = 0.4$), a significant effect for tastant ($F_{1,114} = 534.38$, $p < 0.00001$) and no significant group x tastant interaction ($F_{2,114} = 0.23$, $p = 0.7$), showing that a clear difference existed in the pleasantness rating of the two

tastants without significant differences among the groups. The effect size scores for sweet/bitter pleasantness difference were: Cohen's d = 5.88 for healthy women, Cohen's d =5.64 for AN women and Cohen's d = 2.86 for BN women.

5.4.2 fMRI Activation during Sweet and Bitter Taste Processing

While the main effect of functional activations were largely overlapping across the three groups, comparing sweet and bitter responses (sweet vs bitter contrast) produced opposite polarity patterns in healthy controls compared to AN and BN patients. Indeed, in healthy controls the response to the bitter stimulus was higher overall than the response to the sweet stimulus and this difference was statistically significant in several regions of the taste pathway (Table 15; Figure 32a).

Regions	x	y	z	t	Cluster Size	P value
Right Brainstem	8	-14	-21	5.11	529	<0.0001
Right Putamen	23	-8	15	-4.69	368	<0.0001
Left Caudate	-16	10	15	-3.99	515	0.0002
Left Postcentral Gyrus	-28	-23	15	-4.63	532	<0.0001
Anterior Cingulate Cortex	-4	46	31	-3.67	319	0.0005
Right Postcentral Gyrus	35	-29	36	-4.87	681	<0.0001
Left Putamen	-19	8	9	-3.51	490	0.0009
Left Inferior Insula	-34	10	-12	-3.71	294	0.0005

Table 15: *Main effects obtained by the contrasts sweet vs. bitter in healthy subjects (sweet<bitter)*

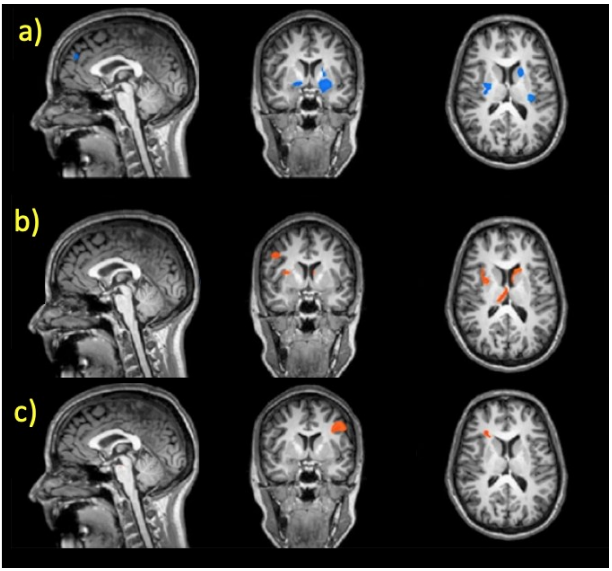

Figure 32: *Maps of main effects after sweet and bitter tastes in HC (a), AN (b) and BN (c).*

Whereas, in both AN and BN patients, the sweet response was higher overall than the bitter response (*Figure 32* b and c; Table 16 and Table 17).

Regions	x	y	z	t	Cluster Size	P value
Left Caudate	-17	19	12	4.60	268	<0.0001
Left Orbitofrontal Cortex	-16	43	9	4.07	569	0.0001
Right Thalamus	8	-20	12	3.92	195	0.0002
Right Anterior Insula	33	10	12	3.34	227	0.0015
Right Dorso-lateral-prefrontal Cortex	38	10	33	5.95	814	<0.0001
Right Putamen	26	1	12	4.15	209	0.0001

Table 16: *Main effects obtained by the contrast sweet vs bitter in women with anorexia nervosa.*

Regions	x	y	z	t	Cluster Size	P value
Left Dorso-lateral-prefrontal Cortex	-43	2	39	4.73	847	<0.0001
Left Brainstem	-10	-15	-21	3.50	350	0.001
Right Brainstem	8	-11	-21	5.21	578	<0.0001
Right Orbito-frontal Cortex	17	42	6	4.42	485	<0.0001
Left Orbito-frontal Cortex	-14	49	3	4.26	201	<0.0001
Right Post-central Gyrus	44	-32	48	5.25	396	<0.0001

Table 17: *Main effects obtained by the contrast sweet vs bitter in women with bulimia nervosa.*

In AN, this effect was statistically significant in the left caudate, left orbitofrontal cortex, right thalamus, right anterior insula, right putamen and right DLPC. In BN, the sweet prevalence was statistically significant in the left DLPC, left and right brainstem, left and right orbitofrontal cortex, right postcentral gyrus. However, the group-by-condition analysis (sweet vs bitter in healthy controls vs AN patients, in healthy controls vs BN patients and in AN patients vs BN patients) did not reveal statistically significant effects.

When comparing healthy controls and patients for single tastes, significantly reduced BOLD responses to the bitter stimulus were detected in both AN and BN women (Figure 33 and Figure 34).

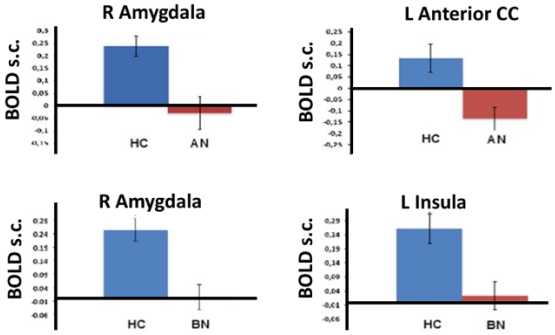

Figure 33: *BOLD signal changes (s.c.) in response to bitter stimulus extracted in the right amygdala and left anterior cingulate cortex (CC), as obtained from the comparison between healthy controls (HC) and patients with anorexia nervosa (AN) (upper row), and in the right amygdala and left insula, as obtained from the comparison between healthy controls (HC) and patients with bulimia nervosa (BN) (lower row).*

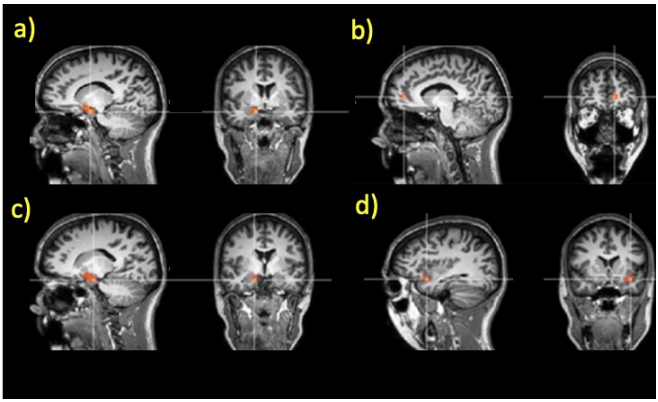

Figure 34: *Maps with differential group effects (healthy controls vs patients with anorexia nervosa or bulimia nervosa) for responses to the bitter stimulus. Significant effects are detected in the right amygdala (a) and anterior cingulate cortex (b) for the comparison between healthy controls and patients with anorexia nervosa, and in the right amygdala (c) and left insula (d) for the comparison between healthy controls and patients with bulimia nervosa.*

In particular, compared to healthy controls, the BOLD responses to the bitter stimulus of AN patients were significantly reduced in the right amygdala ($p < 0.005$) and left ACC ($p < 0.005$) while the BOLD responses to the bitter stimulus of BN patients were significantly reduced in the right amygdala ($p < 0.005$) and left insula ($p < 0.005$). For these analyses, the obtained thresholds for the cluster size (extent cut-off points) resulting from Montecarlo simulations were 432 mm^3 and 459 mm^3 respectively for the comparisons HC vs AN and HC vs BN. No significant differences emerged from the comparison between healthy controls and patients for the sweet stimulus. The peak coordinates, the t- and p-values, the cluster sizes and the post-hoc statistical power of the performed analyses are reported in Table 18.

Group comparison	Region	x	y	z	t	Size (mm^3)	Power
HC vs. AN	RH amygdala	12	-1	-11	5.53	1492	99.9%
HC vs. AN	LH anterior cingulate cortex	-12	47	10	3.98	436	59.2%
HC vs. BN	RH amygdala	15	2	-11	4.2	1338	99.9%
HC vs. BN	LH Insula	-33	14	-11	3.9	679	99.6%

Table 18: *Results of groups by taste effects (bitter) in the regions significantly different in the comparison healthy controls vs patients with anorexia nervosa (AN) and healthy controls vs patients with bulimia nervosa (BN) during bitter perception.*

As no significant group effects were found for the sweet condition, following Wagner et al.'s findings (Wagner et al., 2006) which suggest habituation effects in brain areas responding to sequentially presented sucrose stimuli in healthy subjects, we assessed possible repetition-related suppression effects in the sweet and bitter responses within and between the three groups. More specifically, we looked at the regional effects of the repetition

factor (defined over levels corresponding to three consecutive blocks of two consecutive repetitions of the stimuli) for both sweet and bitter stimuli in all the above reported regions. In all cases, a 2w- ANOVA with repeated measures was performed, and the group repetition interaction was assessed, but no statistically significant effects emerged.

5.4.3 Inter-hemispheric functional connectivity

VMHC comparison: The comparison of both cohorts revealed significantly reduced VMHC in patients with AN and BN compared to HC (Figure 35).

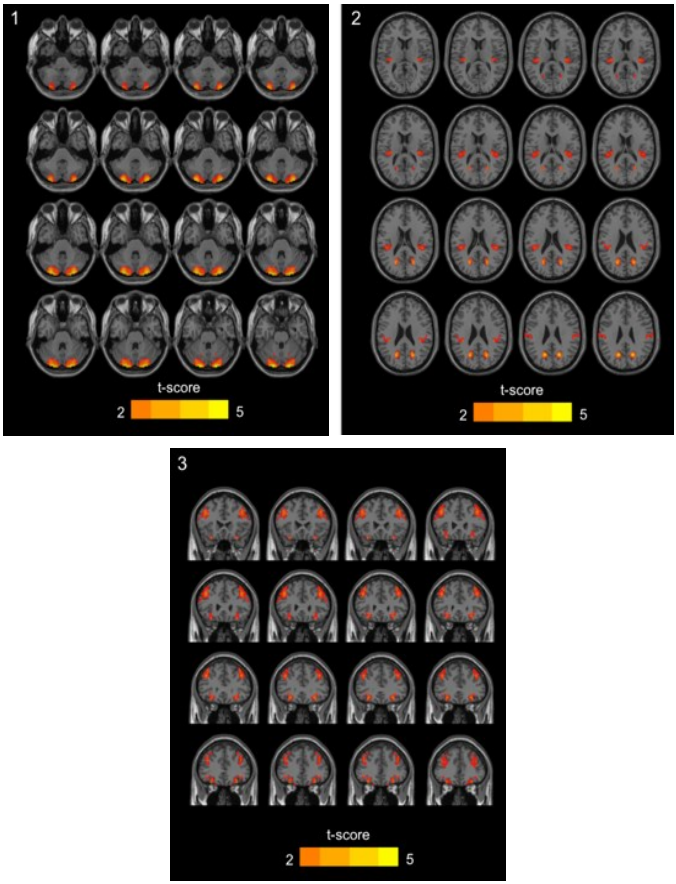

Figure 35: *(1) Clusters of significantly reduced VMHC (P < 0.05 corrected) in AN compared to HC in the cerebellum; (2) Clusters of significantly reduced VMHC (P < 0.05 corrected) in AN compared to HC in the insula and precuneus; (3) Cluster of significantly reduced VMHC (P < 0.05 corrected) in BN compared to HC in the OFC and DLPFC.*

Lower VMHC was observed in the precuneus, cerebellum and in the posterior insula comparing AN versus HC, while lower VMHC was found in the frontal lobe comparing BN and HC. The latter cluster extends from the orbital-frontal cortex (OFC) to the dorso-lateral prefrontal cortex (DLPFC). The cluster peak MNI coordinates are reported in Table 19 and in Table 20. The

comparisons of the regional VMHC values are reported in Figure 36. In none of the highlighted regions, the regional VMHC values were found to be correlated with age, BMI or disease duration.

Brain Region	Cluster Size	MNI Coordinates			T(29)
		x	y	z	
Cerebellum	721	±18	-93	-24	-5.09
Insula	152	±39	-30	24	-3.09
Precuneus	156	±15	-66	30	-4.92

Table 19: *Regions with significantly lower VMHC in AN patients compared to HC: cluster size, peak-location and t-statistic.*

Brain Region	Cluster Size	MNI Coordinates			T(27)
		x	y	z	
Frontal lobe	570	±33	57	-3	-5.22

Table 20 : *Regions with significantly lower VMHC in patients with BN compared to HC: cluster size, peak-location and t-statistic.*

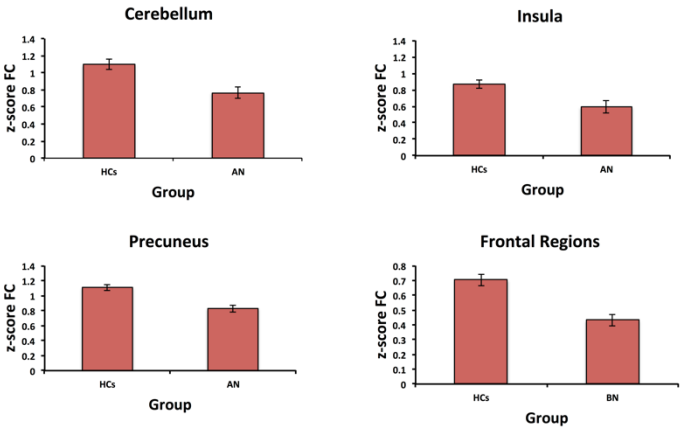

Figure 36: Mean z-score values in the clusters with significant differences in VMHC (both in the comparison between HC and AN and between HC and BN).

VBM comparisons: At the default SPM statistical threshold ($p=0.05$, family-wise corrected for multiple comparisons), the VBM analysis revealed no significant differences between HC and AN and between HC and BN, both in the whole brain analysis and in the ROIs with reduced VMHC in patients. Identical results were obtained using the false discovery rate (FDR) as an alternative correction criterion for voxel-based analyses. At a lower significance threshold ($p=0.001$, uncorrected for multiple comparisons), the VBM analysis returned three clusters of reduced gray matter volumes for the comparison between AN and HC, located in right frontal inferior orbital cortex, left middle frontal gyrus and right post-central gyrus. None of these clusters was found to overlap with regions obtained from the VMHC analysis of resting-state fMRI data. The ANOVA test did not produce statistically significant differences in terms of left-right gray matter volume asymmetry between AN and HC (Cerebellum: $F=1.47$, $df=1$, $p>0.05$; Precuneus: $F=1.05$, $df=1$, $p>0.05$; Insula: $F=3.04$, $df=1$, $p>0.05$) and between BN and HC (Frontal Lobe: $F=0.63$, $df=1$, $p>0.05$).

Performing the ANCOVA analysis considering mean VMHC values in the cerebellum, precuneus, insula and frontal regions and mean FA values in the corpus callosum, no significant effect of FA was found ($p>0.05$). Performing the ANCOVA analysis between regional values of VMHC and FA in each voxel of corpus callosum, a compact cluster was detected in the genu of the corpus callosum, in which FA was significantly correlated ($p<0.05$, corrected for multiple comparisons at the cluster level) with the VMHC values in the insula (Figure 37). This correlation was not different between HC and AN (i.e. no group x FA interaction).

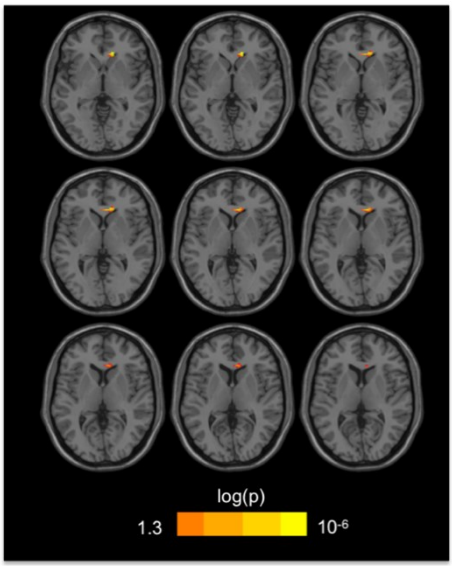

Figure 37 : *Cluster of significant correlations between VMHC in the insula and FA in each voxel of the corpus callosum, considering AN and HC.*

For the spectral coherence analysis, comparing HC and AN patients in the full range of frequencies, mean IHSC values were significantly reduced in AN in cerebellum ($p<0.01$) and precuneus ($p<0.001$) VOIs. Comparing HC and BN patients, in the frontal regions IHSC values were significantly reduced in BN ($p<0.01$). The mean IHSC signals at all frequencies in the considered VOIs are reported in Figure 38.

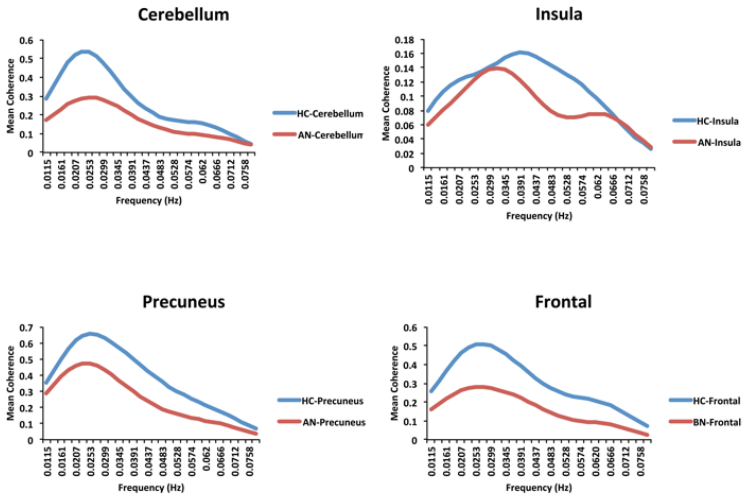

Figure 38 : *Frequency trend of mean coherence signals in the considered VOI in the comparison between HC vs AN and HC vs BN.*

Considering HC and AN, and dividing the spectral band in the two canonical sub-ranges, 1W1B-ANOVA test revealed significant effects of group and frequency range in the cerebellum (Group: F1=13.73 dF1=1 $p<0.001$; Frequency range: F2=20.37 dF2=1 $p<0.0001$; Interaction: F(dF1,dF2)=2.75 $p>0.05$), significant effects of group and frequency range in the precuneus (Group: F1=12.8 dF1=1 $p<0.001$; Frequency range: F2=29.03 dF2=1 $p<0.0001$; Interaction: F(dF1,dF2)=0.00, $p>0.05$), and no significant effect of group and frequency range in the insula (Group: F1=1.1 dF1=1 $p>0.05$; Frequency range: F2=0.00 dF=1 $p>0.05$; Interaction: F(dF1,dF2)=0.08, $p>0.05$).

In the frontal region, only the group (HC and BN) factor was significant (Group: F1=9.64 dF1=1 $p<0.01$; Frequency range: F2=2.06 dF2=1 $p>0.05$; Interaction: F(dF1,dF2)=0.8, $p>0.05$).

Considering the mean IHSC values, post-hoc two-sample t-test performed on two groups separately for each band ('Slow-4', 'Slow-5') revealed a significant difference in the 'Slow-5' range in the cerebellum ($p_{Slow\text{-}4}=0.07$, $p_{Slow\text{-}5}<0.01$, HC vs AN), in the 'Slow-

4’ frequency range in the precuneus ($p_{Slow-4}<0.001$, $p_{Slow-5}=0.06$, HC vs AN) and in both ‘Slow-5’ and ‘Slow-4’ frequency ranges in the DLPFC-OFC ($p_{Slow-4}<0.05$, $p_{Slow-5}<0.05$, HC vs BN), while in the insula a significant difference between AN and HC did not occur in both ‘Slow-5’ and ‘Slow-4’ frequency ranges ($p_{Slow-4}<0.24$, $p_{Slow-5}<0.64$, HC vs AN), albeit a significant difference emerged in a smaller range of frequency in 'Slow 4' (from 0.0299 to 0.0643Hz, $p<0.001$). Figure 39 reports the mean values of regional IHSC of the studied groups in the ‘Slow-4’ and ‘Slow-5’ frequency ranges.

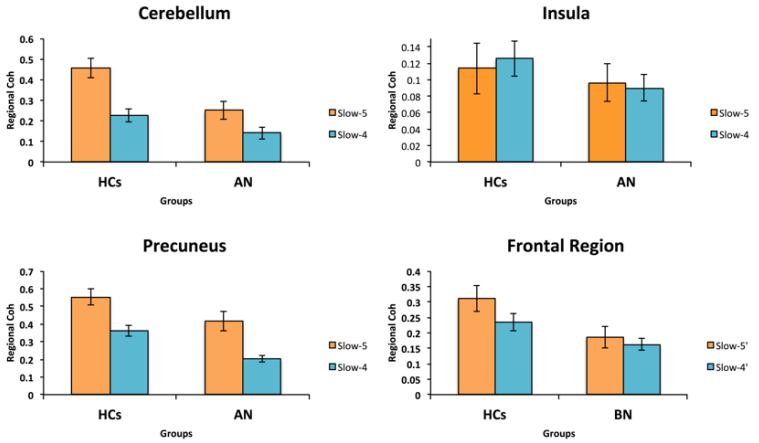

Figure 39: *Main effects of regional spectral coherence in the VOIs extracted from VMHC in the comparison between HC and AN and between HC and BN*

5.5 Discussion

The first finding of this study was that pleasant and aversive taste stimuli activated overlapping brain regions and areas that were specific to each taste in all the groups. In particular, in healthy subjects, the insula, post-central gyrus, medial cingulate cortex (MCC) and brainstem were activated by both sweet and bitter tastes while, in AN patients, both stimuli activated the insula,

MCC and post-central gyrus (as in healthy controls) as well as the striatum, orbitofrontal cortex, amygdala, thalamus and DLPFC; in BN patients, both taste stimuli activated the thalamus (as in AN patients), MCC, insula and post-central gyrus (as in the two other groups). These findings in healthy subjects are in line with previous studies showing that pleasant and aversive tastes have overlapping representations in the brain of healthy humans, although the activated brain areas differed in the various studies, probably because of different experimental paradigms (Haase et al., 2009; O'Doherty et al., 2001). Only one published study has assessed activation of brain areas to both pleasant and aversive taste stimuli in ED patients and it showed that in recovered AN patients the anterior insula was the only area activated by both chocolate (pleasant) and strawberry (aversive) tastes (Cowdrey et al., 2011). Therefore, this study is the first one to show an overlapping activation by pleasant and aversive taste stimuli of brain areas other than the insula, in symptomatic AN and BN patients. Furthermore, it has been found that in both AN and BN patients the brain response to sweet stimulus prevailed over the response to the bitter one in several areas of the taste-reward pathways, whereas the opposite occurred in healthy subjects. These results suggest that the ratio of aversive/pleasant taste stimulation as well as the pattern of brain area activation by each tastant are altered in symptomatic ED patients, who seem to exhibit higher brain activation by a pleasant taste than by an aversive one, despite the fact that there were no significant differences in either the intensity or the pleasantness ratings of sweet and bitter stimuli with respect to healthy controls. Such a discrepancy between the subjective experience of the tastant and the objective neural response pattern is not easy to explain. One hypothetical inference could be that in ED patients the prevalence of brain activation by the sweet stimulus may be linked to an intrinsically higher salience that these subjects attribute to pleasant taste stimuli, since these are potentially linked to foods with a higher calorie content, and they are thus more threatening than unpleasant taste stimuli. Indeed, sweet-induced activation seems to

prevail over that induced by the bitter taste in brain areas implicated in the processes of salience attribution to external stimuli, such as orbitofrontal cortex and anterior insula (Kullmann et al., 2013).

The second major finding of this study is that, compared to healthy women, AN patients displayed significant reduced BOLD responses to the bitter stimulus in the right amygdala and left ACC while symptomatic BN had reduced BOLD responses to the bitter stimulus in the right amygdala and left insula. No significant quantitative differences emerged between patients and controls in brain area responses to the sweet taste although, as stated above, the pattern of brain area activation differed among the groups. In these patients, the normal insula response to the sweet stimulus together with the behavioral findings showing that the intensity and the pleasantness of the sweet perception did not differ from normal controls may suggest that the physiology of basic sweet perception is not altered in symptomatic AN and BN patients. These results contrast with literature data. Indeed, (Wagner et al., 2008) and (Oberndorfer et al., 2013) reported a diminished insula response to sucrose in recovered AN women, and lower glucose-induced activation of ACC and occipital cortex (Frank et al., 2006) or increased insula response to sucrose ingestion (Oberndorfer et al., 2013) were found in women recovered from BN or from bulimic-type EDs, while behavioral studies provided mixed results with both decreased or normal sweet taste perception in symptomatic and/or recovered women with AN and BN (Aschenbrenner et al., 2008; Casper et al., 1980; Fernández-Aranda et al., 2016; Goldzak-kunik et al., 2012; Nozoe et al., 1996). These discrepancies could be mainly dependent on differences in the patients' illness status and/or in the taste test procedures. In this regard it is worth noting that, in order to assess the basic processes of sweet perception, we used a sweet solution whose sucrose concentration matched the sweet taste perception threshold as determined in a preliminary taste perception test. On the same line of research, other groups have assessed fMRI responses to pleasant taste stimuli in AN patients. (Vocks et al., 2011) detected increased right amygdala and

left medial temporal gyrus responses to chocolate milk in symptomatic AN patients. Similarly, (Cowdrey et al., 2014) found increased neural response to the pleasant chocolate taste in the ventral striatum of recovered AN patients. However, the pleasant taste stimulus adopted by (Vocks et al., 2011) and by (Cowdrey et al., 2011) was not a basic pure taste; consequently, cognitive and emotional aspects may have prevailed in those experimental paradigms. In actual fact, (Vocks et al., 2011) interpreted their results as the expression of the patients' fear of weight gain triggered by drinking a potentially harmful high-calorie food such as chocolate milk. Since (Wagner et al., 2006) demonstrated a habituation effect to a sequentially presented sucrose stimulus in the insula, amygdala, DLPFC, hippocampus and ACC of healthy women, we decided to determine whether such an effect may have been responsible for the lack of differences in quantitative brain responses to sweet stimulus between our patients and controls. Our analysis, specifically looking for a progressive reduction in brain area activation by sequentially delivered sweet taste stimulus, showed that this was not the case in any group. Furthermore, our behavioral findings did not show any progressive reduction in the intensity of the sweet perception following the sequential delivery of the sucrose solution.

This study has been the first in reporting that the responses of right amygdala and left ACC to an aversive taste stimulus in acute AN patients were significantly lower than those of healthy controls; similarly, BN patients showed significantly reduced responses of right amygdala and left insula to the bitter stimulus compared to controls, despite there being no significant differences between the groups in the intensity and pleasantness ratings of the bitter solution. Discordant with our findings, (Cowdrey et al., 2011) found increased activation responses of insula and putamen to an aversive taste in recovered AN subjects. Again, in that study, the aversive stimulus was represented by a complex taste stimulus (strawberry drink), which would imply emotional and cognitive consequences other than pure taste responses, and the patients were

not in the acute phase of the illness. No previous studies have explored brain activation following an aversive taste stimulus in symptomatic BN women, so these findings are not comparable to literature data and need confirmation in future studies. In any case, since the amygdala is recognized as a key structure involved in the attribution of affective significance to external stimuli (Irwin et al., 1996), our findings of reduced amygdala activation by the bitter taste in both symptomatic AN and BN women may suggest, for the first time, that these patients assign a reduced aversive fear-related salience to an unpleasant taste stimulus. Moreover, the reduced activation of the insula by the bitter stimulus in our symptomatic BN patients might have pathophysiological implications. Indeed, it is widely acknowledged that disgust perception plays a major role in eating behavior by protecting the subject against the ingestion of non-palatable and/or potentially harmful foods (Chapman and Anderson, 2012); therefore, a reduced sensitivity of the primary gustatory cortex to aversive tastes might represent the neurobiological correlate of the tendency of bulimic patients to ingest both pleasurable and non-pleasurable foods during their binge episodes. Finally, the reduced bitter-induced activation of ACC in our symptomatic AN women might be the expression of a reduced selective attention for food-related aversive stimuli, since ACC plays a major role in attention control and response selection (Critchley et al., 2005). From all the above, these results could potentially infer that symptomatic AN and BN women have an impaired aversion to unpleasant bitter tastants, which are likely to be perceived as less threatening food cues.

The third major finding of this study comes from the inter-hemispheric functional connectivity analysis, reporting reductions in acute AN and BN patients compared to the HC group.
Resting state fMRI studies have reported in AN and BN both reductions and increases within and between specific networks, such as the default mode network (DMN) (Boehm et al., 2014; Cowdrey et al., 2014), the visual and somatosensory networks

(Favaro et al., 2012), the salience network (Boehm et al., 2016), the executive control network (Lao-Kaim et al., 2015) and the cerebellar network (Amianto et al., 2013), but possible alterations in the general inter-hemispheric connectivity in ED were not explored. Furthermore, many studies highlighted the importance of hemispheric interplay for cognitive and emotional processing (Compton et al., 2005; Toro et al., 2008; Wang et al., 2013) as well as for complex behavioral control functioning (Wang et al., 2013). Since it has been also established that patients with ED are characterized by altered reward processing and cognitive control, especially in relation to food-related behavior (see (Kaye et al., 2011) for review), it is reasonable to expect possible deficits in inter-hemispheric functional connectivity.

In a VMHC analysis, possible regions with higher (respectively lower) VMHC values have been previously interpreted as indexing more inter-hemispheric coordinated (respectively more independently segregated) processing in the corresponding neuronal communities (Zuo et al., 2010) and previous studies have speculated about a possible role of a reduced inter-hemispheric cooperation in neurological and other psychiatric diseases. For example, in the study of Luo et. al (Luo et al., 2015), the reduced homotopic connectivity in Parkinson patients in the putamen and in sensori-motor areas have been linked to asymmetrical dopamine depletion and to reduced abilities in handling complex motor tasks. In multiple sclerosis patients (Zhou et al., 2013), both decreased and increased VMHC have been reported, that were respectively linked to sensory, movement, and memory deficits and to possible compensatory phenomena. In psychiatric disorders like Major Depression (Hermesdorf et al., 2016), Unipolar and Bipolar Depression (Wang et al., 2015) and Schizophrenia (Li et al., 2015), reduced VMHC has been associated with reduction in self-referential and reward processing (Hermesdorf et al., 2016), disturbance in cognition, behavior and emotion processing (Wang et al., 2015) and alterations in auditory somatosensory processing (Li et al., 2015).

Present findings demonstrate for the first time that patients with acute AN or BN show specific deficits in inter-hemispheric functional connectivity. In particular, a cluster of reduced VMHC in AN was found in the cerebellum, a brain structure implicated in motor and cognitive control functions (Schmahmann, 2010), social cognition (Hoche et al., 2016), emotion regulation and cognitive flexibility (Dickson et al., 2016). All these aspects are considered relevant for many physiological functions including food intake behavior (Zhu et al., 2006), thereby, our result would support the hypothesis that the cerebellum plays a prominent role in feeding behavior (Zhu and Wang, 2008), and that the observed inter-hemispheric functional dysconnectivity of cerebellar regions could be characteristic of the AN phenotype.

Although reduced inter-hemispheric connectivity in the cerebellum is a novel finding in AN, its involvement in EDs has been previously reported. For instance, reduced activation in the bilateral cerebellar vermis was shown in AN patients when asked to think about eating food after visual cues (Brooks et al., 2013), suggesting a possible dysregulation of the bottom-up appetitive network in AN feeding behavior. In contrast, Amianto et al. (Amianto et al., 2013) reported an increase of intrinsic oscillations in the cerebellar network of AN patients. On the other hand, the intrinsic functional connectivity assessed at the network level, is domain-specific (i.e. relies on preliminary network separation) and concurrently depends on both the amplitudes and the phases of the resting-state fMRI signals, whereas the homotopic functional connectivity, similar to the task-based functional activity, is not domain-specific and mainly depends on the phases of the resting-state fMRI signals.

From this analysis, in addition, a cluster of reduced VMHC in AN was found in the precuneus, which is the central hub of the DMN. Previous studies reported respectively reduced (McFadden et al., 2014) or increased (Boehm et al., 2014; Cowdrey et al., 2014) resting state functional connectivity in the DMN of AN patients in the acute or recovered phase. The DMN and, in particular, the

precuneus support self-related cognitive activities (Buckner et al., 2008) and the reduced network activity as well as reduced inter-hemispheric connectivity in the precuneus may reflect alterations in self-awareness processes of acute AN patients. Thereby, based on the current literature, this result of reduced inter-hemispheric functional connectivity in the precuneus of AN patients could be dependent on the illness state and similarly linked to a mechanism of functional dysconnectivity that is either plastically restored (Boehm et al., 2016) or overcompensated (Cowdrey et al., 2014), after recovery.

Another cluster of reduced VMHC was found in the posterior insula of AN patients. This site is crucial for interoception and for interoceptive awareness, associated with both emotional experience and with processing of emotional stimuli (Craig, 2003). Interoceptive processes activate a well-characterized neuroanatomical pathway that overlaps with several neural systems including the insula, which is thought to be deregulated in individuals with AN (Craig, 2003; Nunn et al., 2011; Tracey and Mantyh, 2007). Indeed, AN patients often display behavioral traits that could be related to impaired interoception such as difficulty in describing and identifying feelings (Bagby et al., 1994a, 1994b; Keller et al., 2006), which raises the possibility that individuals with AN have an impaired ability to effectively use interoceptive information to appropriately value immediate outcomes. Thus, it is possible to speculate that the observed lower inter-hemispheric connectivity in the posterior insula may contribute the anomalous interoceptive state of AN patients, in the form of a loss of functional coordination and cooperation between the two hemispheres. A reduction of functional connectivity in the posterior insula of AN patients, albeit not specific to the inter-hemispheric synchrony, has been also recently reported in (Geisler et al., 2015) in the context of a graph-theoretical analysis. In particular, they found local thalamo-insular network disruption suggesting a less efficient access of AN patients to sensory information and an alteration in integrating exteroceptive and

interoceptive information, emotion and cognition. Also in (Ehrlich et al., 2015), a reduction in functional connectivity in a brain network containing thalamus and posterior insula (as central hub) was found using network based statistics, thus reflecting an altered calibration of signals such as pain, body size and hunger that subsequently contribute to abnormal cognitive behaviors. Thus, our result of reduced inter-hemispheric synchrony in the posterior insula could potentially contribute to further explain the observed alterations in AN disease in terms of impaired cooperation between the hemispheres, an aspect that was not highlighted in previous reports.

Finally, in the comparison between HC and BN patients, we found a significant reduction of VMHC in the DLPFC and the OFC. The DLPFC and the medial prefrontal cortex including the OFC have been reported to be critically involved in impulsive behaviors (Cho et al., 2012) as well as in the cognitive and emotion regulation (Kober et al., 2010). In line with our findings, Chen et al. (Chen et al., 2016) observed reduced homotopic connectivity in the DLPFC of 'restrained eaters'. This reduction was linked to the failure in inhibiting hedonic eating as well as to the lack of top-down control of appetite, which both involve the DLPFC (Brooks et al., 2013; Jasinska et al., 2011). Moreover, previous task-based studies have reported abnormally higher activation of the OFC in BN during the "monetary and food incentive delay" task (Simon et al., 2016) and during the visual perception of reward-food pictures (Schienle et al., 2009), already suggesting a possibly altered reward sensitivity in BN patients.

The observed VMHC reductions in ED patients were not correlated with BMI, age and disease duration and were not linked to global and local atrophy or gray matter asymmetry between the two hemispheres. In fact, although previous volumetric works have often reported substantial differences in gray matter volumes between AN patients and healthy controls (Boghi et al., 2011; Brooks et al., 2012; Titova et al., 2013), our VBM analysis revealed no significant clusters in the same comparison at the default SPM

threshold (p=0.05, family-wise corrected for multiple comparisons), both in the whole-brain analysis and within the mask obtained from all regions with reduced VMHC. Identical results were obtained using the false discovery rate (FDR) as an alternative correction criterion for voxel-based analyses. At a lower significance threshold (p=0.001, uncorrected for multiple comparisons but used in some studies) the VBM analysis returned three clusters with reduced gray matter volumes in AN patients, but none of these clusters overlapped with regions of reduced VMHC. The apparent discrepancy between our VBM findings and previous structural reports could be due to the sample size, the extended range of disease duration, as well as to the variation in the VBM-SPM methodology among different works as highlighted in a recent review (Van Den Eynde et al., 2012).

Furthermore, when performing an ANCOVA analysis between regional inter-hemispheric connectivities and mean FA value of the corpus callosum, no significant correlations were found, albeit this white matter structure is the most important one for inter-hemispheric information transfer. Nonetheless, when we performed the same analyses across all voxels of the corpus callosum, we found a single cluster of significant correlation between FA values and regional VMHC of the insula but not of the cerebellum, precuneus and frontal regions.

Taken together, these results suggest that the observed reductions in the inter-hemispheric connectivity are likely due to a functional deficit of synchronization of BOLD signals between homologue regions in the two hemispheres, possibly secondary to small local microstructural alterations in the corpus callosum, but not to local microstructural alterations in the grey matter. On the other hand, it is also possible that the mechanisms of synchronization across the two hemispheres avoid direct callosal connections (following, e.g., indirect callosal, inter-thalamic, cortico- cerebellar, or other commissural pathways) (Hermesdorf et al., 2016), and this could be the case for the observed reduction in the cerebellum, in the

precuneus and in the frontal regions that were not found to be linked to either global or local FA values in the corpus callosum.
As VMHC investigates functional connectivity by the use of temporal correlations at zero-lag delay across homotopic voxel time-courses, this measure is sensible to the shape of the regional HRF and, consequently, possible interregional variability in the HRF may contribute to decreased VMHC, independent of the underlying neural activity (Sun et al., 2004). Therefore, to assess more comprehensively the differences between groups in the above-mentioned regions, we also performed an IHSC analysis, which is more robust to interregional differences in the HRF (Sun et al., 2004) and additionally allows re-assigning the contributions to the inter-hemispheric functional connectivity according to specific frequency sub-ranges. Specifically, the so-called 'Slow-4' and 'Slow-5' frequency ranges have been previously targeted as these are the two ranges where most of the gray matter oscillations primarily occur (Zuo et al., 2010). In this way, despite the non-electrical nature of the signals, resting-state BOLD fluctuations have been configured as a special type of neuronal oscillations.
It has been originally observed (Buzsaki et al., 2004; Penttonen and Buzsáki, 2003) that neuronal oscillations are distributed linearly on the natural logarithmic scale of frequency and that independent frequency bands are generated by distinct "oscillators" with specific properties and physiological functions. The constellation of brain rhythms is increasingly though to be an important characteristic of individual brains, up to the point that their alterations may lead to mental and neurological disease (Buzsáki et al., 2013).
Even if pivotal studies on the spectral composition of neuronal oscillations were conducted on neuro-electrical signals recorded in animals, a similar approach was proposed by Zuo et al. (Zuo et al., 2010) for resting-state fMRI in humans. This approach consisted in the decomposition of resting state fMRI signal fluctuations into four distinct frequency bands: slow-5 (0.01–0.027 Hz), slow-4 (0.027–0.073 Hz), slow-3 (0.073–0.198 Hz), and slow-2 (0.198–

0.25 Hz). Among these, the BOLD dynamics have been proven to be maximally informative in the slow-4 and slow-5 bands. In particular, the analysis of these two spectral components as distinct entities has led to the discovery of interesting effects in several neural systems. For example, in the healthy brain, behavioral traits such as extraversion and neuroticism were correlated with the amplitude of frequency fluctuations in the slow-4 and slow-5 bands in different regions related to emotion processing (Wei et al., 2014). In some pathological conditions, significant alterations were found preferentially in slow-5 (see, e. g., (Han et al., 2011; Huang et al., 2014; La et al., 2016; Martino et al., 2016) or slow-4 (see, e. g., (Yu et al., 2013; Zhan et al., 2016) frequency bands; even in pharmacological conditions, an acute effect of the first levodopa challenge on the sensori-motor resting state network was specifically highlighted for the slow-4 band in drug-naive Parkinson patients (Esposito et al., 2013).

In the present study, we have extracted the IHSC values to separate contribution of slow-4 and slow-5 BOLD fluctuations to the interhemispheric functional connectivity and to examine whether these components differed in specific brain structures where the functional homotopicity was affected by an ED. We, in fact, believe that the differentiation of spectral components would be important given the current notion that the same neural circuit can generate different kinds of rhythms depending on the more local or more distant synaptic interaction between the two hemispheres. In this case, different oscillatory patterns could also help to represent different psychophysiological states or functions.

When performing a full band IHSC analysis, a significant reduction of the IHSC in AN and BN patients compared to HC was confirmed in all the considered VOIs, except for the posterior insula. Thereby, the reduction in VMHC observed in the posterior insula could be either due to the HRF variability between the groups or rather be a more frequency-selective effect. When separating the full band into canonical bands 'Slow-5' and 'Slow-4', a higher coherence in the ‘Slow-5’ range compared to the ‘Slow-4’ range was observed in all

detected regions except the posterior insula, and a significant effect of frequency was observed in the cerebellum and in the precuneus but not in the posterior insula and in the frontal regions. Instead, a reduction in the IHSC was observed in the posterior insula in the (non-canonical) sub-band of frequencies ranging from 0.0299 Hz to 0.0643 Hz. Moreover, considering the frequency ranges separately in post-hoc comparisons, we found that the significant change of regional IHSC between AN and BN patients and HC was variably dependent on the specific frequency range of signal oscillations. In fact, AN patients had reduced IHSC only in the 'Slow-5' frequency range in the cerebellum, only in the 'Slow-4' frequency range in the precuneus and between 0.0299 and 0.0643 Hz in the posterior insula, whereas BN patients had reduced IHSC values both in the 'Slow-4' and in the 'Slow-5' ranges in the frontal regions.

Taken together, these findings may possibly shed more light on the spatio-temporal scale of the observed VMHC effects in the two groups of patients. In fact, (Buzsaki et al., 2004) previously reported that lower frequency dynamics are typically associated to larger-scale neural networks and longer-term cortico-cortical connectivity, whereas higher frequency dynamics preferentially pertain to shorter-scale neural networks and shorter-term (subcortical-cortical) connectivity. Thus, it is reasonable to expect that higher coherence and therefore higher inter-hemispheric connectivity should prevail at the lower frequencies. Along this line, especially in the posterior insula and in the frontal regions, the IHSC analysis seems to suggest a different balance between lower and higher frequencies, and this aspect may linked to the special role of these regions as network hubs for both large and short-scale functional connectivity (Liao et al., 2015).

Chapter 6:

General Discussion and Conclusion

The presented thesis has been organized into two main sections: in the first part, it focused on the evaluation of the gustatory processes elicited by basic tastes in healthy subjects, in the second part on the analyses of possible impairments of the gustatory processing of basic tastes and of the possible inter-hemispheric functional asymmetries in people affected by Anorexia Nervosa and Bulimia Nervosa.

More in details, in the first section, after a description of the state of the art about what is known regarding taste processing in human brain, I firstly described the implementation of a novel device for gustatory experiments allowing the injection of tastants' solutions during not only fMRI experiments but also during any other possible imaging techniques. Besides the full description of the device, I proposed the results of a pilot single-subject 3 Tesla fMRI study, in which the working gustometer was used to control the injection of different basic taste qualities and concentrations.
The developed gustometer has been demonstrated to be able to deliver small volumes of taste solutions at high flow rates, and this aspect is potentially crucial, particularly in the study of gustatory processing with high temporal resolution imaging techniques. In addition, this gustometer has been the first implementation of a low-cost device, usable for multi-center studies because of its miniaturized structure, that may contribute to an increased standardization of experimental designs in human imaging studies of taste perception.

The second main finding of this thesis concerns the study of the PGC response to increasing taste intensities. To perform this study, I administered two tastes with opposite valences, sweet and bitter, in five different concentrations using (i) high resolution fMRI data with relatively small voxel size (2.5mm isotropic) at 3 Tesla, (ii) an event-related stimulation paradigm to maximally reduce the impact of tongue movements during taste perception, and (iii) high resolution cortical registration methods to maximize the spatial correspondence of the insular cortex across all individual brains in determining the cortical distribution of intensity-related taste activations. This study has revealed that (i) the left insular cortex includes a compact specialized cluster for processing taste intensities, independently of the quality and valence of the tastant, that (ii) exhibits a highly non-linear trend of the responses to the concentration for both sweet and bitter tastants, as previously reported in animal studies; (iii) the spatial distribution of the highest responses across the main effects of the insular activation delineate an anterior-posterior spatial gradient for high-to-low concentrations, highlighting a distributed spatial coding of responses to different taste intensities within the bilateral insular cortex.

The third major finding of this thesis has been the localization of the areas within the insular cortex that primarily respond to basic taste stimuli. It is the first study investigating gustatory cortex with the use of ultra-high spatial resolution functional imaging (7 Tesla) and it was aimed at defining (i) the clusters within the insula responding to all the known basic tastes, sweet, bitter, salty, sour and umami both following a group-based and a single-subject based approaches, and (ii) at determining whether the activations obtained in response to the different basic taste qualities may follow a spatial distribution (chemotopy) within the insular cortex. Results obtained from this study have, firstly, provided evidences of bilateral insula activation to basic taste quality in the anterior and middle insula. The activations obtained with the single-subject based analysis, differently from that performed at a group level, show how peaks of activation to all

basic tastes and to the neutral solution appear in the same location within the insular cortex. Thus, at least from these initials results, the hypothesis of a spatially segregated pattern of responses (chemotopy), specific for each of basic tastant, is poorly supported.

The fourth major finding of this thesis came from the study performed on AN and BN patients, for both the evaluation of possible impairments in the processing of rewarding and aversive taste stimuli and for the analysis of possible alterations in the inter-hemispheric functional connectivities. Results from the first analysis suggest that the ratio of aversive/pleasant taste stimulation as well as the pattern of brain area activations by each tastant are altered in symptomatic ED patients in several areas of the reward pathway, as the amygdala, the cingulate cortex and the insula. Altered inter-hemispheric functional connectivity was found across several brain regions implicated in cognitive controls and in the emotion regulation, as the cerebellum, the precuneus, the posterior insula for the AN patients, and as the dorsolateral prefrontal cortex for the BN patients, suggesting the resting state inter-hemispheric functional (dis-)connectivity as a novel marker for the study of AN and BN pathologies.

Bibliography

Abdollahi, R.O., Kolster, H., Glasser, M.F., Robinson, E.C., Coalson, T.S., Dierker, D., Jenkinson, M., Van Essen, D.C., Orban, G.A., 2014. Correspondences between retinotopic areas and myelin maps in human visual cortex. Neuroimage 99, 509–524. https://doi.org/10.1016/j.neuroimage.2014.06.042

Accolla, R., Bathellier, B., Petersen, C.C.H., Carleton, A., 2007. Differential Spatial Representation of Taste Modalities in the Rat Gustatory Cortex. J. Neurosci. 27, 1396–1404. https://doi.org/10.1523/JNEUROSCI.5188-06.2007

Accolla, R., Carleton, A., 2008. Internal body state influences topographical plasticity of sensory representations in the rat gustatory cortex. Proc. Natl. Acad. Sci. 105, 4010–4015. https://doi.org/10.1073/pnas.0708927105

Aharoni, R., Hertz, M.M., 2012. Disgust sensitivity and anorexia nervosa. Eur. Eat. Disord. Rev. 20, 106–110. https://doi.org/10.1002/erv.1124

Amianto, F., D'Agata, F., Lavagnino, L., Caroppo, P., Abbate-Daga, G., Righi, D., Scarone, S., Bergui, M., Mortara, P., Fassino, S., 2013. Intrinsic connectivity networks within cerebellum and beyond in eating disorders. Cerebellum 12, 623–631. https://doi.org/10.1007/s12311-013-0471-1

Andersson, J.L.R., Skare, S., Ashburner, J., 2003. How to correct susceptibility distortions in spin-echo echo-planar images: Application to diffusion tensor imaging. Neuroimage 20, 870–888. https://doi.org/10.1016/S1053-8119(03)00336-7

Antinucci, M., Risso, D., 2017. A Matter of Taste: Lineage-Specific Loss of Function of Taste Receptor Genes in Vertebrates. Front. Mol. Biosci. 4, 1–8. https://doi.org/10.3389/fmolb.2017.00081

Araujo, I.E.T. De, Kringelbach, M.L., Rolls, E.T., Mcglone, F., 2003. Human Cortical Responses to Water in the Mouth , and the Effects of Thirst. j. Neurophysiol 90, 1865–1876. https://doi.org/10.1152/jn.00297.2003

Aschenbrenner, K., Scholze, N., Joraschky, P., Hummel, T., 2008. Gustatory and olfactory sensitivity in patients with anorexia and bulimia in the course of treatment. J. Psychiatr. Res. 43, 129–137. https://doi.org/10.1016/j.jpsychires.2008.03.003

Ashburner, J., 2007. A fast diffeomorphic image registration algorithm. Neuroimage 38, 95–113. https://doi.org/10.1016/j.neuroimage.2007.07.007

Avery, J.A., Gotts, S.J., Kerr, K.L., Burrows, K., Ingeholm, J.E., Bodurka, J., Martin, A., Simmons, W.K., 2017. Convergent Gustatory and Viscerosensory Processing in the Human Dorsal Mid-Insula. Hum. Brain Mapp. 2164, 2150–2164. https://doi.org/10.1002/hbm.23510

Avery, J.A., Kerr, K.L., Ingeholm, J.E., Burrows, K., Bodurka, J., Simmons, W.K., 2016. A common gustatory and interoceptive representation in the human mid-insula. Hum. Brain Mapp. 36, 2996–3006. https://doi.org/10.1002/hbm.22823

Bagby, R.M., Parker, J.D.A., Taylor, G.J., 1994a. The twenty-item Toronto Alexithymia scale-I. Item selection and cross-validation of the factor structure. J. Psychosom. Res. 38, 23–32. https://doi.org/10.1016/0022-3999(94)90005-1

Bagby, R.M., Taylor, G.J., Parker, J.D.A., 1994b. The twenty-item Toronto Alexithymia scale-II. Convergent, discriminant, and concurrent validity. J. Psychosom. Res. 38, 33–40. https://doi.org/10.1016/0022-3999(94)90006-X

Bamiou, D.E., Musiek, F.E., Luxon, L.M., 2003. The insula (Island of Reil) and its role in

auditory processing: Literature review. Brain Res. Rev. 42, 143–154. https://doi.org/10.1016/S0165-0173(03)00172-3
Barry, M.A., Gatenby, J.C., Zeiger, J.D., Gore, J.C., 2001. Hemisperic Dominance of Cortical Activity Evoked by Focal Electrogustatory Stimuli. Chem Senses 26, 471–485. https://doi.org/10.1093/chemse/26.5.471
Baumgartner, U., Iannetti, G.D., Zambreanu, L., Stoeter, P., Treede, R.-D., Tracey, I., 2010. Multiple Somatotopic Representations of Heat and Mechanical Pain in the Operculo-Insular Cortex: A High-Resolution fMRI Study. J. Neurophysiol. 104, 2863–2872. https://doi.org/10.1152/jn.00253.2010
Bender, G., Veldhuizen, M.G., Meltzer, J.A., Gitelman, D.R., Small, D.M., 2009. Neural correlates of evaluative compared with passive tasting. Eur. J. Neurosci. 30, 327–338. https://doi.org/10.1111/j.1460-9568.2009.06819.x
Bermudez-Rattoni, F., 2014. The forgotten insular cortex: Its role on recognition memory formation. Neurobiol. Learn. Mem. 109, 207–216. https://doi.org/10.1016/j.nlm.2014.01.001
Berridge, K.C., 2009. "Liking" and "wanting" food rewards: Brain substrates and roles in eating disorders. Physiol. Behav. 97, 537–550. https://doi.org/10.1016/j.physbeh.2009.02.044
Berridge, K.C., Kringelbach, M.L., 2008. Affective neuroscience of pleasure: reward in humans and animals. Psychopharmacology (Berl). 199, 457–480. https://doi.org/10.1007/s00213-008-1099-6.Affective
Boehm, I., Geisler, D., King, J.A., Ritschel, F., Seidel, M., Deza Araujo, Y., Petermann, J., Lohmeier, H., Weiss, J., Walter, M., Roessner, V., Ehrlich, S., 2014. Increased resting state functional connectivity in the fronto-parietal and default mode network in anorexia nervosa. Front. Behav. Neurosci. 8, 1–11. https://doi.org/10.3389/fnbeh.2014.00346
Boehm, I., Geisler, D., Tam, F., King, J.A., Ritschel, F., Seidel, M., Bernardoni, F., Murr, J., Goschke, T., Calhoun, V.D., Roessner, V., Ehrlich, S., 2016. Partially restored resting-state functional connectivity in women recovered from anorexia nervosa. J. Psychiatry Neurosci. 41, 1–9. https://doi.org/10.1503/jpn.150259
Boghi, A., Sterpone, S., Sales, S., Agata, F.D., Boris, G., Zullo, G., Munno, D., 2011. In vivo evidence of global and focal brain alterations in anorexia nervosa. Psychiatry Res. Neuroimaging 192, 154–159. https://doi.org/10.1016/j.pscychresns.2010.12.008
Brandt, T., Dieterich, M., 1999. The vestibular cortex: Its locations, functions, and disorders. Ann. N. Y. Acad. Sci. https://doi.org/10.1111/j.1749-6632.1999.tb09193.x
Brooks, S.J., Cedernaes, J., Schiöth, H.B., 2013. Increased Prefrontal and Parahippocampal Activation with Reduced Dorsolateral Prefrontal and Insular Cortex Activation to Food Images in Obesity: A Meta-Analysis of fMRI Studies. PLoS One 8, e60393--1:8. https://doi.org/10.1371/journal.pone.0060393
Brooks, S.J., O'Daly, O., Uher, R., Friederich, H.C., Giampietro, V., Brammer, M., Williams, S.C.R., Schioth, H.B., Treasure, J., Campbell, I.C., 2012. Thinking about eating food activates visual cortex with reduced bilateral cerebellar activation in females with anorexia nervosa: An fmri study. PLoS One 7, e34000--1:11. https://doi.org/10.1371/journal.pone.0034000
Buckner, R.L., Andrews-Hanna, J.R., Schacter, D.L., 2008. The brain's default network: Anatomy, function, and relevance to disease. Ann. N. Y. Acad. Sci. 1124, 1–38. https://doi.org/10.1196/annals.1440.011

Buettner, A., Beer, A., Hannig, C., Settles, M., 2001. Observation of the swallowing process by application of videofluoroscopy and real-time magnetic resonance imaging-consequences for retronasal aroma stimulation. Chem. Senses 26, 1211–1219. https://doi.org/10.1093/chemse/26.9.1211

Bulik, C.M., Berkman, N.D., Brownley, K.A., Sedway, J.A., Lohr, K.N., 2008. Anorexia Nervosa Treatment: A Systematic Review of Randomized Controlled Trials. Int. J. Eat. Disord. 41, 174–179. https://doi.org/10.1002/eat

Buzsaki, G., Draughn, A., Buzsáki, G., Draguhn, A., Buzsaki, G., Draughn, A., 2004. Neuronal Oscillations in Cortical Networks. Science 304, 1926–1930. https://doi.org/10.1126/science.1099745

Buzsáki, G., Logothetis, N., Singer, W., 2013. Scaling brain size, keeping timing: Evolutionary preservation of brain rhythms. Neuron 80, 751–764. https://doi.org/10.1016/j.neuron.2013.10.002

Canna, A., Prinster, A., Fratello, M., Puglia, L., Magliulo, M., Cantone, E., Pirozzi, M.A., Salle, F. Di, Esposito, F., 2018. A low-cost open-architecture taste delivery system for gustatory fMRI and BCI experiments Article. J. Neurosci. Methods, Press 311, 1–12. https://doi.org/10.1016/J.JNEUMETH.2018.10.003

Carleton, A., Accolla, R., Simon, S.A., 2010. Coding in the mammalian gustatory system. Trends Neurosci. 33, 326–334. https://doi.org/10.1016/j.tins.2010.04.002

Casper, R., Kirschner, B., Sandstead, H., Jacob, R., Davis, J., 1980. An evaluation taste function of trace metals , vitamins , in anorexia nervosa. Am J Clin Nutr 33, 1801–1808.

Cerf-Ducastel, B., Haase, L., Murphy, C., 2013. Effect of Magnitude Estimation of Pleasantness and Intensity on fMRI Activation to Taste. Chemosens Percept. 5, 100–109. https://doi.org/10.1007/s12078-011-9109-1.Effect

Cerf-ducastel, B., Murphy, C., 2004. Validation of a stimulation protocol suited to the investigation of odor – taste interactions with fMRI. Physiol. Behav. 81, 389–396. https://doi.org/10.1016/j.physbeh.2003.12.018

Cerf-ducastel, B., Van De Moortele, P., Macleod, P., Bihan, D. Le, Faurion, A., 2001. Interaction of Gustatory and Lingual Somatosensory Perceptions at the Cortical Level in the Human : a Functional Magnetic Resonance Imaging Study. Chem Senses 26, 371–383.

Chang, L.J., Smith, A., Dufwenberg, M., Sanfey, A.G., 2011. Triangulating the Neural, Psychological, and Economic Bases of Guilt Aversion. Neuron 70, 560–572. https://doi.org/10.1016/j.neuron.2011.02.056

Chang, L.J., Yarkoni, T., Khaw, M.W., Sanfey, A.G., 2013. Decoding the role of the insula in human cognition: Functional parcellation and large-scale reverse inference. Cereb. Cortex 23, 739–749. https://doi.org/10.1093/cercor/bhs065

Chapman, H.A., Anderson, A.K., 2012. Understanding disgust. Ann. N. Y. Acad. Sci. 1251, 62–76. https://doi.org/10.1111/j.1749-6632.2011.06369.x

Chen, S., Dong, D., Jackson, T., Su, Y., Chen, H., 2016. Altered frontal inter-hemispheric resting state functional connectivity is associated with bulimic symptoms among restrained eaters. Neuropsychologia 81, 22–30. https://doi.org/10.1016/j.neuropsychologia.2015.06.036

Chen, X., Gabitto, M., Peng, Y., Ryba, N.J.P., Zuker, C.S., 2011. A gustotopic map of taste qualities in the mammalian brain. Science 333, 1262–1266. https://doi.org/10.1126/science.1204076

Cho, S.S., Pellecchia, G., Aminian, K., Ray, N., Segura, B., Obeso, I., Strafella, A.P., 2012. Morphometric Correlation of Impulsivity in Medial Prefrontal Cortex

Morphometric Correlation of Impulsivity in Medial Prefrontal. Brain Topogr. 26, 479–487. https://doi.org/10.1007/s10548-012-0270-x
Compton, R.J., Feigenson, K., Widick, P., 2005. Take it to the bridge: An interhemispheric processing advantage for emotional faces. Cogn. Brain Res. 24, 66–72. https://doi.org/10.1016/j.cogbrainres.2004.12.002
Cooper, J.L., Ph, D., Morrison, T.L., Bigman, O.L., Abramowitz, S.I., Levin, S., Krener, P., 1988. Mood Changes and Affective Disorder in the Bulimic Binge- Purge Cycle. Int. J. Eat. Disord. 7, 469–474.
Cowdrey, F.A., Filippini, N., Park, R.J., Smith, S.M., McCabe, C., 2014. Increased resting state functional connectivity in the default mode network in recovered anorexia nervosa. Hum. Brain Mapp. 35, 483–491. https://doi.org/10.1002/hbm.22202
Cowdrey, F.A., Park, R.J., Harmer, C.J., McCabe, C., 2011. Increased neural processing of rewarding and aversive food stimuli in recovered anorexia nervosa. Biol. Psychiatry 70, 736–743. https://doi.org/10.1016/j.biopsych.2011.05.028
Craig, A.D., 2009. How do you feel - now? The anterior insula and human awareness. Nat. Rev. Neurosci. 10, 59–70. https://doi.org/10.1038/nrn2555
Craig, A.D., 2003. How do you feel? Interoception: The sense of the physiological condition of the body. Nat. Rev. Neurosci. 13, 500–505. https://doi.org/10.1016/S0959-4388(03)00090-4
Critchley, H.D., Tang, J., Glaser, D., Butterworth, B., Dolan, R.J., 2005. Anterior cingulate activity during error and autonomic response. Neuroimage 27, 885–895. https://doi.org/10.1016/j.neuroimage.2005.05.047
Crouzet, S.M., Busch, N.A., Ohla, K., 2015. Taste quality decoding parallels taste sensations. Curr. Biol. 25, 890–896. https://doi.org/http://dx.doi.org/10.1016/j.cub.2015.01.057
Dalenberg, J.R., Hoogeveen, H.R., Renken, R.J., Langers, D.R.M., Gert, J., 2015. Functional specialization of the male insula during taste perception. Neuroimage 119, 210–220. https://doi.org/10.1016/j.neuroimage.2015.06.062
Dalenberg, J.R., Weitkamp, L., Renken, R.J., Nanetti, L., Ter Horst, G.J., 2017. Flavor pleasantness processing in the ventral emotion network. PLoS One 12, 1–20. https://doi.org/10.1371/journal.pone.0170310
Damasio, A.R., Grabowski, T.J., Bechara, A., Damasio, H., Ponto, L.L.B., Parvizi, J., Hichwa, R.D., 2000. Subcortical and cortical brain activity during the feeling of self-generated emotions. Nat. Neurosci. 3, 1049–1056. https://doi.org/10.1038/79871
Davey, G.C.L., 2011. Disgust: The disease-avoidance emotion and its dysfunctions. Philos. Trans. R. Soc. B Biol. Sci. 366, 3453–3465. https://doi.org/10.1098/rstb.2011.0039
Davey, G.C.L., Buckland, G., Tantow, B., Dallos, R., 1998. Disgust and eating disorders. Eur. Eat. Disord. Rev. 6, 201–211.
Davidovic, M., Starck, G., Olausson, H., 2017. Processing of affective and emotionally neutral tactile stimuli in the insular cortex. Dev. Cogn. Neurosci. 17. https://doi.org/10.1016/j.dcn.2017.12.006
De Araujo, I., Rolls, E.T., Kringelbach, M.L., McGlone, F., Phillips, N., 2003. Taste-olfactory convergence, and the representation of the pleasantness of flavour, in the human brain. Eur. J. Neurosci. 18, 2059–2068. https://doi.org/10.1046/j.1460-9568.2003.02915.x
De Araujo, I.E., Rolls, E.T., 2004. Representation in the Human Brain of Food Texture and Oral Fat. J. Neurosci. 24, 3086–3093.

https://doi.org/10.1523/JNEUROSCI.0130-04.2004
De Martino, F., Moerel, M., Van De Moortele, P.F., Ugurbil, K., Goebel, R., Yacoub, E., Formisano, E., 2013. Spatial organization of frequency preference and selectivity in the human inferior colliculus. Nat. Commun. 4, 1386–1388. https://doi.org/10.1038/ncomms2379
Dickson, P.E., Cairns, J., Goldowitz, D., Mittleman, G., 2016. Cerebellar contribution to higher and lower order rule learning and cognitive flexibility in mice. Neuroscience 1–11. https://doi.org/10.1016/j.neuroscience.2016.03.040
Doty, R.L., Tourbier, I.A., Pham, D.L., Cuzzocreo, J.L., Udupa, J.K., Karacali, B., Beals, E., Fabius, L., Leon-Sarmiento, F.E., Moonis, G., Kim, T., Mihama, T., Geckle, R.J., Yousem, D.M., 2016. Taste dysfunction in multiple sclerosis. J. Neurol. 263, 677–688. https://doi.org/10.1007/s00415-016-8030-6
Duncan, J., Owen, A.M., 2000. Common regions of the human frontal lobe recruted by diverse cognitive demands. Trends Neurosci. 23, 475–483. https://doi.org/10.1016/S0166-2236(00)01633-7
Eckert, M. a, Menon, V., Walczak, A., Ahlstrom, J., Denslow, S., Horwitz, A., Dubno, J.R., 2010. At the Heart of the Ventral Attention System: the Right Anterior Insula Mark. Hum. Brain Mapp. 30, 2530–2541. https://doi.org/10.1002/hbm.20688.At
Ehrlich, S., Lord, A.R., Geisler, D., Borchardt, V., Boehm, I., Seidel, M., Ritschel, F., Schulze, A., King, J.A., Weidner, K., Roessner, V., Walter, M., 2015. Reduced functional connectivity in the thalamo-insular subnetwork in patients with acute anorexia nervosa. Hum. Brain Mapp. 36, 1772–1781. https://doi.org/10.1002/hbm.22736
Esposito, F., Tessitore, A., Giordano, A., De Micco, R., Paccone, A., Conforti, R., Pignataro, G., Annunziato, L., Tedeschi, G., 2013. Rhythm-specific modulation of the sensorimotor network in drug-naïve patients with Parkinson's disease by levodopa. Brain 136, 710–725. https://doi.org/10.1093/brain/awt007
Favaro, A., Santonastaso, P., Manara, R., Bosello, R., Bommarito, G., Tenconi, E., Di Salle, F., 2012. Disruption of visuospatial and somatosensory functional connectivity in anorexia nervosa. Biol. Psychiatry 72, 864–870. https://doi.org/10.1016/j.biopsych.2012.04.025
Feinberg, D.A., Moeller, S., Smith, S.M., Auerbach, E., Ramanna, S., Glasser, M.F., Miller, K.L., Ugurbil, K., Yacoub, E., 2010. Multiplexed echo planar imaging for sub-second whole brain fmri and fast diffusion imaging. PLoS One 5, 1–11. https://doi.org/10.1371/journal.pone.0015710
Fernández-Aranda, F., Agüera, Z., Fernández-García, J.C., Garrido-Sanchez, L., Alcaide-Torres, J., Tinahones, F.J., Giner-Bartolomé, C., Baños, R.M., Botella, C., Cebolla, A., de la Torre, R., Fernández-Real, J.M., Ortega, F.J., Frühbeck, G., Gómez-Ambrosi, J., Granero, R., Islam, M.A., Jiménez-Murcia, S., Tárrega, S., Menchón, J.M., Fagundo, A.B., Sancho, C., Estivill, X., Treasure, J., Casanueva, F.F., 2016. Smell–taste dysfunctions in extreme weight/eating conditions: analysis of hormonal and psychological interactions. Endocrine 51, 256–267. https://doi.org/10.1007/s12020-015-0684-9
First, M.B., Williams, J.B.W., Karg, R.S., Spitzer, R.L., 2015. User's Guide to Structured Clinical Interview for Dsm-5 Disorders (Scid-5-cv): Clinician Version Title : User's Guide to Structured Clinical 5–7.
Fletcher, M.L., Ogg, M.C., Lu, L., Ogg, R.J., Boughter, J.D., 2017. Overlapping Representation of Primary Tastes in a Defined Region of the Gustatory Cortex. J. Neurosci. 37, 7595–7605. https://doi.org/10.1523/JNEUROSCI.0649-17.2017

Forman, S.D., Cohen, J.D., Fitzgerald, M., Eddy, W.F., Mintun, M.A., Noll, D.C., 1995. Improved assessment of significant activation in functional magnetic resonance imaging (fMRI): use of a cluster-size threshold. Magn Reson Med 33, 636–647. https://doi.org/10.1002/mrm.1910330508

Fossati, A., Cloninger, C.R., Villa, D., Borroni, S., Grazioli, F., Giarolli, L., Battaglia, M., Maffei, C., 2007. Reliability and validity of the Italian version of the Temperament and Character Inventory-Revised in an outpatient sample. Compr. Psychiatry 48, 380–387. https://doi.org/10.1016/j.comppsych.2007.02.003

Frank, D., 2015. On Joseph Spengler's "Have Values a Place in Economics?" Ethics 125, 559–561. https://doi.org/10.1086/678378

Frank, G.K., Kaye, W.H., Carter, C.S., Brooks, S., May, C., Fissell, K., Stenger, V.A., 2003. The evaluation of brain activity in response to taste stimuli - A pilot study and method for central taste activation as assessed by event-related fMRI. J. Neurosci. Methods 131, 99–105. https://doi.org/10.1016/S0165-0270(03)00240-1

Frank, G.K., Wagner, A., Achenbach, S., McConaha, C., Skovira, K., Aizenstein, H., Carter, C.S., Kaye, W.H., 2006. Altered brain activity in women recovered from bulimic-type eating disorders after a glucose challenge: A pilot study. Int. J. Eat. Disord. 39, 76–79. https://doi.org/10.1002/eat.20210

Frank, G.K.W., 2014. Advances from neuroimaging studies in eating disorders. CNS Spectr. 20, 391–400. https://doi.org/10.1017/S1092852915000012

Frank, M., 1973. An analysis of hamster afferent taste nerve response functions. J. Gen. Physiol. 61, 588–618. https://doi.org/10.1085/jgp.61.5.588

Frey, S., Petrides, M., 1999. SHORT COMMUNICATION Re-examination of the human taste region : a positron emission tomography study. Eur. J. Neurosci. 11, 2985–2988.

Frost, M.A., Esposito, F., Goebel, R., 2014. Improved correspondence of resting-state networks after macroanatomical alignment. Hum. Brain Mapp. 35, 673–682. https://doi.org/10.1002/hbm.22191

Frost, M.A., Goebel, R., 2012. Measuring structural-functional correspondence: Spatial variability of specialised brain regions after macro-anatomical alignment. Neuroimage 59, 1369–1381. https://doi.org/10.1016/j.neuroimage.2011.08.035

Ganchrow, J.R., Erikson, R.P., 2018. Neural Correlates of Gustatory Intensity and Quality. J Neurophysiol 33, 768– 783.

Garner, D.M., 1991. Eating disorder inventory-2 manual. Int J Eat Disord. 14, 59–64.

Geisler, D., Borchardt, V., Lord, A.R., Boehm, I., Ritschel, F., Zwipp, J., Clas, S., King, J.A., Wolff-Stephan, S., Roessner, V., Walter, M., Ehrlich, S., 2015. Abnormal functional global and local brain connectivity in female patients with anorexia nervosa. J. Psychiatry Neurosci. 41, 1–7. https://doi.org/10.1503/jpn.140310

Goebel, R., Esposito, F., Formisano, E., 2006. Analysis of Functional Image Analysis Contest (FIAC) data with BrainVoyager QX: From single-subject to cortically aligned group General Linear Model analysis and self-organizing group Independent Component Analysis. Hum. Brain Mapp. 27, 392–401. https://doi.org/10.1002/hbm.20249

Goldzak-kunik, G., Friedman, R., Spitz, M., Sandler, L., Leshem, M., 2012. Intact sensory function in anorexia nervosa. Am J Clin Nutr 272–282. https://doi.org/10.3945/ajcn.111.020131.1

Good, C.D., Johnsrude, I.S., Ashburner, J., Henson, R.N.A., Friston, K.J., Frackowiak, R.S.J., 2001. A voxel-based morphometric study of ageing in 465 normal adult human brains. Neuroimage 14, 21–36. https://doi.org/10.1006/nimg.2001.0786

Goto, T.K., Yeung, A.W.K., Suen, J.L.K., Fong, B.S.K., Ninomiya, Y., 2015. High resolution time-intensity recording with synchronized solution delivery system for the human dynamic taste perception. J. Neurosci. Methods 245, 147–155. https://doi.org/10.1016/j.jneumeth.2015.02.023
Grabenhorst, F., Rolls, E.T., 2008. Selective attention to affective value alters how the brain processes taste stimuli. Eur. J. Neurosci. 27, 723–729. https://doi.org/10.1111/j.1460-9568.2008.06033.x
Green, B.G., Dalton, P., Cowart, B., Shaffer, G., Rankin, K., Higgins, J., 1996. Evaluating the “labeled magnitude scale” for measuring sensations of taste and smell. Chem. Senses 21, 323–334. https://doi.org/10.1093/chemse/21.3.323
Green, B.G., Nachtigal, D., 2014. Somatosensory factors in taste perception: Effects of active tasting and solution temperature. Physiol Behav. 107, 1–23. https://doi.org/10.1088/1367-2630/15/1/015008.Fluid
Guldin, W.O., Grüsser, O.J., 1998. Is there a vestibular cortex? Trends Neurosci. 21, 254–259. https://doi.org/10.1016/S0166-2236(97)01211-3
Gutierrez, R., Simon, S.A., 2011. Chemosensory processing in the taste - reward pathway. Flavour Fragr. J. 26, 231–238. https://doi.org/10.1002/ffj.2050
Haase, L., Cerf-Ducastel, B., Buracas, G., Murphy, C., 2007. On-line psychophysical data acquisition and event-related fMRI protocol optimized for the investigation of brain activation in response to gustatory stimuli. J. Neurosci. Methods 159, 98–107. https://doi.org/10.1016/j.jneumeth.2006.07.009
Haase, L., Cerf-Ducastel, B., Murphy, C., 2009. Cortical activation in response to pure taste stimuli during the physiological states of hunger and satiety. Neuroimage 44, 1008–1021. https://doi.org/10.1016/j.neuroimage.2008.09.044
Han, Y., Wang, J., Zhao, Z., Min, B., Lu, J., Li, K., He, Y., Jia, J., 2011. NeuroImage Frequency-dependent changes in the amplitude of low-frequency fluctuations in amnestic mild cognitive impairment : A resting-state fMRI study. Neuroimage 55, 287–295. https://doi.org/10.1016/j.neuroimage.2010.11.059
Harvey, T., Troop, N.A., Treasure, J.L., Murphy, T., 2002. Fear, disgust, and abnormal eating attitudes: A preliminary study. Int. J. Eat. Disord. 32, 213–218. https://doi.org/10.1002/eat.10069
Hermesdorf, M., Sundermann, B., Feder, S., Schwindt, W., Minnerup, J., Arolt, V., Berger, K., Pfleiderer, B., Wersching, H., 2016. Major depressive disorder: Findings of reduced homotopic connectivity and investigation of underlying structural mechanisms. Hum. Brain Mapp. 37, 1209–1217. https://doi.org/10.1002/hbm.23097
Hirata, S.I., Nakamura, T., Ifuku, H., Ogawa, H., 2005. Gustatory coding in the precentral extension of area 3 in Japanese macaque monkeys; comparison with area G. Exp. Brain Res. 165, 435–446. https://doi.org/10.1007/s00221-005-2321-y
Hoche, F., Guell, X., Sherman, J.C., Vangel, M.G., Schmahmann, J.D., 2016. Cerebellar Contribution to Social Cognition. Cerebellum 15, 732–743. https://doi.org/10.1007/s12311-015-0746-9
Hoogeveen, H.R., Dalenberg, J.R., Renken, R.J., Horst, G.J. ter, Lorist, M.M., 2015. Neural processing of basic tastes in healthy young and older adults — an fMRI study. Neuroimage 119, 1–12. https://doi.org/10.1016/j.neuroimage.2015.06.017
Hort, J., Ford, R.A., Eldeghaidy, S., Francis, S.T., 2016. Thermal Taster Status : Evidence of Cross-Modal Integration. Hum. Brain Mapp. 37, 2263–2275. https://doi.org/10.1002/hbm.23171
Huang, Z., Wang, Z., Zhang, J., Dai, R., Wu, J., Li, Y., Liang, W., Mao, Y., Yang, Z.,

Holland, G., Zhang, J., Northoff, G., 2014. Altered Temporal Variance and Neural Synchronization of Spontaneous Brain Activity in Anesthesia. Hum. Brain Mapp. 35, 5368–5378. https://doi.org/10.1002/hbm.22556
Humphries, C., Liebenthal, E., Binder, J.R., 2010. Tonotopic organization of human auditory cortex. Neuroimage 50, 1202–1211. https://doi.org/10.1016/j.neuroimage.2010.01.046
Iannilli, E., Singh, P.B., Schuster, B., Gerber, J., Hummel, T., 2012. Taste laterality studied by means of umami and salt stimuli: An fMRI study. Neuroimage 60, 426–435. https://doi.org/10.1016/j.neuroimage.2011.12.088
Irwin, W., Davidson, R.J.R., Lowe, M.J.M., Mock, B.J.B., Sorenson, J.A., Turski, P.A., 1996. Human amygdala activation detected with echo-planar functional magnetic resonance imaging. Neuroreport.
Jasinska, A.J., Ramamoorthy, A., Crew, C.M., 2011. Toward a neurobiological model of cue-induced self-control in decision making: Relevance to addiction and obesity. J. Neurosci. 31, 16139–16141. https://doi.org/10.1523/JNEUROSCI.4477-11.2011
Jezzini, A., Mazzucato, L., La Camera, G., Fontanini, A., 2013. Processing of Hedonic and Chemosensory Features of Taste in Medial Prefrontal and Insular Networks. J. Neurosci. 33, 18966–18978. https://doi.org/10.1523/JNEUROSCI.2974-13.2013
Jones, L.M., Fontanini, A., Katz, D.B., 2006. Gustatory processing: a dynamic systems approach. Curr. Opin. Neurobiol. 16, 420–428. https://doi.org/10.1016/j.conb.2006.06.011
Katz, D.B., Simon, S. a, Nicolelis, M. a L., 2002. Taste-specific neuronal ensembles in the gustatory cortex of awake rats. J. Neurosci. 22, 1850–1857. https://doi.org/22/5/1850 [pii]
Kaye, W.H., Fudge, J.L., Paulus, M., 2009. New insights into symptoms and neurocircuit function of anorexia nervosa. Nat. Rev. Neurosci. 10, 573–84. https://doi.org/10.1038/nrn2682
Kaye, W.H., Wagner, A., Fudge, J.L., Paulus, M., 2011. Neurocircuity of Eating Disorders Walter, Behavioral Neurobiology of Eating Disorders. https://doi.org/DOI 10.1007/7854_2010_85
Keating, C., Tilbrook, A.J., Rossell, S.L., Enticott, P.G., Fitzgerald, P.B., 2012. Reward processing in anorexia nervosa. Neuropsychologia 50, 567–575. https://doi.org/10.1016/j.neuropsychologia.2012.01.036
Keller, H., Schwarze, M., Filipic, S., Traue, H.C., Joern von Wietersheim, 2006. Alexithymia and Facial Emotion Recognition in Patients with Eating Disorders. Int J Eat Disord 39, 245–251.
Kinomura, S., Kawashima, R., Yamada, K., Ono, S., Itoh, M., Yoshioka, S., Yamaguchi, T., Matsui, H., Miyazawa, H., Itoh, H., Goto, R., Fujiwara, T., Satoh, K., Fukuda, H., 1994. Functional anatomy of taste perception in the human brain studied with positron emission tomography. Brain Res. 659, 263–266.
Kobayakawa, T., Endo, H., Ayabe-Kanamura, S., Kumagai, T., Yamaguchi, Y., Kikuchi, Y., Takeda, T., Saito, S., Ogawa, H., 1996. The primary gustatory area in human cerebral cortex studied by magnetoencephalography. Neurosci. Lett. 212, 155–158.
Kobayakawa, T., Ogawa, H., Kaneda, H., Ayabe-kanamura, S., HiroshiEndo, Saito, S., 1999. Spatio-temporal Analysis of Cortical Activity Evoked by Gustatory Stimulation in Humans. Chem. Senses 24, 201–209.
Kobayakawa, T., Saito, S., Gotow, N., Ogawa, H., 2008. Representation of salty taste stimulus concentrations in the primary gustatory Area in humans. Chemosens. Percept. 1, 227–234. https://doi.org/10.1007/s12078-008-9030-4

Kober, H., Mende-siedlecki, P., Kross, E.F., Weber, J., Mischel, W., Hart, C.L., Ochsner, K.N., 2010. Prefrontal-striatal pathway underlies cognitive regulation of craving. Proc. Natl. Acad. Sci. U. S. A. 107, 14811–14816. https://doi.org/10.1073/pnas.1007779107
Kriegeskorte, N., Goebel, R., 2001. An efficient algorithm for topologically correct segmentation of the cortical sheet in anatomical MR volumes. Neuroimage 14, 329–346. https://doi.org/10.1006/nimg.2001.0831
Kringelbach, M.L., 2005. The human orbitofrontal cortex: linking reward to hedonic experience. Nat. Rev. Neurosci. 6, 691–702. https://doi.org/10.1038/nrn1748
Kringelbach, M.L., De Araujo, I.E.T., Rolls, E.T., 2004. Taste-related activity in the human dorsolateral prefrontal cortex. Neuroimage 21, 781–788. https://doi.org/10.1016/j.neuroimage.2003.09.063
Kullmann, S., Pape, A.A., Heni, M., Ketterer, C., Schick, F., Häring, H.U., Fritsche, A., Preissl, H., Veit, R., 2013. Functional network connectivity underlying food processing: Disturbed salience and visual processing in overweight and obese adults. Cereb. Cortex 23, 1247–1256. https://doi.org/10.1093/cercor/bhs124
Kurth, F., Zilles, K., Fox, P.T., Laird, A.R., Eickhoff, S.B., 2010. A link between the systems: functional differentiation and integration within the human insula revealed by meta-analysis. Brain Struct. Funct. 214, 519–534. https://doi.org/10.1007/s00429-010-0255-z
La, C., Nair, V.A., Mossahebi, P., Young, B.M., Chacon, M., Jensen, M., Birn, R.M., Meyerand, M.E., Prabhakaran, V., 2016. Implication of the Slow-5 Oscillations in the Disruption of the Default-Mode Network in Healthy Aging and Stroke. Brain Connect. 6, 482–495. https://doi.org/10.1089/brain.2015.0375
Lao-Kaim, N.P., Fonville, L., Giampietro, V.P., Williams, S.C.R., Simmons, A., Tchanturia, K., 2015. Aberrant function of learning and cognitive control networks underlie inefficient cognitive flexibility in Anorexia Nervosa: A cross-sectional fMRI study. PLoS One 10, e0124027: 1-16. https://doi.org/10.1371/journal.pone.0124027
Li, H.J., Xu, Y., Zhang, K.R., Hoptman, M.J., Zuo, X.N., 2015. Homotopic connectivity in drug-naïve, first-episode, early-onset schizophrenia. J. Child Psychol. Psychiatry Allied Discip. 56, 432–443. https://doi.org/10.1111/jcpp.12307
Liao, X., Yuan, L., Zhao, T., Dai, Z., Shu, N., Xia, M., Yang, Y., Evans, A., He, Y., 2015. Spontaneous functional network dynamics and associated structural substrates in the human brain. Front. Hum. Neurosci. 9. https://doi.org/10.3389/fnhum.2015.00478
Lundström, J.N., Boesveldt, S., Albrecht, J., 2011. Central processing of the chemical senses: An overview. ACS Chem. Neurosci. 2, 5–16. https://doi.org/10.1021/cn1000843
Luo, C., Guo, X., Song, W., Zhao, B., Cao, B., Yang, J., Gong, Q., Shang, H., 2015. Decreased Resting-State Interhemispheric Functional Connectivity in Parkinson ' s Disease. Biomed Res. Int. 2015. https://doi.org/10.1155/2015/692684
Macdonald, C.J., Meck, W.H., Simon, S.A., 2012. Distinct neural ensembles in the rat gustatory cortex encode salt and water tastes. J. Physiol. 590, 3169–3184. https://doi.org/10.1113/jphysiol.2012.233486
Maffei, A., Haley, M., Fontanini, A., 2013. Neural processing of gustatory information in insular circuits. Curr Opin Neurobiol. 22, 709–716. https://doi.org/10.1016/j.conb.2012.04.001.NEURAL
Marciani, L., Pfeiffer, J.C., Hort, J., Head, K., Bush, D., Taylor, A.J., Spiller, R.C.,

Francis, S., Gowland, P.A., 2006. Improved methods for fMRI studies of combined taste and aroma stimuli. J. Neurosci. Methods 158, 186–194. https://doi.org/10.1016/j.jneumeth.2006.05.035
Martino, M., Magioncalda, P., Saiote, C., Conio, B., Escelsior, A., Rocchi, G., Piaggio, N., Marozzi, V., Huang, Z., Ferri, F., Amore, M., Inglese, M., Northoff, G., 2016. Abnormal functional–structural cingulum connectivity in mania: combined functional magnetic resonance imaging-diffusion tensor imaging investigation in different phases of bipolar disorder. Acta Psychiatr. Scand. 134, 339–349. https://doi.org/10.1111/acps.12596
Martins, Y., Pliner, P., 2005. Human food choices: An examination of the factors underlying acceptance/rejection of novel and familiar animal and nonanimal foods. Appetite 45, 214–224. https://doi.org/10.1016/j.appet.2005.08.002
Martınez-Gonzalez, M.A., Corella, D., Salas-Salvado, J., Ros, E., Covas, M.I., Fiol, M., Warnberg, J., Aros, F., Ruız-Gutierrez, V., Lamuela-Raventos, R.M., Lapetra, J., Munoz, M.A., Martınez, J.A., Saez, G., Serra-Majem, L., Pinto´, X., Mitjavila, M.T., Tur, J.A., Portillo, M. del P., Estruch, R., 2012. Cohort Profile: Design and methods of the PREDIMED study. Int. J. Epidemiol. 41, 377–385. https://doi.org/doi:10.1093/ije/dyq250
McFadden, K.L., Tregellas, J.R., Shott, M.E., Frank, G.K.W., 2014. Reduced salience and default mode network activity in women with anorexia nervosa. J. Psychiatry Neurosci. 39, 178–88. https://doi.org/10.1503/jpn.130046
Mehler, P.S., Krantz, M.J., Sachs, K. V., 2015. Treatments of medical complications of anorexia nervosa and bulimia nervosa. J. Eat. Disord. 3, 1–7. https://doi.org/10.1186/s40337-015-0041-7
Menon, V., Uddin, L.Q., 2010. Saliency, switching, attention and control: a network model of insula function. Brain Srruct Func 214, 655–667.
Miskovic, V., Anderson, A.K., 2018. Modality general and modality specific coding of hedonic valence. Curr. Opin. Behav. Sci. 19, 91–97. https://doi.org/10.1016/j.cobeha.2017.12.012
Mizoguchi, C., Kobayakawa, T., Saito, S., Ogawa, H., 2002. Gustatory Evoked Cortical Activity in Humans Studied by Simultaneous EEG and MEG Recording. Chem. Senses 27, 629–634.
Moeller, S., Yacoub, E., Olman, C. a, Auerbach, E., Strupp, J., Harel, N., Uğurbil, K., 2011. Multiband Multislice GE-EPI at 7 Tesla, With 16-Fold Acceleration Using Partial Parallel Imaging With Application to High Spatial and Temporal Whole-Brain FMRI. Magn. Reson. Med. 63, 1144–1153. https://doi.org/10.1002/mrm.22361.Multiband
Monteleone, A.M., Monteleone, P., Esposito, F., Prinster, A., Volpe, U., Cantone, E., Pellegrino, F., Canna, A., Milano, W., Aiello, M., Di Salle, F., Maj, M., 2017. Altered processing of rewarding and aversive basic taste stimuli in symptomatic women with anorexia nervosa and bulimia nervosa: An fMRI study. J. Psychiatr. Res. 90, 94–101. https://doi.org/10.1016/j.jpsychires.2017.02.013
Monteleone, P., Maj, M., 2013. Dysfunctions of leptin, ghrelin, BDNF and endocannabinoids in eating disorders: Beyond the homeostatic control of food intake. Psychoneuroendocrinology 38, 312–330. https://doi.org/10.1016/j.psyneuen.2012.10.021
Nakamura, Y., Goto, T.K., Tokumori, K., Yoshiura, T., Kobayashi, K., Nakamura, Y., Honda, H., Ninomiya, Y., Yoshiura, K., 2011. Localization of brain activation by umami taste in humans. Brain Res. 1406, 18–29.

https://doi.org/10.1016/j.brainres.2011.06.029
Nitschke, J.B., Dixon, G.E., Sarinopoulos, I., Short, S.J., Cohen, J.D., Smith, E.E., Kosslyn, S.M., Rose, R.M., Davidson, R.J., 2006. Altering expectancy dampens neural response to aversive taste in primary taste cortex. Nat. Neurosci. 9, 435–442. https://doi.org/10.1038/nn1645
Nozoe, S., Masuda, A., Naruo, T., Soejima, Y., Nagai, N., Tanaka, H., 1996. Changes in taste responsiveness in patients with anorexia nervosa during behavior therapy. Physiol. Behav. 59, 549–553. https://doi.org/10.1016/0031-9384(95)02105-1
Nunn, K., Frampton, I., Fuglset, T.S., Törzsök-Sonnevend, M., Lask, B., 2011. Anorexia nervosa and the insula. Med. Hypotheses 76, 353–357. https://doi.org/10.1016/j.mehy.2010.10.038
O'Doherty, J., Rolls, E.T., Francis, S., Bowtell, R., McGlone, F., 2001. Representation of Pleasant and Aversive Taste in the Human Brain. J. Neurophysiol. 85, 1315–1321. https://doi.org/10.1152/jn.2001.85.3.1315
O'Doherty, J.P., Deichmann, R., Critchley, H.D., Dolan, R.J., 2002. Neural responses during anticipation of a primary taste reward. Neuron 33, 815–826. https://doi.org/10.1016/S0896-6273(02)00603-7
Oberndorfer, T.A., Frank, G.K.W., Simmons, A.N., Wagner, A., McCurdy, D., Fudge, J.L., Yang, T.T., Paulus, M.P., Kaye, W.H., 2013. Altered insula response to sweet taste processing after recovery from anorexia and bulimia nervosa. Am. J. Psychiatry 170, 1143–1151. https://doi.org/10.1176/appi.ajp.2013.11111745
Ogawa, H., Murayama, N., Hasegawa, K., 1992. Difference in receptive field features of taste neurons in rat granular and dysgranular insular cortices. Exp. Brain Res.
Ogawa, H., Wakita, M., Hasegawa, K., Kobayakawa, T., Sakai, N., Hirai, T., Yamashita, Y., Saito, S., 2005. Functional MRI Detection of Activation in the Primary Gustatory Cortices in Humans. Chem. Senses 30, 583–592. https://doi.org/10.1093/chemse/bji052
Ogawa, H., Yamashita, S., Noma, A., Sato, M., 1972. Taste responses in the macaque monkey chorda tympani. Physiol. Behav. 9, 325–331.
Oh, S., Boegle, R., Ertl, M., Stephan, T., Dieterich, M., 2018. Multisensory vestibular, vestibular-auditory, and auditory network effects revealed by parametric sound pressure stimulation. Neuroimage 176, 354–363. https://doi.org/10.1016/j.neuroimage.2018.04.057
Penttonen, M., Buzsáki, G., 2003. Natural logarithmic relationship between brain oscillators. Thalamus Relat. Syst. 2, 145–152. https://doi.org/10.1016/S1472-9288(03)00007-4
Pfaffmann, C., 1980. Wundt's schema of sensory affect in the light of research on gustatory preferences. Psychol. Res. 42, 165–174. https://doi.org/10.1007/BF00308700
Phillips, M.L., Drevets, W.C., Rauch, S.L., Lane, R., 2003. Neurobiology of emotion perception I: The neural basis of normal emotion perception. Biol. Psychiatry 54, 504–514. https://doi.org/10.1016/S0006-3223(03)00168-9
Phillips, M.L., Young, A.W., Senior, C., Brammer, M., Andrew, C., Calder, A.J., Bullmore, E.T., Perrett, D.I., Rowland, D., Williams, S.C.R., Gray, J.A., David, A.S., 1997. A specific neural substrate for percieving facial expressions of disgust. Nature 389, 495–498.
Prinster, A., Cantone, E., Verlezza, V., Magliulo, M., Sarnelli, G., Iengo, M., Cuomo, R., Salle, F. Di, Esposito, F., 2017. Cortical representation of different taste modalities on the gustatory cortex: A pilot study. PLoS One 12, 1–15.

https://doi.org/https://doi.org/10.1371/journal. pone.0190164
Rolls, E.T., 2016. Functions of the anterior insula in taste, autonomic, and related functions. Brain Cogn. 110, 4–19. https://doi.org/10.1016/j.bandc.2015.07.002
Rolls, E.T., 2006. Brain mechanisms underlying flavour and appetite. Philos. Trans. R. Soc. B Biol. Sci. 361, 1123–1136. https://doi.org/10.1098/rstb.2006.1852
Roper, S.D., Chaudhari, N., 2017. Taste buds: Cells, signals and synapses. Nat. Rev. Neurosci. 18, 485–497. https://doi.org/10.1038/nrn.2017.68
Royet, J.P., Plailly, J., Delon-Martin, C., Kareken, D.A., Segebarth, C., 2003. fMRI of emotional responses to odors: Influence of hedonic valence and judgment, handedness, and gender. Neuroimage 20, 713–728. https://doi.org/10.1016/S1053-8119(03)00388-4
Rudenga, K., Green, B., Nachtigal, D., Small, D.M., 2010. Evidence for an integrated oral sensory module in the human anterior ventral insula. Chem. Senses 35, 693–703. https://doi.org/10.1093/chemse/bjq068
Samuelsen, C.L., Gardner, M.P.H., Fontanini, A., 2012. Effects of cue-triggered expectation on cortical processing of taste. Neuron 74, 410–422. https://doi.org/10.1016/j.neuron.2012.02.031.Effects
Sanfey, A.G., Rilling, J.K., Aronson, J.A., Nystrom, L.E., Cohen, J.D., 2003. The Neural Basis of Economic Decision-Making in the ultimatum game. Science 300, 1755–1759.
Sarinopoulos, I., Dixon, G.E., Short, S.J., Davidson, R.J., Nitschke, J.B., 2006. Brain mechanisms of expectation associated with insula and amygdala response to aversive taste: Implications for placebo. Brain. Behav. Immun. 20, 120–132. https://doi.org/10.1016/j.bbi.2005.11.006
Schienle, A., Schafer, A., Hermann, A., Vaitl, D., 2009. Binge-Eating Disorder: Reward Sensitivity and Brain Activation to Images of Food. Biol. Psychiatry 65, 654–661. https://doi.org/10.1016/j.biopsych.2008.09.028
Schmahmann, J.D., 2010. The role of the cerebellum in cognition and emotion: Personal reflections since 1982 on the dysmetria of thought hypothesis, and its historical evolution from theory to therapy. Neuropsychol. Rev. 20, 236–260. https://doi.org/10.1007/s11065-010-9142-x
Schoenfeld, M.A., Neuer, G., Tempelmann, C., Heinze, H., 2004. Functional magnetic resonance tomography correlates of taste perception in the human primary cortex. Neuroscience 127, 347–353. https://doi.org/10.1016/j.neuroscience.2004.05.024
Scott, K., 2004. The sweet and the bitter of mammalian taste. Curr. Opin. Neurobiol. 14, 423–427. https://doi.org/10.1016/j.conb.2004.06.003
Scott, T.R., Plata-Salamán, C.R., Smith-Swintosky, V.L., Giza, B.K., 1991. Gustatory Neural Coding in the Monkey Cortex: Stimulus Intensity. J. Neurophysiol. 65. https://doi.org/10.1152/jn.1996.75.6.2369
Scott, T.R.J., Erickson, R.P., 1971. Synaptic processing of taste-quality information in thalamus of the rat. J. Neurophysiol. 34, 868–883. https://doi.org/10.1152/jn.1971.34.5.868
Seeley, W.W., Menon, V., Schatzberg, A.F., Keller, J., Glover, G.H., Kenna, H., Reiss, A.L., Greicius, M.D., 2007. Dissociable Intrinsic Connectivity Networks for Salience Processing and Executive Control. J. Neurosci. 27, 2349–2356. https://doi.org/10.1523/JNEUROSCI.5587-06.2007
Seifritz, E., Di Salle, F., Esposito, F., Herdener, M., Neuhoff, J.G., Scheffler, K., 2006. Enhancing BOLD response in the auditory system by neurophysiologically tuned fMRI sequence. Neuroimage 29, 1013–1022.

https://doi.org/10.1016/j.neuroimage.2005.08.029
Sescousse, G., Caldú, X., Segura, B., Dreher, J.C., 2013. Processing of primary and secondary rewards: A quantitative meta-analysis and review of human functional neuroimaging studies. Neurosci. Biobehav. Rev. 37, 681–696. https://doi.org/10.1016/j.neubiorev.2013.02.002
Sheehan, D. V., Lecrubier, Y., Sheehan, K.H., Amorim, P., Janavs, J., Weiller, E., Hergueta, T., Baker, R., Dunbar, G.C., 1998. The Mini-International Neuropsychiatric Interview (M.I.N.I.): The development and validation of a structured diagnostic psychiatric interview for DSM-IV and ICD-10. J. Clin. Psychiatry 59, 22–33. https://doi.org/10.1016/S0924-9338(99)80239-9
Simon, J.J., Skunde, M., Walther, S., Bendszus, M., Herzog, W., Friederich, H.-C., 2016. Neural signature of food reward processing in bulimic-type eating disorders. Soc. Cogn. Affect. Neurosci.
Simon, S.A., Araujo, I.E. De, Stapleton, J.R., Nicolelis, M.A.L., 2008. Multisensory Processing of Gustatory Stimuli. Chemosens Percept 1, 95–102. https://doi.org/10.1007/s12078-008-9014-4.Multisensory
Simon, S.A., De Araujo, I.E., Gutierrez, R., Nicolelis, M.A.L., 2006. The neural mechanisms of gustation: A distributed processing code. Nat. Rev. Neurosci. 7, 890–901. https://doi.org/10.1038/nrn2006
Small, D.M., 2010. Taste representation in the human insula. Brain Struct Funct 214, 551–561. https://doi.org/10.1007/s00429-010-0266-9
Small, D.M., Gregory, M.D., Mak, Y.E., Gitelman, D., Mesulam, M.M., Parrish, T., 2003. Dissociation of Neural Representation of Intensity and Affective Valuation in Human Gustation. Neuron 39, 701–711.
Small, D.M., Jones-gotman, M., Zatorre, R.J., Petrides, M., Evans, A.C., 1997. A Role for the Right Anterior Temporal Lobe in Taste Quality Recognition. J. Neurosci. 17, 5136–5142.
Small, D.M., Voss, J., Mak, Y.E., Simmons, K.B., Parrish, T., Gitelman, D., 2004. Experience-Dependent Neural Integration of Taste and Smell in the Human Brain. J. Neurophysiol. 92, 1892–1903. https://doi.org/10.1152/jn.00050.2004
Smith, S.M., Jenkinson, M., Woolrich, M.W., Beckmann, C.F., Behrens, T.E.J., Johansen-Berg, H., Bannister, P.R., De Luca, M., Drobnjak, I., Flitney, D.E., Niazy, R.K., Saunders, J., Vickers, J., Zhang, Y., De Stefano, N., Brady, J.M., Matthews, P.M., 2004. Advances in functional and structural MR image analysis and implementation as FSL. Neuroimage 23, 208–219. https://doi.org/10.1016/j.neuroimage.2004.07.051
Smith, D. V., Li, C.S., 2000. GABA-mediated corticofugal inhibition of taste-responsive neurons in the nucleus of the solitary tract. Brain Res. 858, 408–415. https://doi.org/10.1016/S0006-8993(99)02484-1
Smith, D. V., St. John, S.J., Boughter, J.D., 2000. Neuronal cell types and taste quality coding. Physiol. Behav. 69, 77–85. https://doi.org/10.1016/S0031-9384(00)00190-6
Song, X.-W., Dong, Z.-Y., Long, X.-Y., Li, S.-F., Zuo, X.-N., Zhu, C.-Z., He, Y., Yan, C.-G., Zang, Y.-F., 2011. REST: A Toolkit for resting-state functional magnetic resonance imaging data processing. PLoS One 6, e25031: 1--12. https://doi.org/10.1371/journal.pone.0025031
Sosulski, D.L., Lissitsyna Bloom, M., Cutforth, T., Axel, R., Datta, S.R., 2011. Distinct representations of olfactory information in different cortical centres. Nature 472, 213–219. https://doi.org/10.1038/nature09868

Spetter, M.S., Smeets, P.A.M., de Graaf, C., Viergever, M.A., 2010. Representation of sweet and salty taste intensity in the brain. Chem. Senses 35, 831–840. https://doi.org/10.1093/chemse/bjq093
Sridharan, D., Levitin, D.J., Menon, V., 2008. A critical role for the right fronto-insular cortex in switching between central-executive and default-mode networks. Proc. Natl. Acad. Sci. 105, 12569–12574. https://doi.org/10.1073/pnas.0800005105
Stapleton, J.R., Lavine, M.L., Wolpert, R.L., Nicolelis, M.A.L., Simon, S.A., 2006. Rapid Taste Responses in the Gustatory Cortex during Licking. J. Neurosci. 26, 4126–4138. https://doi.org/10.1523/JNEUROSCI.0092-06.2006
Sugita, M., Shiba, Y., 2005. Neuroscience: Genetic tracing shows segregation of taste neuronal circuitries for bitter and sweet. Science (80-.). 309, 781–785. https://doi.org/10.1126/science.1110787
Sun, F.T., Miller, L.M., D'Esposito, M., 2004. Measuring interregional functional connectivity using coherence and partial coherence analyses of fMRI data. Neuroimage 21, 647–658. https://doi.org/10.1016/j.neuroimage.2003.09.056
Titova, O.E., Hjorth, O.C., Schiöth, H.B., Brooks, S.J., 2013. Anorexia nervosa is linked to reduced brain structure in reward and somatosensory regions : a meta-analysis of VBM studies. BMC Psychiatry 13.
Toro, R., Fox, P.T., Paus, T., 2008. Functional coactivation map of the human brain. Cereb. Cortex 18, 2553–2559. https://doi.org/10.1093/cercor/bhn014
Tracey, I., Mantyh, P.W., 2007. The Cerebral Signature for Pain Perception and Its Modulation. Neuron 55, 377–391. https://doi.org/10.1016/j.neuron.2007.07.012
Treasure, J., Claudino, A.M., Zucker, N., 2010. Eating disorders. Lancet (London, England) 375, 583–593. https://doi.org/10.1016/S0140-6736(03)12378-1
Van Den Eynde, F., Suda, M., Broadbent, H., Guillaume, S., Eynde, M. Van Den, Steiger, H., Israel, M., Berlim, M., Giampietro, V., Simmons, A., Treasure, J., Campbell, I., Schmidt, U., 2012. Structural Magnetic Resonance Imaging in Eating Disorders : A Systematic Review of Voxel-Based Morphometry Studies. Eur. Eat. Disord. Rev. 20, 94–105. https://doi.org/10.1002/erv.1163
Van Den Heuvel, M.P., Mandl, R.C.W., Kahn, R.S., Hulshoff Pol, H.E., 2009. Functionally linked resting-state networks reflect the underlying structural connectivity architecture of the human brain. Hum. Brain Mapp. 30, 3127–3141. https://doi.org/10.1002/hbm.20737
Van der Laan, L.N., de Ridder, D.T.D., Viergever, M.A., Smeets, P.A.M., 2011. The first taste is always with the eyes: A meta-analysis on the neural correlates of processing visual food cues. Neuroimage 55, 296–303. https://doi.org/10.1016/j.neuroimage.2010.11.055
Veldhuizen, M.G., Albrecht, J., Zelano, C., Boesveldt, S., Breslin, P., Lundström, J.N., 2011. Identification of Human Gustatory Cortex by Activation Likelihood Estimation. Hum. Brain Mapp. 32, 1–23. https://doi.org/10.1088/1367-2630/15/1/015008.Fluid
Veldhuizen, M.G., Bender, G., Constable, R.T., Small, D.M., 2007. Trying to Detect Taste in a Tasteless Solution : Modulation of Early Gustatory Cortex by Attention to Taste. Chem. Senses 32, 569–581. https://doi.org/10.1093/chemse/bjm025
Veldhuizen, M.G., Nachtigal, D., Teulings, L., Gitelman, D.R., Small, D.M., 2010. The insular taste cortex contributes to odor quality coding. Front. Hum. Neurosci. https://doi.org/10.3389/fnhum.2010.00058
Vicario, C.M., 2013. Altered insula response to sweet taste processing in recovered anorexia and bulimia nervosa: A matter of disgust sensitivity? Am. J. Psychiatry

170, 1497. https://doi.org/10.1176/appi.ajp.2013.13060748
Vocks, S., Herpertz, S., Rosenberger, C., Senf, W., Gizewski, E.R., 2011. Effects of gustatory stimulation on brain activity during hunger and satiety in females with restricting-type anorexia nervosa: An fMRI study. J. Psychiatr. Res. 45, 395–403. https://doi.org/10.1016/j.jpsychires.2010.07.012
Wager, T.D., Barrett, L.F., 2004. From affect to control: Functional specialization of the insula in motivation and regulation. Emotion 129, 2865. https://doi.org/http://dx.doi.org/10.1101/102368
Wagner, A., Aizenstein, H., Frank, G.K., Figurski, J., May, J.C., Putnam, K., Fischer, L., Bailer, U.F., Henry, S.E., McConaha, C., Vogel, V., Kaye, W.H., 2006. Neural correlates of habituation to taste stimuli in healthy women. Psychiatry Res. - Neuroimaging 147, 57–67. https://doi.org/10.1016/j.pscychresns.2005.11.005
Wagner, A., Aizenstein, H., Mazurkewicz, L., Fudge, J., Frank, G.K., Putnam, K., Bailer, U.F., Fischer, L., Kaye, W.H., 2008. Altered insula response to taste stimuli in individuals recovered from restricting-type anorexia nervosa. Neuropsychopharmacology 33, 513–523. https://doi.org/10.1038/sj.npp.1301443
Walsh, B.T., 2013. The enigmatic persistence of anorexia nervosa. Am. J. Psychiatry 170, 477–484. https://doi.org/10.1176/appi.ajp.2012.12081074
Wang, L., Gillis-Smith, S., Peng, Y., Zhang, J., Chen, X., Salzman, C.D., Ryba, N.J.P., Zuker, C.S., 2018. The coding of valence and identity in the mammalian taste system. Nature 558, 127–131. https://doi.org/10.1038/s41586-018-0165-4
Wang, L., Li, K., Zhang, Q.-E., Zeng, Y.-W., Jin, Z., Dai, W.-J., Su, Y.-A., Wang, G., Tan, Y.-L., Yu, X., Si, T.-M., 2013. Interhemispheric Functional Connectivity and Its Relationships with Clinical Characteristics in Major Depressive Disorder: A Resting State fMRI Study. PLoS One 8, e60191. https://doi.org/10.1371/journal.pone.0060191
Wang, Q.J., Spence, C., 2017. "A sweet smile": the modulatory role of emotion in how extrinsic factors influence taste evaluation. Cogn. Emot. https://doi.org/10.1080/02699931.2017.1386623
Wang, Y., Zhong, S., Jia, Y., Zhou, Z., Wang, B., Pan, J., Huang, L., 2015. Interhemispheric resting state functional connectivity abnormalities in unipolar depression and bipolar depression. Bipolar Disord. 17, 486–495. https://doi.org/10.1111/bdi.12315
Wegman, J., van Loon, I., Smeets, P.A.M., Cools, R., Aarts, E., 2018. Top-down expectation effects of food labels on motivation. Neuroimage 173, 13–24. https://doi.org/10.1016/j.neuroimage.2018.02.011
Wei, L., Duan, X., Zheng, C., Wang, S., Gao, Q., Zhang, Z., Lu, G., Chen, H., 2014. Specific Frequency Bands of Amplitude Low- Frequency Oscillation Encodes Personality. Hum. Brain Mapp. 35, 331–339. https://doi.org/10.1002/hbm.22176
Wicker, B., Keysers, C., Plailly, J., Royet, J.P., Gallese, V., Rizzolatti, G., 2003. Both of us disgusted in My insula: The common neural basis of seeing and feeling disgust. Neuron 40, 655–664. https://doi.org/10.1016/S0896-6273(03)00679-2
Xu, J., Moeller, S., Auerbach, E.J., Strupp, J., Smith, S.M., Feinberg, D.A., Yacoub, E., Ugurbil, K., 2013. Evaluation of slice accelerations using multiband echo planar imaging at 3 Tesla. Neuroimage 14, 384–399. https://doi.org/10.1080/10810730902873927.Testing
Yamamoto, C., Takehara, S., Morikawa, K., Nakagawa, S., Yamaguchi, M., Iwaki, S., Tonoike, M., Yamamoto, T., 2003. Magnetoencephalographic Study of Cortical Activity Evoked by Electrogustatory Stimuli. Chem. Senses 28, 245–251.

https://doi.org/10.1093/chemse/28.3.245
Yamamoto, T., Yuyama, N., Kato, T., Kawamura, Y., 1984. Gustatory responses of cortical neurons in rats. I. Response characteristics. J Neurophysiol 51, 616–635.
Yan Chao-Feng and Zang Yu-Feng, 2010. DPARSF: a MATLAB toolbox for "pipeline" data analysis of resting-state fMRI. Front. Syst. Neurosci. 4, 1–7. https://doi.org/10.3389/fnsys.2010.00013
Yarkoni, T., Barch, D.M., Gray, J.R., Conturo, T.E., Braver, T.S., 2009. BOLD correlates of trial-by-trial reaction time variability in gray and white matter: A multi-study fMRI analysis. PLoS One 4. https://doi.org/10.1371/journal.pone.0004257
Yeomans, M.R., 1998. Taste, palatability and the control of appetite. Proc. Nutr. Soc. 57, 609–615. https://doi.org/10.1079/PNS19980089
Yeung, A.W. K., Goto, T.K., Leung, W.K., 2017. Basic taste processing recruits bilateral anteroventral and middle dorsal insulae : An activation likelihood estimation analysis of fMRI studies. Brain Behav. 7, 1–12. https://doi.org/10.1002/brb3.655
Yeung, A.W.K., Goto, T.K., Leung, W.K., 2018. Affective value , intensity and quality of liquid tastants / food discernment in the human brain : An activation likelihood estimation meta-analysis. Neuroimage 169, 189–199. https://doi.org/10.1016/j.neuroimage.2017.12.034
Yiannakas, A., Rosenblum, K., 2017. The Insula and Taste Learning. Front. Mol. Neurosci. 10. https://doi.org/10.3389/fnmol.2017.00335
Yokota, T., Eguchi, K., Hiraba, K., 2011. Functional properties of putative pyramidal neurons and inhibitory interneurons in the rat gustatory cortex. Cereb. Cortex 21, 597–606. https://doi.org/10.1093/cercor/bhq126
Yu, R., Hsieh, M.H., Wang, H.S., Liu, C., Liu, C., Hwang, J., Chien, Y., Hwu, H., Tseng, W.I., 2013. Frequency Dependent Alterations in Regional Homogeneity of Baseline Brain Activity in Schizophrenia. PLoS One 8, 1–8. https://doi.org/10.1371/journal.pone.0057516
Zald, D.H., Hagen, M.C., Pardo, J. V, 2002. Neural Correlates of Tasting Concentrated Quinine and Sugar Solutions. j. Neurophysiol 87, 1068–1075. https://doi.org/10.1152/jn.00358.2001. Neural
Zald, D.H., Pardo, J., 1997. Emotion , olfaction , and the human amygdala : Amygdala activation during aversive olfactory stimulation. PNAS 94, 4119–4124.
Zald, D.H., Pardo, V., 1999. The Functional Neuroanatomy of Voluntary Swallowing. Ann. Neurol. 46, 281–286.
Zald, D.H., Pardo, J. V, 2000. Cortical Activation Induced by Intraoral Stimulation with Water in Humans. Chem. Senses 25, 267–275.
Zhan, J., Gao, L., Zhou, F., Bai, L., Kuang, H., He, L., 2016. Amplitude of Low-Frequency Fluctuations in Multiple-Frequency Bands in Acute Mild Traumatic Brain Injury. Front. Hum. Neurosci. 10. https://doi.org/10.3389/fnhum.2016.00027
Zhang, Y., Wang, K., Yue, C., Mo, N., Wu, D., Wen, X., Qiu, J., 2018. The motor features of action verbs: fMRI evidence using picture naming. Brain Lang. 179, 22–32. https://doi.org/10.1016/j.bandl.2018.02.002
Zhou, Y., Milham, M., Zuo, X.-N., Kelly, C., Jaggi, H., Herbert, J., Grossman, R.I., Ge, Y., 2013. Functional homotopic changes in multiple sclerosis with resting-state functional MR imaging. AJNR. Am. J. Neuroradiol. 34, 1180–7. https://doi.org/10.3174/ajnr.A3386
Zhu, J.-N., Wang, J.-J., 2008. The cerebellum in feeding control: Possible function and mechanism. Cell. Mol. Neurobiol. 28, 469–478. https://doi.org/10.1007/s10571-007-9236-z

Zhu, J.-N., Yung, W.-H., Kwok-Chong Chow, B., Chan, Y.-S., Wang, J.-J., 2006. The cerebellar-hypothalamic circuits: potential pathways underlying cerebellar involvement in somatic-visceral integration. Brain Res. Rev. 52, 93–106. https://doi.org/10.1016/j.brainresrev.2006.01.003

Zuo, X.-N., Di Martino, A., Kelly, C., Shehzad, Z.E., Gee, D.G., Klein, D.F., Castellanos, F.X., Biswal, B.B., Milham, M.P., 2010. The oscillating brain: complex and reliable. Neuroimage 49, 1432–1445. https://doi.org/10.1016/j.neuroimage.2009.09.037

Publications:

Papers:

Antonietta Canna, Anna Prinster, Michele Fratello, Luca Puglia, Mario Magliulo, Elena Cantone, Maria Agnese Pirozzi, Francesco Di Salle, Fabrizio Esposito : ***A low-cost open-architecture taste delivery system for gustatory fMRI and BCI experiments*.** Journal of Neuroscience Methods. doi - https://doi.org/10.1016/j.jneumeth.2018.10.003

Antonietta Canna, Anna Prinster, Elena Cantone, Sara Ponticorvo, Andrea G. Russo, Francesco Di Salle, Fabrizio Esposito: "***Intensity related distribution of sweet and bitter taste fMRI responses in the insular cortex. Human Brain Mapping***" (Submitted).

Canna Antonietta*, Russo Andrea Gerardo*, Ponticorvo Sara, Manara Renzo, Pepino Alessandro, Sansone Mario, Di Salle Francesco, Esposito Fabrizio :"***Automated search of control points in surface-based morphometry***" NeuroImage 176 (2018) 5670. doi - 10.1016 j.neuroimage.2018.04.035

Antonietta Canna*, Sara Ponticorvo*, Andrea G. Russo, Renzo Manara, Francesco Di Salle, Renato Saponiero, Martina Callaghan, Nikolaus Weiskopf, Fabrizio Esposito: "***A Group-level Comparison of Volumetric and Combined Volumetric-Surface Normalization for Whole Brain Analyses of Myelin and Iron Maps***". Magnetic Resonance Imaging 2018. doi: 10.1016/j.mri.2018.08.021

Canna Antonietta, Prinster Anna, Monteleone Alessio Maria, Cantone Elena, Monteleone Palmiero, Volpe Umberto, Maj Mario, Di Salle Francesco, Esposito Fabrizio: "***Interhemispheric Functional Connectivity in Anorexia and Bulimia Nervosa*.**" European Journal of Neuroscience, 2016 Dec 19: 10.1111 - ejn.13507

Monteleone Alessio Maria, Monteleone Palmiero, Esposito Fabrizio, Prinster Anna, Volpe Umberto, Cantone Elena, Pellegrino Francesca, Canna Antonietta, Milano Walter, Aiello Marco, Di Salle Francesco, Maj Mario.: "***Altered processing of rewarding and aversive basic taste stimuli in symptomatic women with anorexia nervosa and bulimia nervosa: An fMRI study.***" J Psychiatr Res. 2017 Feb 21;90:94-101. doi: 10.1016 - j.jpsychires.2017.02.013.

Monteleone Alessio Maria, Monteleone Palmiero, Esposito Fabrizio, Prinster Anna, Ruzzi Vincenzo, Canna Antonietta, Aiello Marco, Di Salle Francesco, Maj Mario: "***The effects of childhood maltreatment on brain structure in adults with eating disorders.***" World J Biol Psychiatry. 2017 Nov 20:1-10. doi: 10.1080 - 15622975.2017.1395071.

Conferences:

Antonietta Canna, Sara Ponticorvo, Andrea Gerardo Russo, Renzo Manara, Francesco Di Salle, Martina Callaghan, Nicolaus Weiskopf, Fabrizio Esposito: "***MRI-Based Iron and Myelin Mapping with Volumetric vs. Combined Volumetric-Surface Normalization.***" Organization for Human Brain Mapping (OHBM) 2017, Vancouver, Canada, 25 June- 29 June.

Antonietta Canna, Andrea Gerardo Russo, Sara Ponticorvo, Fabrizio Esposito: "***Automatic Search of Control Points in Cortical Thickness Analysis.***" Organization for Human Brain Mapping (OHBM) 2017, Vancouver, Canada, 25 June- 29 June.

Antonietta Canna, Anna Prinster, Alessio Maria Monteleone, Palmiero Monteleone, Roberta Amodio, Elena Cantone, Francesco Di Salle, Fabrizio Esposito: "***Extrinsic and Intrinsic Functional Connectivity Changes along the Taste Pathway in Eating Disorders***." Organization for Human Brain Mapping (OHBM) 2016, Geneva, Switzerland, 25 June- 30 June.

Acknowledgments

I would like to thank Professor Fabrizio Esposito for his teaching and constant support. I am also grateful with Professor Renzo Manara, Professor Francesco Di Salle, Professor Palmiero Monteleone and Dr. Anna Prinster for the important scientific discussions.
I thank all people I met in Maastricht because they made my experience unforgettable. I thank Prof. Elia Formisano and Prof. Anne Roefs for the opportunity they gave me to acquire data at ultra-high field and I thank Niels, Vittoria, Roy, Federica, Marco, Lars, Martha, Sieske, Clara, Leonie and Alida, and all the others, for the time we had together.
Ringrazio voi, mamma e papa, semplicemente perché siete la mia forza e il mio coraggio. Accettate ogni mia scelta, facendomi sentire sempre protetta e al sicuro in qualsiasi parte del mondo in cui mi trovi, e per me questo vale più di ogni altra cosa.
Ringrazio te, Ale, semplicemente perché io e te siamo sempre stati e saremo una cosa sola. Sei fondamentale, e non solo per tutte le volte che ti chiedo di aggiustare le mie fantastiche opera d'arte.
Ringrazio te, Angela, perché io con te ho trovato una sorella, oltre che un'amica.
Ringrazio te, Michele, perché sei stato il mio mentore e perché ci sei stato quando ne avevo più bisogno, sia lavorativamente che personalmente.
Ringrazio te, Sara, perché sei paziente e riesci ad accettare ogni mio stato d'animo. Sei una cara amica davvero, la mia ranocchietta.
Ringrazio te, Brontolo (Andrea), perché so che di qualsiasi cosa avrò bisogno, sebbene brontolando, tu dirai di si.
Ringrazio le mie amiche secolari, Giovanna, Federica, Marilena, Carme, Marisa ed Anna, gli anni passano ma noi siamo sempre presenti le une per le altre.
Ringrazio chi c'è stato in questo percorso, anche chi non ho menzionato personalmente, per averlo reso uno dei percorsi più importanti e divertenti della mia vita.

Anto